# THREE-PHASE AC ARC HEATER

*R. PHILLIPS, D. GEISTER, P. HANDY, S. BOWEN*

*THE UNIVERSITY OF MICHIGAN*
*ANN ARBOR, MICHIGAN*

FEBRUARY 1964

## FOREWORD

This Final Technical Documentary Report was prepared by the Aircraft Propulsion Laboratory, Department of Aeronautical and Astronautical Engineering, The University of Michigan, on Contract AF 33(657)-8630 for the Aerospace Research Laboratories, Office of Aerospace Research, United States Air Force. The work reported herein was accomplished on Task 7065-01, "Fluid Dynamics Facilities Research" of Project 7065, "Aerospace Simulation Techniques Research" under the cognizance of Capt. Ralph Prete of the Fluid Dynamics Facilities Laboratory, ARL. At The University of Michigan the project supervisor was Prof. J. A. Nicholls. This report covers work done during the period 1 May 1963 to 15 November 1963.

# ABSTRACT

Experimental and theoretical investigations into the technology associated with three-phase AC arc heaters is presented and critically discussed. The behavior of the three-phase arc is extensively considered and it is shown that a previously reported analysis can adequately predict this behavior.

The problems of designing arc heater components are discussed and in particular those associated with the pressure vessel. It is shown that the present, low pressure chamber extracts an unacceptable amount of energy from the arc heated gas resulting in a rather low unit efficiency.

Finally, the benefits which might result from coupling a magnetogasdynamic accelerator to the arc heater for flight simulation are discussed and on the basis of perfect accelerator performance (no losses) it seems that significant increases in stagnation properties can be effected.

# TABLE OF CONTENTS

# LIST OF ILLUSTRATIONS

## LIST OF ILLUSTRATIONS (continued)

# I. INTRODUCTION

During the subject reporting period basic investigations into the problems associated with AC arc heating were continued. In the spirit of our past work these investigations were of a theoretical as well as experimental nature. The progress to date will be reported in several specific categories. Experimentally, that which has been learned from the operation of the large 3-phase facility will be discussed as well as the information gleaned from some related small scale experiments.

In almost all instances theoretical work has either preceded or accompanied our experimental efforts and this report will serve to document the most thorough and/or most important of these analyses. Included among these will be certain tasks which were performed prior to the subject reporting period and they are described herein for the sake of completeness. Since such a variety of subjects will be covered, the investigations will be described as separate entities with little or no cohesive material joining their presentations.

Subjects to be covered include the properties of AC arcs subjected to both normal and axial flow, the feasibility of using a magnetogasdynamic accelerator for hypersonic simulation, the prediction of pressure vessel heating due to an arc heated gas, the design of a water cooled magnetic field coil, and finally some general design considerations for both high and low pressure arc heaters.

# II. EXPERIMENTAL INVESTIGATIONS

In this section the highlights of the arc heater experimental program will be discussed with the emphasis being placed upon the lessons learned therefrom rather than simply displaying large amounts of data. The data which are presented are of a typical (summarizing) nature and show trends associated with the pertinent phenomena. In addition to the information gleaned from the low pressure 3-phase arc heater, the results of certain small scale experiments will be presented and discussed. With these small experiments it has been possible to isolate and closely examine certain phenomena which are present in the larger device but are usually obscured by complex interaction with other events.

Some of the experimental programs described herein are quite complete and are essentially closed subjects. Others, however, are really only preliminary and more data needs to be gathered when improved facilities, i. e., the high pressure arc heater, become available.

## A. THE CHARACTERISTICS OF THE 3-PHASE ARC AND ITS ROLE AS A CIRCUIT ELEMENT

Quite early in the arc heater developmental program considerable effort was directed toward obtaining data related to the characteristics of a 3-phase AC discharge and attempting to fit those data into the framework of a relatively simple circuit theory. The advantages of having such a theory are, it seems, quite evident.

Using oscillographic analysis it was hoped that a great deal could be learned about the arc characteristics as they are influenced by the magnetic field, pressure level, and flow rate. This approach has proved to be quite successful but the effect of the magnetic field should be examined in still more detail. With the present arrangement the magnetic field which the arcs experience cannot be varied too greatly. In particular, at high power operation the field strength cannot be varied at all without allowing the electrodes to be destroyed.

2

Consider first the behavior of the arc voltage and the line current when both the magnetic field and chamber pressure are held constant. In Figure 1 a typical oscillogram of these quantities is reproduced. Traces 1 through 3 are the arc voltages corresponding to phase voltages 1-2, 2-3, 3-1, respectively while the remaining active traces are the line currents. The circuit is shown in Figure 2 and it is seen that the arc behaves somewhat like a lossy neutral point in a wye-connected inductive circuit. It should be pointed out that the arc characteristics for a 4-wire circuit would be quite different from those shown in Figure 1, see Reference 1. In Figure 1 the galvanometers used on voltage traces 2 and 3 had a high frequency response and were driven with a large fraction of the actual signal voltage. It is clear that there is a great amount of random behavior which is attributable, it is felt, to the forced spot motion caused by the magnetic field. This is not surprising since the location of electrode spots on cooled metallic electrodes is a rather random affair anyway without the further disturbing action of an external magnetic field. Oscillograms similar to Figure 1 have been made when there was no magnetic field present and the voltage waveforms were considerably smoother.

It is clear that when such random high frequency disturbances are present in a phenomenon very little information about its behavior in the large can be determined by using high frequency response galvanometers. For comparison, the first voltage trace has been recorded with a galvanometer which will not pass much of the randomness and which, moreover, is driven with a smaller signal so as to decrease the maximum required writing rate of the recorder. Here the large scale behavior of the arc voltage is far clearer than in traces 2 and 3 and it is possible to determine a type of square wave behavior. According to this pattern the arc burns with a positive polarity for $2\pi/3$ radians, is extinguished and remains dormant for $\pi/3$ radians, and is then reignited to burn with a negative polarity for $2\pi/3$ radians followed by the 1/6 cycle dormant period. Of course, the arcs burning between the other phases must behave identically but shifted in time by $2\pi/3$ and $4\pi/3$ radians respectively. The arcing pattern is something
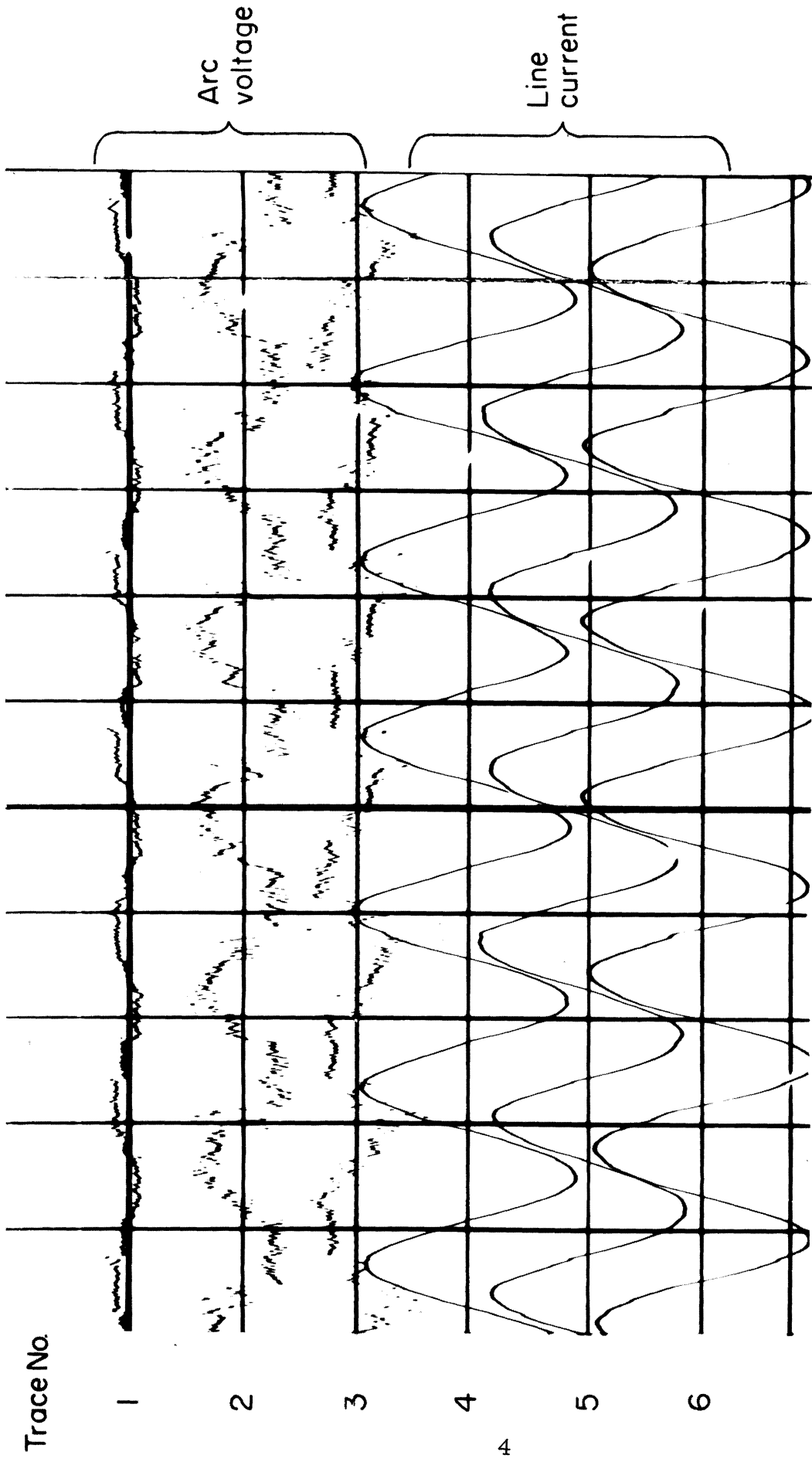
3

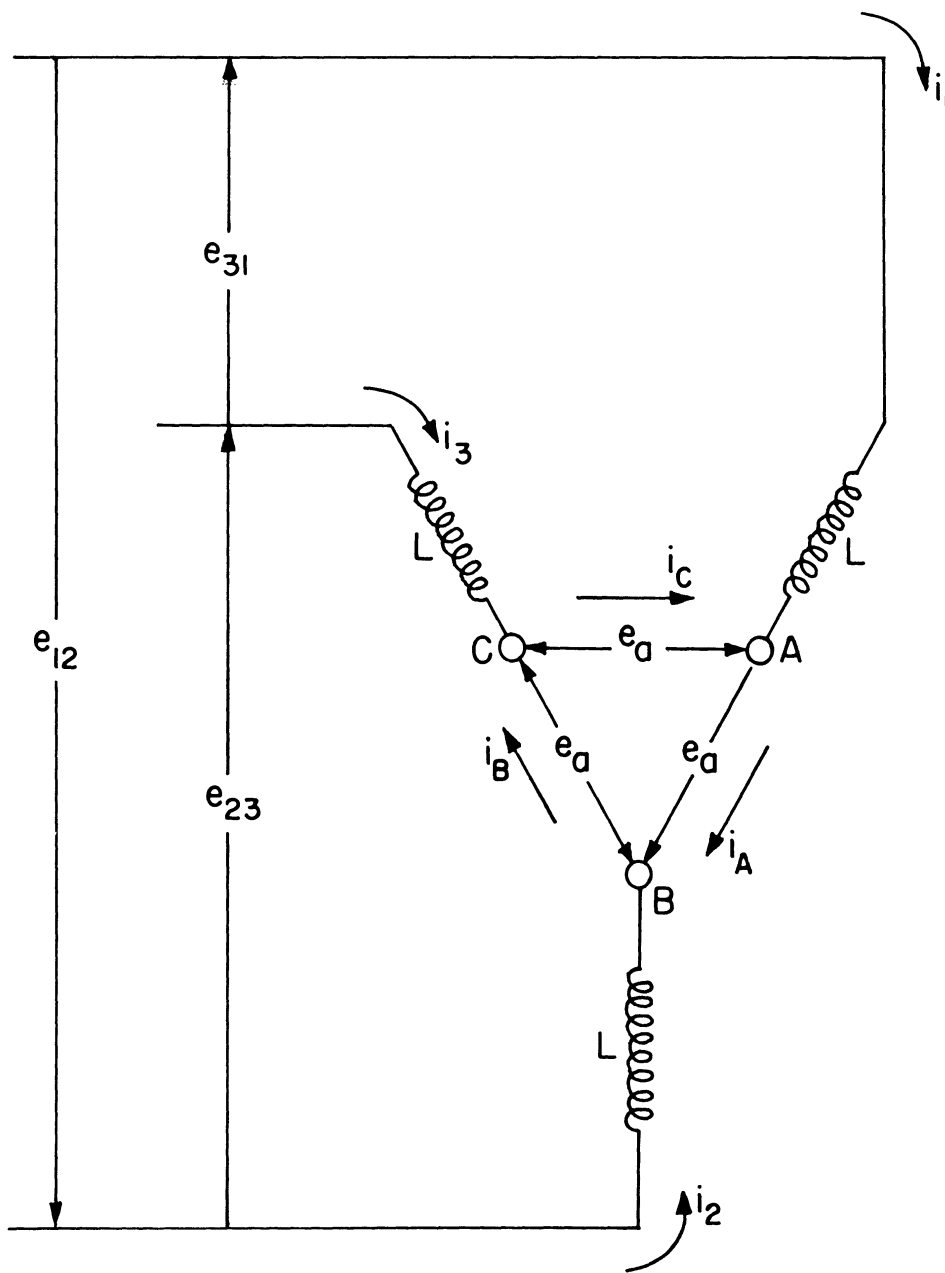FIGURE 1. VOLTAGE AND CURRENT TRACES FOR THREE PHASE ARC HEATER.

FIGURE 2. CIRCUIT ARRANGEMENT FOR THREE PHASE ARC HEATER.

like that shown in Figure 3. For the three wire system shown in Figure 2 the instantaneous sum of the voltages $e_{AB}$, $e_{BC}$, $e_{CA}$ must <u>always</u> be zero, implying, of course, that there is some relation between the arc voltages which must be satisfied for every instant of time. The pattern shown in Figure 3 is just such an arrangement but mathematically it is not the <u>only</u> one possible. It is interesting to examine the physical reasons behind the arcing arrangement which the system exhibits. Before proceeding to discuss this, however, it will be helpful to have a more lucid picture available of the actual arcing phenomenon.

In order to obtain voltage and current waveforms for a 3-phase arc system which is not subjected to the random disturbances of blowing and magnetic field effects a small model arc was constructed which duplicates the electrical characteristics of the large 3-phase unit. That is, the arcs were inductively stabilized and the inductors were wound so that the resistive portion of their impedance was the same fraction as the large scale inductors. A variety of electrode materials were used including tungsten, carbon, brass, and water-cooled copper. There was no externally applied magnetic field and the only blowing which the arcs experienced was due to free convection. The rms current level was of the order of 30 amps and the open circuit voltage was as high as 600 volts. Figure 4 is a rather busy oscillogram of the arc voltages for all three phases upon which is superimposed the corresponding line voltages. The single low amplitude sine curve at the bottom is the <u>line</u> current corresponding to the arc voltage at that location. Its polarity is reversed for the sake of clarity. It is seen that the arcing arrangement is strikingly similar to that depicted in Figure 3. With the aid of this oscillogram (which was taken with tungsten electrodes) it is possible to discuss the physical aspects of this three phase mode of arcing.

First one observes that for a given arc gas, electrode material, and electrode spacing, there is a unique burning voltage corresponding to the current imposed upon the arc. This is quite evident for the DC arc where the voltage-current characteristic is nearly hyperbolic and elementary considerations can show there is but one stable burning condition. While harder to demonstrate
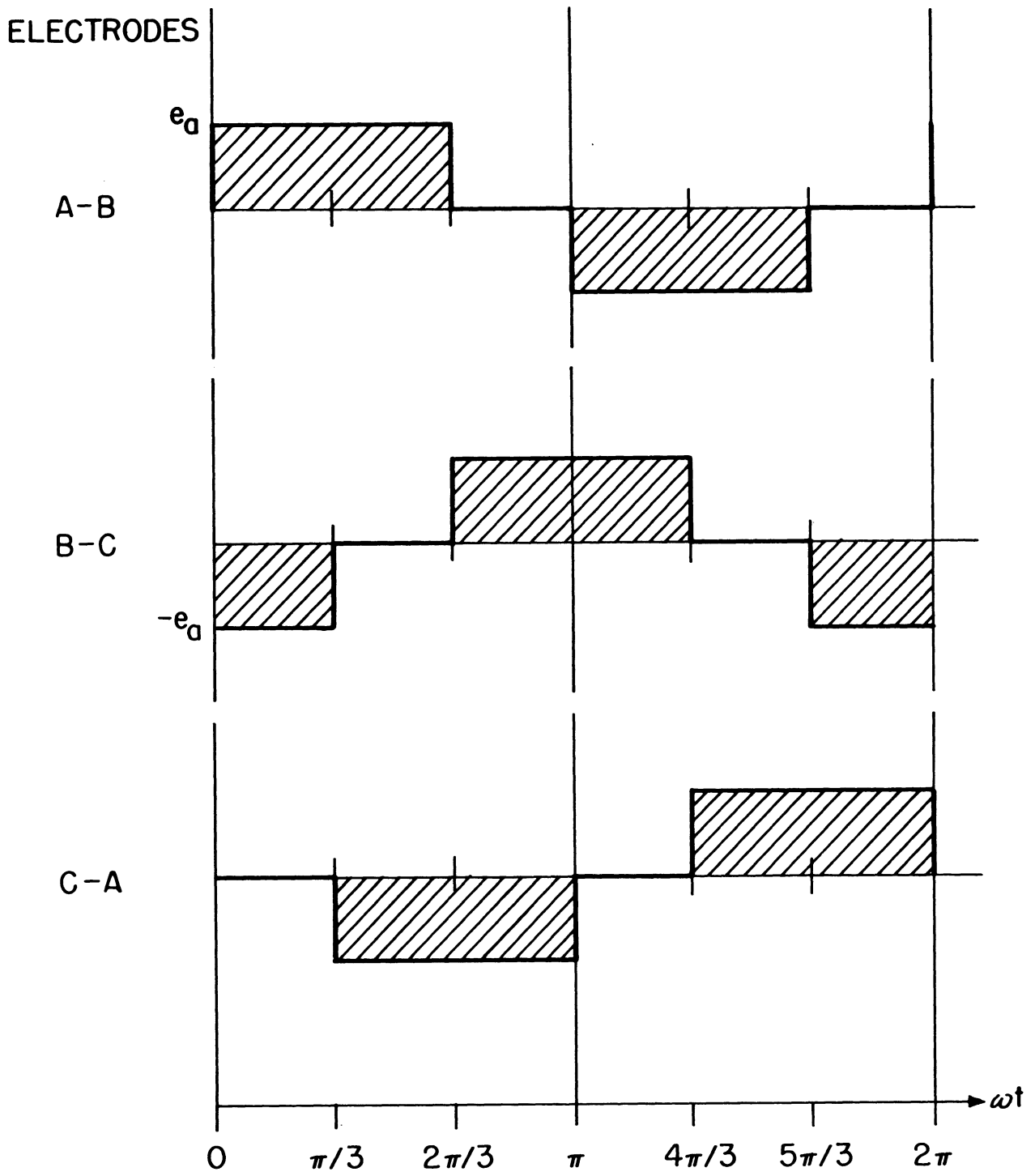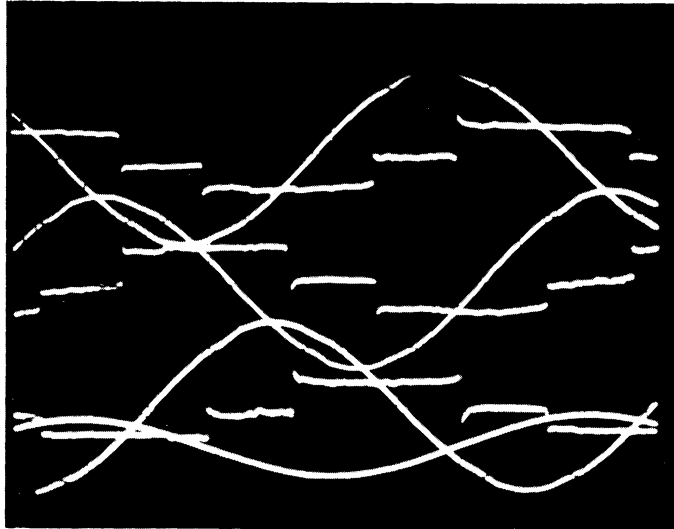
FIGURE 3. DIAGRAM OF MODEL ARC VOLTAGES.

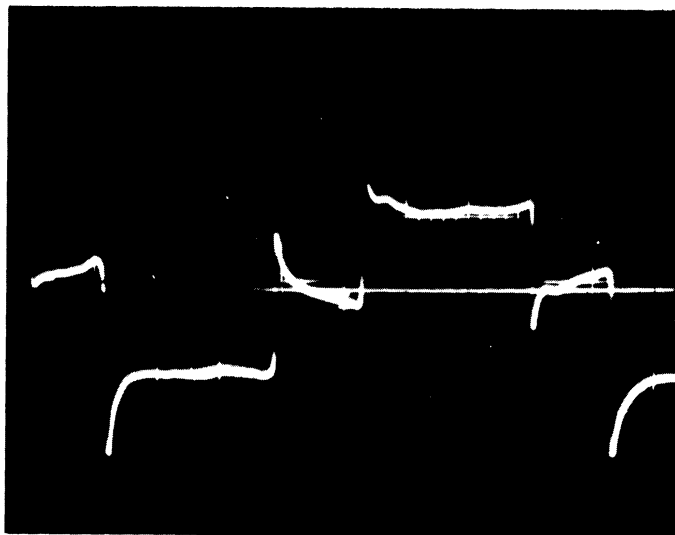FIGURE 4. THREE PHASE MODEL ARC WAVEFORMS.



FIGURE 5. THREE PHASE ARC VOLTAGE (One electrode pair).
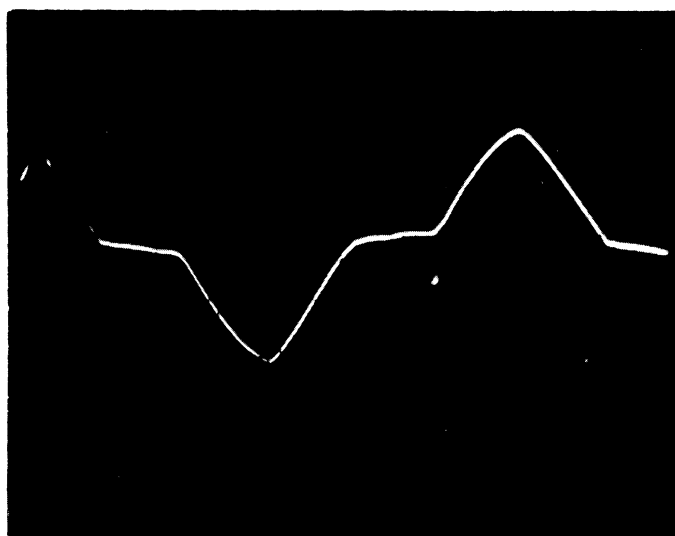


FIGURE 6. THREE PHASE ARC CURRENT (One electrode pair).

8

the same is nonetheless true of an AC arc (see Reference 2). Then in a perfectly balanced 3-phase circuit one would not expect an arc to burn between one pair of electrodes with a voltage, say, $e_a$, while between another pair there exists an arc burning with a potential difference of $2e_a$. Hence when an arc exists it burns at the unique voltage of $e_a$ which may either be positive or negative. Since there are three possible locations for arcing in the three-phase, three-wire circuit it follows from the above arguments that only two arcs may exist simultaneously at a given instant of time. Moreover, they must be of opposite polarity because of the zero voltage summability condition mentioned earlier. As mentioned before, there are other mathematical arrangements which can fulfill this condition than the one shown in Figures 3 and 4 but the physics of the system dictates only one.

To see this, consider an instant in time for which the arc of trace 3 (Figure 4) is burning with a positive polarity. Also suppose the arc of trace 2 is burning negatively so that arc number 1 is dormant. As the line current which feeds arcs 1 and 3 approaches its zero passage the arc of trace 3 must begin to extinguish. As its voltage drops to zero the voltage across the dormant arc must rise proportionately to preserve the null summability condition for the circuit. Arc number 2 continues to burn unchanged. The just extinguished arc (number 3) experiences the instantaneous open circuit voltage existing across its terminals which however is not sufficient to reignite it. In the other phase, however, across arc number 1, the line voltage is near its maximum and reignites the previously dormant arc. It is here that one can see the advantages of a three phase arc burning in this three wire mode. The extinction transient of one arc is the reignition transient for another; a feature which promotes arc stability. The extinction and ignition process described above is repeated 1/6 cycle later where the arc of trace 2 extinguishes and arc number 3 ignites again.

The long dormant period which an arc experiences suggests that it carries no current during this time. That this is indeed the case is shown quite clearly in Figures 5 and 6. Here one finds the arc voltage waveform for a single

electrode pair along with the corresponding arc current. Again tungsten electrodes were used and it is seen that during the periods of non-conduction the arc voltage is nearly zero.

This simple arc voltage behavior has suggested an analysis of a three phase inductive circuit containing idealized, square wave-type arcs. This analysis is presented in its entirety in Reference 3 and has proved to be quite valuable in predicting the performance of the large 3-phase arc heater. In fact it is quite interesting to compare these predictions with actual data since a maximum in attainable useful power was predicted if the arc voltage reached a certain critical level. Now it was predicted that this critical arc voltage would be a significant fraction of the available line voltage so that there was some doubt as to whether this condition could be realized experimentally. If, however, the high arc voltage is attained by causing the arc to burn in a high pressure environment it has been found that the realization of this maximum point is indeed possible. To see this consider the following presentation of data.

In Reference 3 it was predicted that the power factor, $F$, of a three phase circuit containing arcs which are inductively stabilized is a function only of the ratio of the arc voltage, $e_a$, to the peak line voltage, $E_m$. Figure 7 shows this relationship and it is shown to be very nearly linear. Now both variables of Figure 7 can be measured so it is possible to check the validity of the curve quite precisely. The power dissipated by the arcs as well as the circuit KVA is measured continuously throughout a run and their quotient is the power factor regardless of any waveform non-harmonics. Figure 8 shows such a set of traces. The arc voltage is easily measured on an oscilloscope and the results obtained from several typical runs are shown as open circles in Figure 7. The agreement is quite satisfactory so one may reasonably assume that arc voltage can be inferred by entering Figure 7 knowing only the power factor and reading off $e_a/E_m$ from the theoretical curve. In Figure 9 a non-dimensional power is plotted as a function of the ubiquitous voltage ratio $e_a/E_m$. Again the open circles summarize the data gleaned from many runs of the 3 phase arc heater. The data point nearest

Eq.:

$$F = \frac{2\sqrt{3}}{\pi}\left(\frac{e_a}{E_m}\right)\left(\frac{I_x}{I_\ell}\right)\left[1 - \frac{1}{3}\left(\frac{4\pi^2}{9}\right)\left(\frac{e_a}{E_m}\right)^2\right]^{-\frac{1}{2}}$$

O   Summary of typical data
—   Theoretical prediction
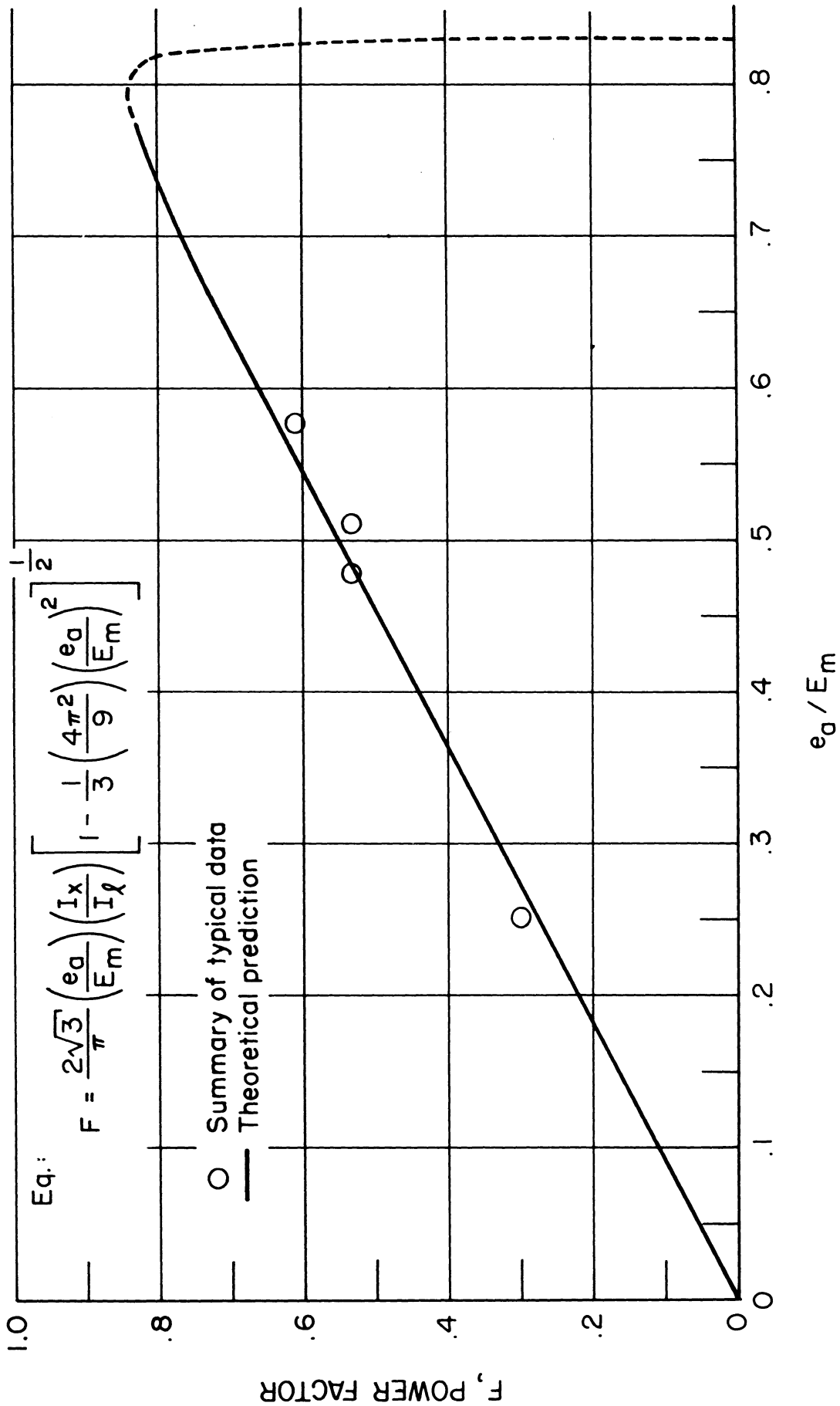
$e_a / E_m$

F, POWER FACTOR

FIGURE 7.  POWER FACTOR OF 3 PHASE ARC — THEORY AND EXPERIMENT.

11
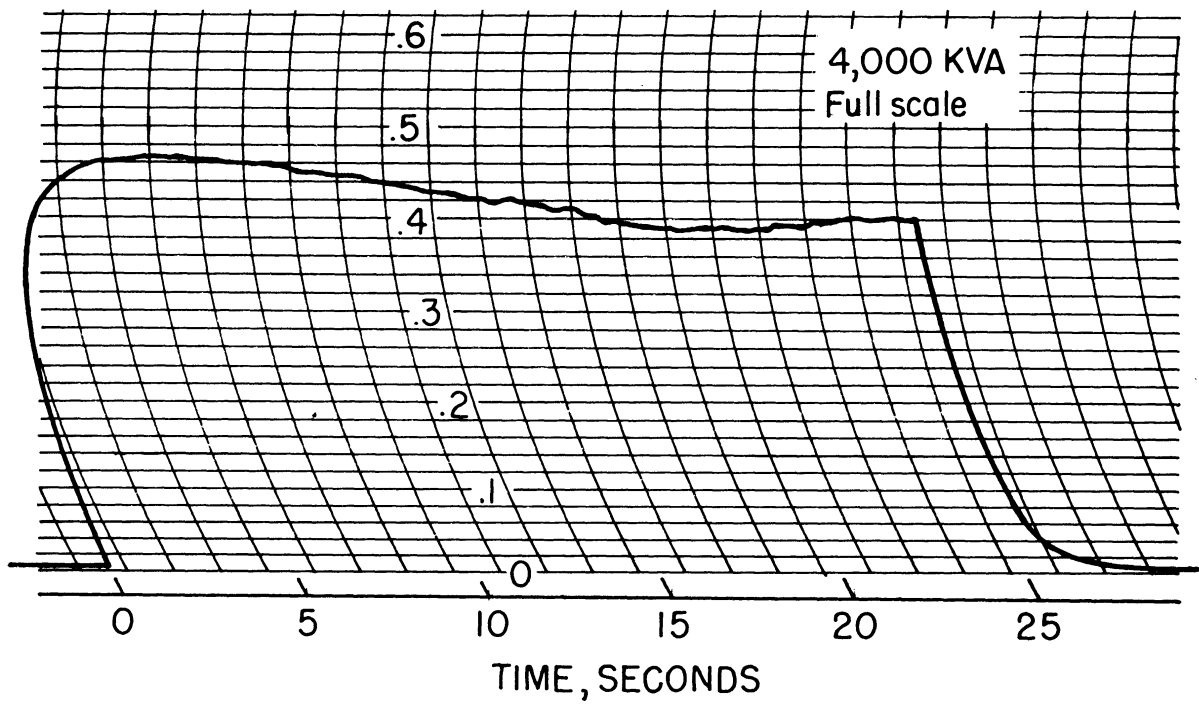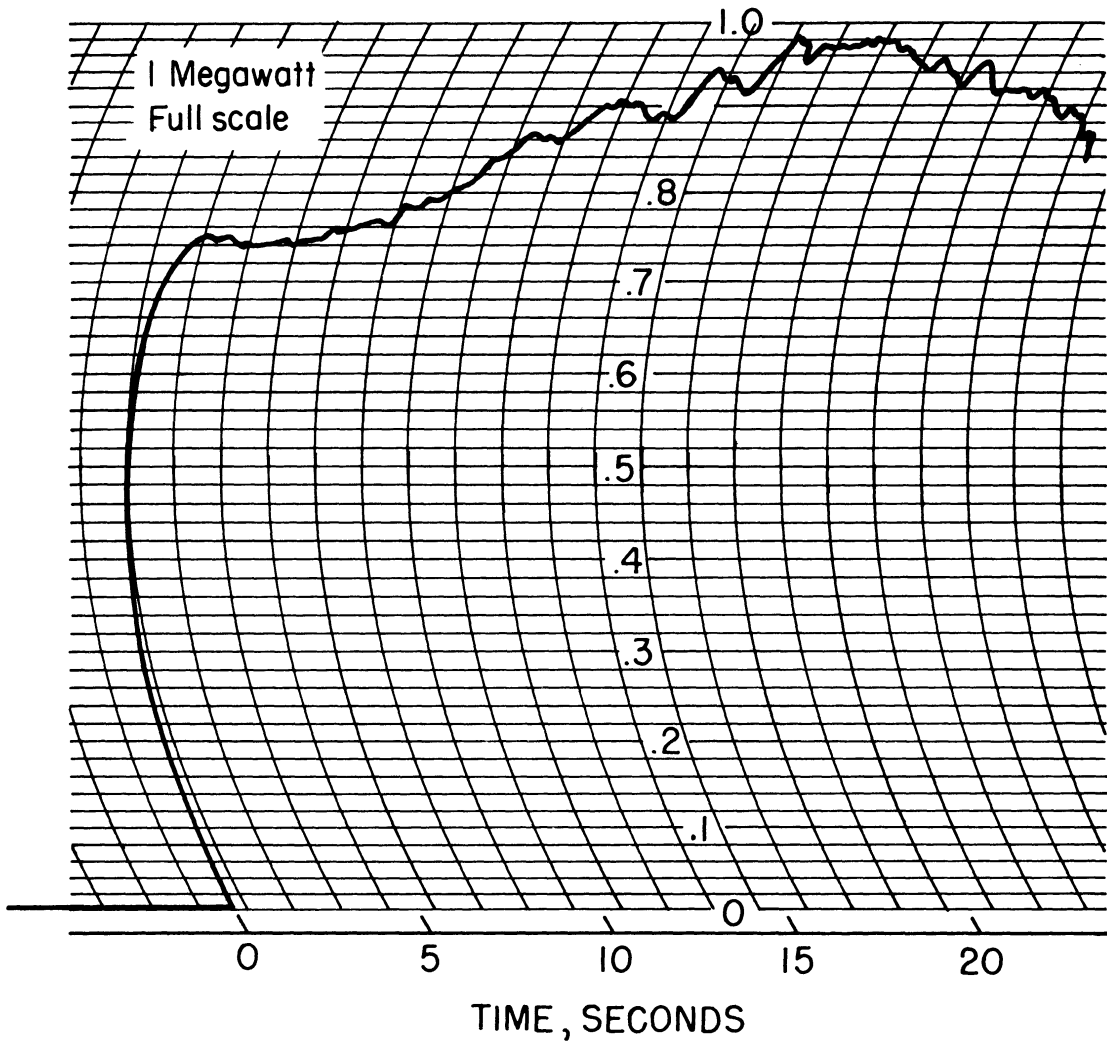
FIGURE 8. POWER AND KVA TRACES.

12
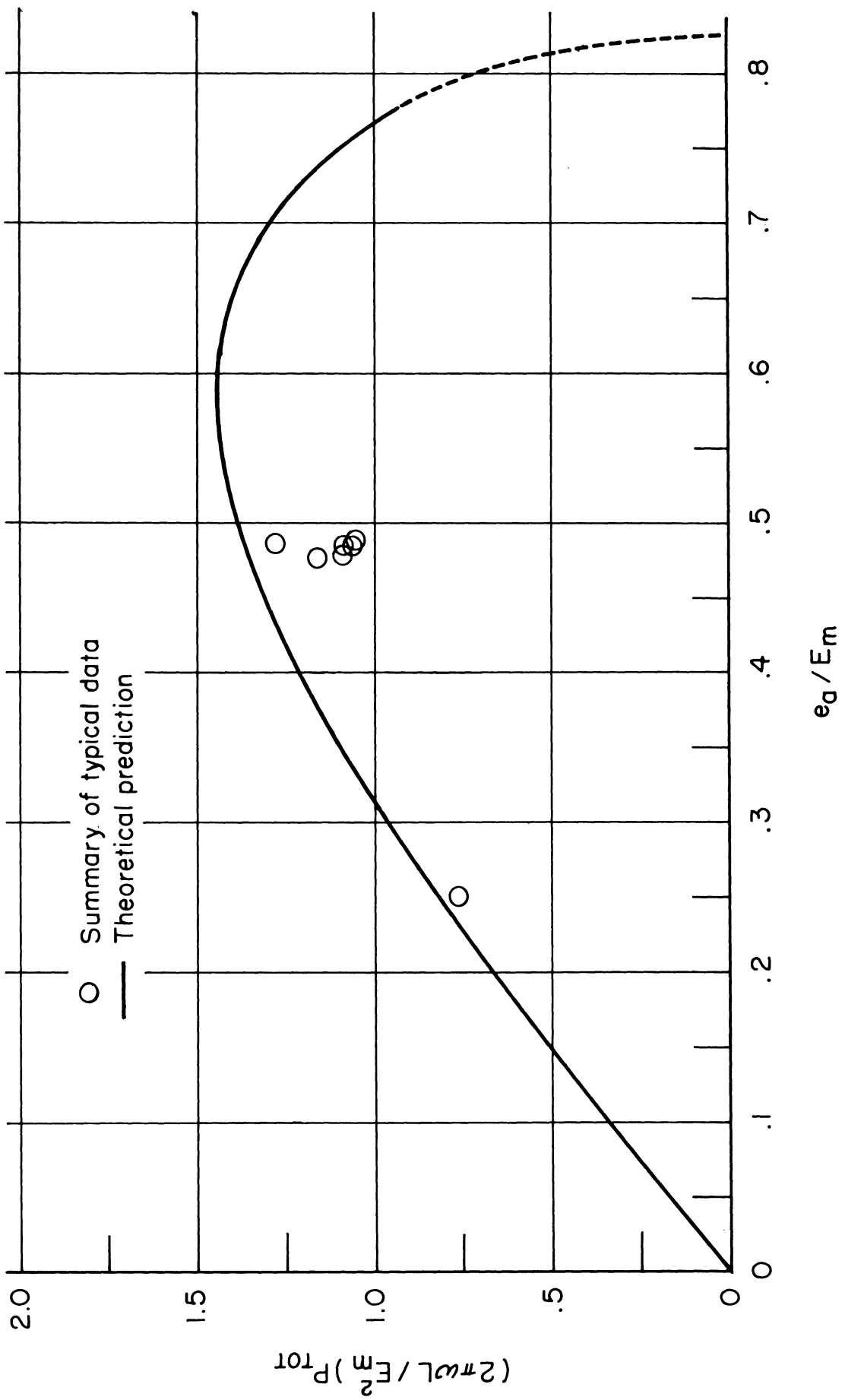
FIGURE 9. NON-DIMENSION POWER IN THREE PHASE ARC – THEORY AND EXPERIMENT.

○ Summary of typical data
— Theoretical prediction

$e_a/E_m$

$(2\pi\omega L/E_m^2)P_{TOT}$

the power maximum corresponds to the actual extremum in the measured power of Figure 8. The deviation from the solid curve is due to the fact that the circuit resistance was neglected in the analysis. It is concluded that if one knows the voltage ratio, $e_a/E_m$, the performance of a three phase arc heater system can be predicted rather accurately. It is quite difficult, however, to have prescience of the arc voltage unless experimental data are available. One knows that such parameters as electrode spacing, the type of arc gas, and the pressure level should influence the arc voltage by varying amounts but to say a priori what their combined effect will be for a specific arc chamber is indeed quite beyond the present state of technology.

The effects of the aforementioned agents upon the arc voltage in the three phase facility have been examined experimentally and the findings are interesting but not too unexpected.

Since a wide variety of sonic orifices have not been available for these studies nor has the air injection system been entirely adequate it is not possible to separate the effects of mass flow loading and pressure level on the arc voltage measurements to be presented. The indicated parameter will be the pressure but it should be borne in mind that the arc is probably affected equally as much by convective column loading. In Figure 10 the results of several typical elevated pressure runs are presented where the power level has been selected as the dependent variable and is plotted versus the logarithm of the chamber pressure in atmospheres. The data are presented in this manner because it is known that the effect of high gas pressure should be to increase the arc burning voltage according to the relation

$$e_a = A \ln P + B$$

when all other variables are held constant. Furthermore, for the range of conditions presented in Figure 10 the power is a proportional indicator of the voltage level and an unambiguous power measurement is easy to obtain. It is seen that a linear relation between the power and $\ln P$ does not hold and this deviation is
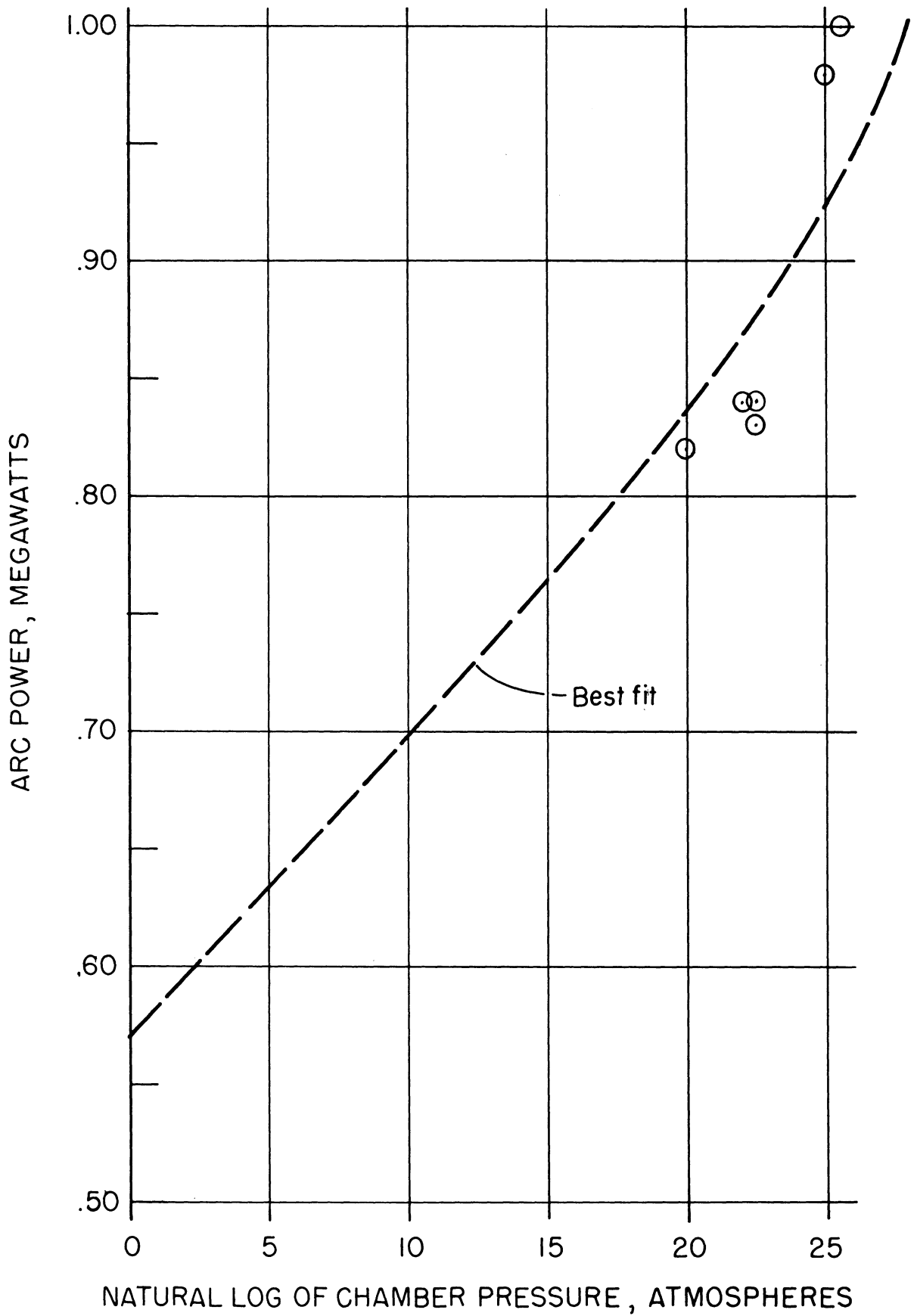
FIGURE 10. EFFECT OF PRESSURE / MASS FLOW ON ARC POWER.

preliminarily ascribed to the presence of mass flow effects. In subsequent investigations the variables of mass flow and pressure will be much more independently controllable and better data on this matter can be obtained.

The effect of electrode spacing on $e_a$, the arc voltage, is exactly what one would expect, there exists a linear relation between the two. Gap sizes ranging from 3/4 inch to 2 1/2 inches have been studied and for all other variables held constant there is a proportional effect upon the arc voltage when the electrode spacing is increased.

The presence of an externally applied magnetic field is felt in many profound ways by the three phase arc. Of course, it induces rapid electrode spot motion which in turn prevents electrode attrition. This is the primary reason for having a magnetic field. In addition the magnetic field interacts with the arc in such a way as to increase the burning voltage; undoubtedly by lengthening the arc column. This voltage increase is immediately apparent in the power measurements and within the range of variation of field strength that has been possible it appears that there is nearly a linear effect of magnetic field on power dissipation. Since the arc voltage was quite low for the measurements in question, the arc power proportionately follows the arc voltage so it can safely be inferred that there is a linear relation between arc voltage and magnetic field strength for the range of conditions considered. The data supporting this statement are shown in Figure 11. Here the chamber pressure was one atmosphere, the electrode spacing about one inch, and the magnetic field strength indicated on the abscissa is that field which existed at the approximate arc location as measured by a gaussmeter.

The arc stability is greatly affected by the presence of a magnetic field through the induced motion but no conclusive data are available on this phenomenon. The problem is being studied analytically at this time (Section III-A) and further experimental investigations will be made later in the program.
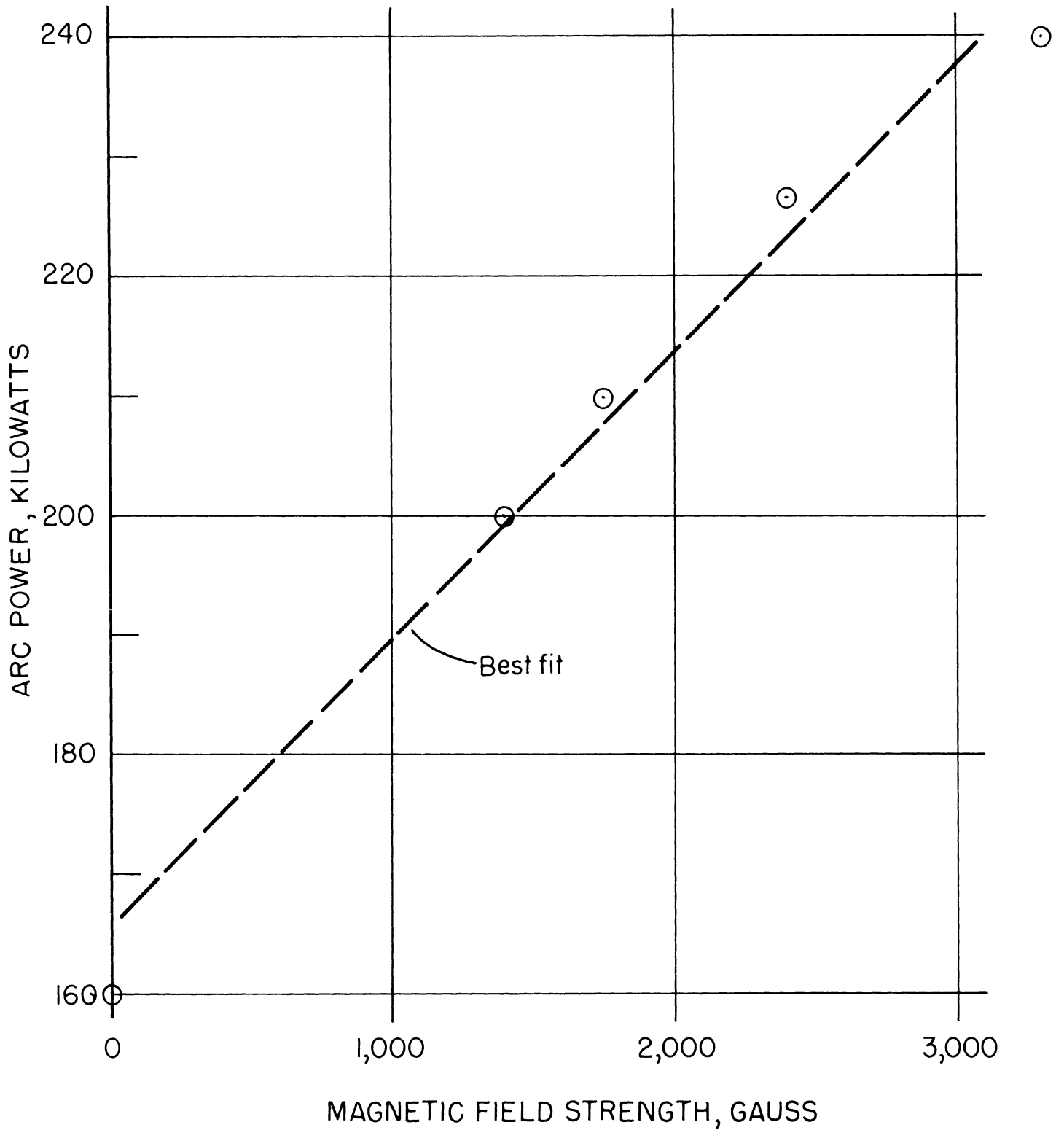
FIGURE II. EFFECT OF MAGNETIC FIELD STRENGTH
ON ARC POWER.

# B. UNIT EFFICIENCY AND ACHIEVABLE STAGNATION CONDITIONS

Since it is the prime function of an arc heater to produce a stream of high enthalpy gas all attention must inevitably focus on how well it performs this job. Disregarding for the moment questions of contamination and stability one must ask how much of the energy which is being added to the gas in the arc chamber eventually shows up in the gas stream which one wishes to study. This leads one to a study of how much energy is being extracted from the water cooled hardware of the system. One would, of course, like to minimize losses to the cooled components but in a high power device which must operate for periods of time greater than one minute a certain amount of water cooling is absolutely necessary. In the present facility water cooled electrodes are used to reduce effluent contamination and they seem to extract an almost fixed fraction of the arc power (about 25%). The exit nozzle, of course, must be water cooled but losses to that component have proved to be insignificant. The only other major component which extracts energy from the heated gas is the chamber or pressure vessel. This unit is a copper cylinder 20 inches long, with a 10 inch inside diameter and 1 1/2 inch thick walls. This is obviously quite a massive component and one would predict that it would rob the heated gas of much of its energy. The chamber has this particular size for a number of reasons. The original set of electrodes were patterned after those first used by General Electric and the internal diameter of the chamber, of course, had to be large enough to accommodate them. Second, it was felt that the nonuniformities in temperature and velocity which would be added to the flow by the arc heating process could be evened out only by the stilling effect of a rather long chamber. Hence, the seemingly undue length of the pressure vessel. It was recognized that flow uniformity would be obtained only at the expense of lower stagnation conditions but this was deemed unavoidable at that time. In brief, the chamber losses have proved to be excessive.

A rough analysis of the situation shows that one might expect rather severe losses to the chamber and also indicates to what extent they can be mitigated. Suppose the distance x is measured from the electrode location in the chamber and at x = S the hot gas has left the pressure vessel. If $\dot{q}_w$ is the heat transferred to the chamber walls at each axial station, x, H is the stagnation enthalpy of the flow, and D the internal diameter of the chamber, one can write the following differential equation

$$\frac{dH}{dx} = -\frac{\pi D}{\dot{w}}\dot{q}_w$$

where $\dot{w}$ is the mass rate of flow of the heated gas. The wall heat flux $\dot{q}_w$ will, in general, include radiative as well as convective contributions. The radiative component is not easy to express analytically in terms of chamber properties but according to Section V the convective heat transfer has the following form

$$\dot{q}_{con} = C_1 H/x^{1/2}$$

where $C_1$ is a function of chamber conditions and varies only slightly from end to end. Then the above differential equation can be written as

$$\frac{dH}{dx} + \frac{\pi DC_1}{\dot{w}}Hx^{-1/2} = \frac{-\pi D\dot{q}_{rad}}{\dot{w}}$$

where $\dot{q}_{rad}$ is assumed to be constant. This is easily integrated to give at x = S

$$H_f e^{aS^{1/2}} = H_i - \frac{\dot{q}_{rad}}{C_1 a}\left[e^{aS}(aS - 1) + 1\right]$$

where $H_i$ and $H_f$ are the enthalpies corresponding to conditions at x = 0 and x = S, respectively and a = $2\pi DC_1/\dot{w}$. For the arc chamber presently being used S $\cong$ 10 in., D = 10 in., and $\dot{w} \cong$ 0. 10 lb/sec. In Figure 12 the above expression for $H_f/H_i$ is plotted for two typical stagnation pressures, 15 atmospheres and 30 atmospheres.

19
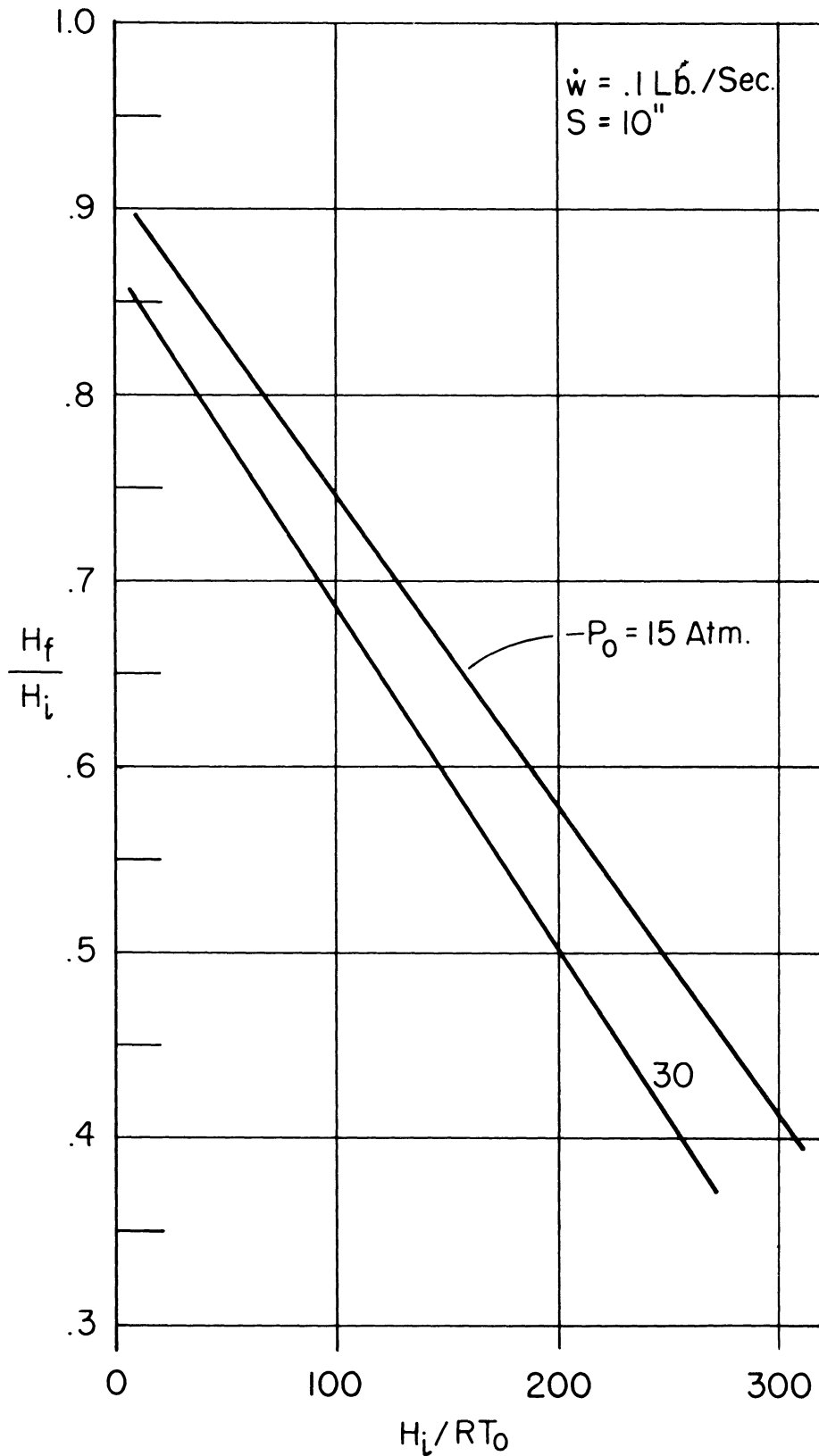
FIGURE 12. LOSS IN STAGNATION ENTHALPY TO
PRESSURE VESSEL.

It is seen that a large fraction of the energy initially imparted to the gas is extracted before the gas can reach the chamber exit, leaving a relatively cool effluent.

Consider now some typical measured results. Table I presents the results of six very typical arc heater runs. The greatest difference between these runs is that their duration varies considerably. Run number 8744 is the only true steady state run, that is all components reached their respective equilibrium temperature before the run was terminated. The results show quite clearly that about one minute must elapse before equilibrium running conditions will exist. The energy losses accountable to each major component are listed as well as the maximum energy input to the system. Electrical circuit conditions such as KVA consumed and power factor are also listed. The most dismal fact which is discernible from this table is that the unit efficiency, defined as arc power less power lost all divided by arc power, drops to 14% for steady conditions at about 6 atmospheres chamber pressure. There is some uncertainty in the air mass flow for these runs but it appears that the effluent produced under conditions for which run number 8744 is typical has a stagnation temperature which is less than $4000^{\circ}K$ but at least $3200^{\circ}K$. This is a large uncertainty but further measurements will refine the determination of this parameter.

One can obviously conclude that the amount of energy being claimed by the pressure vessel is intolerable and must be reduced. Toward this end new electrode configurations are being studied which will not require so large an enclosure and the chamber length on future arc heaters will certainly be less than in the present case.

Attention is called to the fact that up to now the maximum arc power has seldom exceeded one megawatt. Even with a low efficiency higher final stagnation conditions can be obtained if one simply adds more energy at the beginning. In fact, with the present highly lossy facility it should be possible to nearly double the stagnation enthalpy in this way.

21

## TABLE I

### TYPICAL ARC HEATER RUNS

| Run Number | Chamber Pressure (Atm) | Arc Power (Megawatts) | Circuit KVA | Power Factor | Power to Nozzle (kw) | Power to Electrodes (kw) | Power to Chamber (kw) | Total Losses to Components (kw) | System Efficiency % |
|---|---|---|---|---|---|---|---|---|---|
| 8637 | 12.2 | .98 | 1800 | .544 | 33.6 | 294 | 159 | 486 | 50.4 |
| 8739 | 9.5 | .83 | 1540 | .540 | 28.8 | 258 | 304 | 592 | 28.7 |
| 8740 | 9.0 | .84 | 1550 | .542 | 33.6 | 258 | 340 | 633 | 24.7 |
| 8741 | 9.5 | .84 | 1590 | .528 | 38.5 | 284 | 304 | 626 | 25.4 |
| 8742 | 7.4 | .82 | 1500 | .547 | 33.6 | 296 | 202 | 532 | 35.1 |
| 8744 | 6.3 | .91 | 1720 | .529 | 38.5 | 296 | 450 | 783 | 14.0 |

# III. THE ELECTRIC ARC IN A FLOWING ENVIRONMENT

Present day applications of the electric arc as a gas heater have led to the need for a better understanding of the interaction of the flowing stream and the arc column. This need arises, not only so that the enthalpy distribution in and around the arc can be predicted, but because the flow has a profound effect upon the stability of the arc discharge. Although this latter remark certainly applies to DC arcs the stability problems which exist for AC arcs are much more complex. In fact, a complete stability analysis of the non-linear system of equations offered by the dynamic arc has never been attempted. Only the method of small disturbances introduced by Kauffmann (4) has been employed with any success. This method assumes that small AC perturbations are imposed upon an otherwise stable steady-state discharge and by examining the roots of a secular equation one can obtain sufficient conditions for complete stability. These conditions thus obtained are only necessary to cause instability but not, unfortunately, sufficient since one cannot say whether disturbances which seem to cause instability for a linear problem will indeed lead to arc extinction when the amplitude of the disturbances has grown too large to be considered linear. Of course, these same considerations apply in the study of the stability of any non-linear system. Perhaps the advanced techniques of Liapunov which have been used so successfully in the study of non-linear control systems could be applied to the present problem but this has not as yet been investigated.

Presented herein is a first attempt at an understanding of the behavior of the dynamic arc which is subjected to two simple flow configurations. The first is an analysis of the arc in cross-flow (convection determined arc), that is, normal to its axis. Here an extention of the method used by Rother (5) is employed and it will be seen that even for the simple flow field that is assumed the problem is quite complex.

The second problem concerns an AC arc burning in a tube (wall stabilized arc) with a flow along the axis of the tube. Here, following the approach of Stine and Watson (6), one can show that the behavior of the arc as it approaches the fully developed column can be predicted, as well as the ultimate character of the asymptotic column. It should be borne in mind, however, that both of these models are quite crude and their shortcomings will be pointed out at appropriate instances.

## A. THE DYNAMIC ARC IN CROSS-FLOW

It is well known that when an electrode stabilized arc is blown normal to the arc axis the column assumes a new shape which is determined by the flow velocity and the nature of the gas which comprises the discharge. For moderate blowing this new shape is nearly circular and one may characterize the column geometry by a radius of curvature, $\rho$. Furthermore, the distortion of the electric field due to the blowing may be determined by assuming that the field lines follow the arc and that, since the integral of $\vec{E} \cdot \vec{ds}$ along any path through the arc and between the electrodes is constant, the field strength will be greater on the concave (windward) side of the arc than on the convex side (leeward). Figure 13, which follows, illustrates this situation. Here one sees that the electrode axis is along the coordinate axis and that the blowing is along the x axis from left to right. The radius of curvature, $\rho$, is not known a priori but must be determined from a solution of the problem to be posed. It is assumed now that the cross-section A - A is characteristic of the entire arc since it is there that the velocity has its full component. Then this region should determine the stability of the entire column since energy removal processes by convection are the most severe there. It is simple to show that the field strength in the Section A - A can be represented by $E = E_o/(1 + x/\rho)$, where $E_o$ is the field strength at x = 0. Eventually it will be
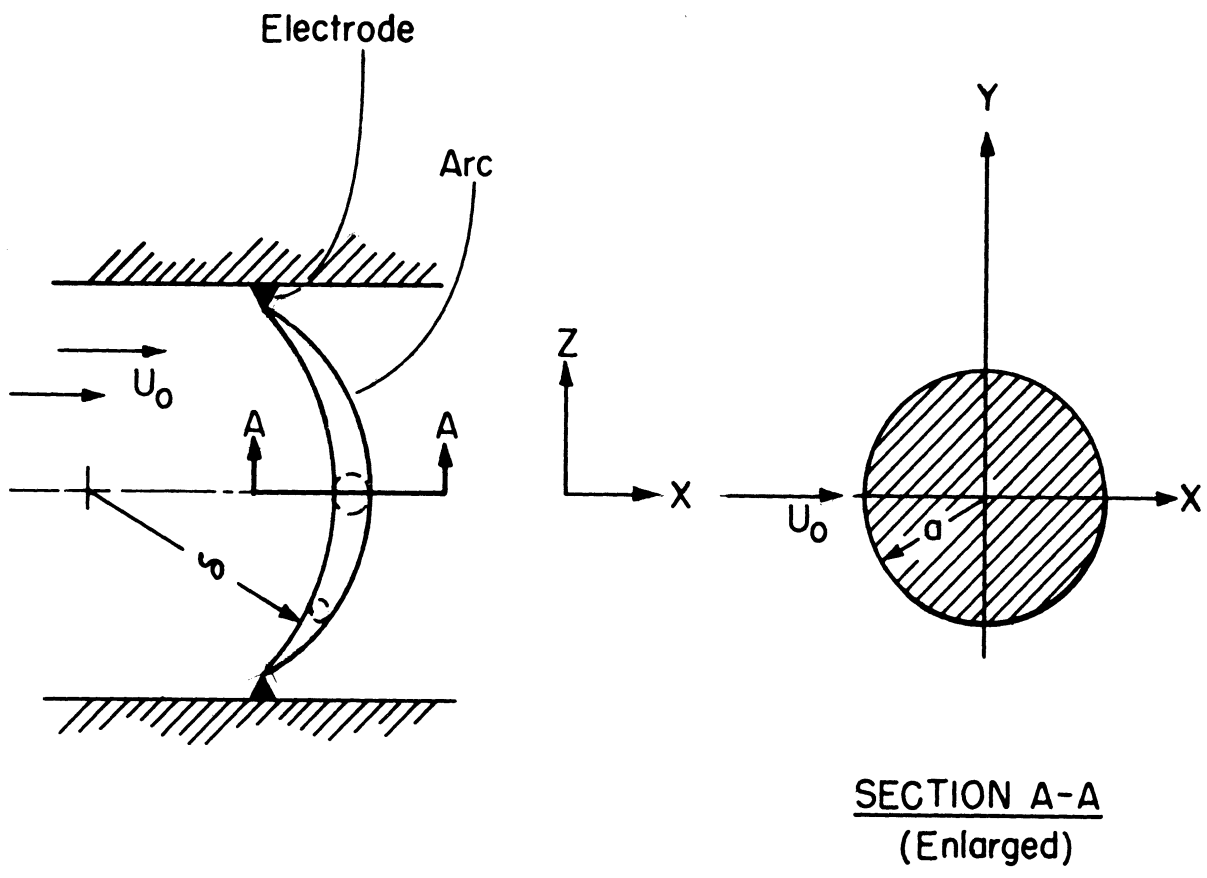
FIGURE 13. SKETCH OF BLOWN ARC COORDINATE SYSTEM.

necessary to assume that Joule heat can only be produced within a circle of radius "a" (essentially the arc radius) but the analysis can be carried up to a point with greater generality and this assumption will not be invoked until necessary.

One proceeds now by writing an energy equation for the arc and its surroundings which includes the effects of convection. Subsequent developments assume that thermodynamic equilibrium prevails everywhere, a quite justifiable assumption for the pressures (greater than one atmosphere) and the alternation frequencies (of the order of a kilocycle or less) which shall be of interest here. Neglecting diffusion of species due to mechanisms such as baro- and thermal-diffusion as well as that due to concentration gradients implies that thermal conduction and forced convection are the dominant modes of energy transfer. Again, this is easily justified.

In vector notation the energy equation becomes:

$$\eta \left\{ \frac{\partial h}{\partial t} + \vec{U} \cdot \nabla h \right\} - \nabla \cdot (\kappa \nabla T) = \sigma E^2 \; (x, t) \tag{3-1}$$

Here $\eta$ is the mass density, h the static enthalpy, $\kappa$ and $\sigma$ the thermal and electrical conductivities respectively, and $\vec{U}$ is the velocity vector of the imposed flow field. To be precise one should also write the equations of conservation of mass and momentum as well as an equation of state. This would, however, lead to insurmountable complexities so, as usual, one makes some rather stringent assumptions. Here it is assumed $\vec{U}$ has a component along the x-axis only and is constant at a value $U_o$. Before making further simplifications notice that the Equation (3-1) is made far more tractable by introducing the transformation

$$S = \int_{T_o}^{T} \kappa \, dT'$$

where S is often called the heat flux potential and $T_o$ is some convenient reference temperature. Then, since $dh = c_p \, dT$, one can write Equation (3-1) in the form:

26

$$\eta \, \frac{c_p}{\kappa} \left( \frac{\partial S}{\partial t} + \vec{U}_o \cdot \nabla S \right) - \nabla^2 S = \sigma E^2 \ (x, t)$$

where $c_p$ is the specific heat at constant pressure. The group of parameters $(\eta \, c_p / \kappa)$ is the reciprocal of what is commonly known as the thermal diffusivity and is not, strictly speaking a constant. However, its variation with S, the new dependent variable, is not severe over rather wide ranges of temperature so that it will be assumed to be constant at some representative value. Defining $\lambda = \kappa / \eta \, c_p$ one can write the above equation in cartesian coordinates

$$\frac{1}{\lambda} \left( \frac{\partial S}{\partial t} + U_o \frac{\partial S}{\partial x} \right) - \frac{\partial^2 S}{\partial x^2} - \frac{\partial^2 S}{\partial y^2} = \sigma E^2 \ (x, t)$$

Finally, one assumes that the complex dependence of $\sigma$ upon S can be legitimately mitigated by assuming a linear relationship between the two variables. Then write

$$\sigma = C_1 S + C_2$$

and introduce for facility of computation $\alpha(x, t) = C_1 E^2 \ (x, t)$ and $4\pi f \ (x, t) = C_2 E^2 \ (x, t)$. The equation then assumes the form:

$$\frac{\partial^2 S}{\partial x^2} + \frac{\partial^2 S}{\partial y^2} - \frac{U_o}{\lambda} \frac{\partial S}{\partial x} - \frac{1}{\lambda} \frac{\partial S}{\partial t} + \alpha(x, t) S = - 4\pi f (x, t) \tag{3-2}$$

This equation must be solved subject to the initial condition $S \ (x, y, 0) = S_o$ and the boundedness condition,

$$\lim_{|x|, \ |y| \to \infty} S \ (x, y, t) = 0 \quad .$$

Notice that if a non-zero temperature exists at infinity a simple transformation will bring the problem into the above form. Now the problem is facilitated by transforming out the term involving $\partial S / \partial x$ and this is done by introducing

$$S = \psi \, e^{\frac{U_o}{2\lambda} x}$$

27

This casts Equation (3-2) into the form

$$\frac{\partial^2 \psi}{\partial x^2} + \frac{\partial^2 \psi}{\partial x^2} - \frac{1}{\lambda} \frac{\partial \psi}{\partial t} + \left[ \alpha(x, t) - \frac{U_o^2}{4\lambda^2} \right] \psi = - 4\pi e^{-\frac{U_o x}{2\lambda}} f(x, t) \qquad (3-3)$$

Since Equation (3-3) applies in the infinite domain and there are no boundaries it is possible to find a Green's function by the method of multiple fourier integrals (Reference 4). In the following, $g(R, \tau)$ denotes the Green's function where $R = |\vec{r} - \vec{r}_o|$, the distance between source and field points, and $\tau = (t - t_o)$, the time between source emission and field observation. This Green's function must satisfy the equation

$$\nabla^2 g - \frac{1}{\lambda} g_t + \left[ \alpha(R, \tau) - \frac{U_o^2}{4\lambda^2} \right] g = - 4\pi \delta(\vec{R}) \delta(\tau) \qquad (3-4)$$

where the continuous function $\exp(-U_o x/2\lambda) f(x, t)$ is replaced by a product of delta "functions", $\delta(\vec{R}) \cdot \delta(\tau)$. Next one assumes that $g(R, \tau)$ has the form

$$g(R, \tau) = \frac{1}{(2\pi)^2} \int e^{i\vec{p} \cdot \vec{R}} \gamma(\vec{p}, \tau) \, dV_p$$

where $dV_p$ is the volume element in $\vec{p}$-space which is two dimensional in this case. Applying the operator of Equation (3-4) to the above Fourier integral one obtains

$$\frac{1}{4\pi^2} \int e^{i\vec{p} \cdot \vec{R}} \left\{ - p^2 \gamma - \frac{1}{\lambda} \frac{d\gamma}{d\tau} + \left[ \alpha(R, \tau) - \frac{U_o^2}{4\lambda^2} \right] \gamma \right\} dV_p = - 4\pi \delta(\vec{R}) \delta(\tau)$$

However it is known that

$$\frac{1}{4\pi^2} \int e^{i\vec{p} \cdot \vec{R}} dV_p = \delta(\vec{R})$$

28

so one can write

$$\frac{d\gamma}{d\tau} + \lambda \left[ p^2 - \alpha(R, \tau) + \frac{U_o^2}{4\lambda^2} \right] \gamma = 4\pi\lambda\delta(\tau)$$

This is a first order, ordinary differential equation for $\gamma(p, \tau)$ whose solution is easily found to be

$$\gamma(p, \tau) = 4\pi\lambda\, u(\tau) \exp\left[ -\lambda\tau\left(p^2 + \frac{U_o^2}{4\lambda^2}\right) + \lambda \int_0^\tau \alpha(R, \xi)\, d\xi \right]$$

where the properties of the $\delta$ function and the unit step function $u(\tau)$ have been employed; namely

$$u(\tau) = \int_{-\infty}^\tau \delta(\xi)\, d\xi = \begin{cases} 0, & \tau < 0 \\ 1, & \tau > 0 \end{cases}$$

and

$$\int_{-\infty}^\tau h(\xi)\, \delta(\xi)\, d\xi = u(\tau)\, h(0)$$

where h is any function $\xi$. Finally the expression for the Green's function becomes:

$$g(R, \tau) = \frac{\lambda u(\tau)}{\pi} \exp\left[ -\lambda\left(\frac{\tau U_o^2}{4\lambda^2} - \int_0^\tau \alpha(R, \xi)\, d\xi\right) \right] \int dV_p \exp\left[ i\vec{p}\cdot\vec{R} - \lambda\tau\vec{p}\cdot\vec{p} \right]$$

This can be integrated to yield

$$g(R, \tau) = \frac{u(\tau)}{\tau} \exp\left[ -\lambda\left(\frac{\tau U_o^2}{4\lambda^2} - \int_0^\tau \alpha(R, \xi)\, d\xi\right) \right] e^{-\frac{R^2}{4\lambda\tau}} \qquad (3\text{-}5)$$

29

which is the Green's function being sought. Notice that even though the original Equation (3-3) is written in cartesian coordinates the Green's function is quite general and is not tied to any specific coordinate system. By superposition of sources one can write the general solution of Equation (3-3) as

$$\psi(x, y, t) = \int_0^t dt_0 \int dx_0 \, dy_0 \, e^{\frac{U_0 x_0}{2\lambda}} f(x_0, t_0) \, g\left[(x - x_0), (y - y_0), (t - t_0)\right]$$

$$+ \frac{1}{4\pi\lambda} \int dx_0 \, dy_0 \, [\psi g]_{t_0 = 0} \quad .$$

The second term in the right hand member represents the effects of initial conditions and will henceforth be neglected since one is only interested in the quasi-steady state. Notice that the original differential equation has been cast into the form of an integral equation by introducing the notion of the Green's function. Such is always the case when one solves a differential equation in this manner and even though the resulting integral equation is not readily solvable there is a wider variety of methods available to attack it.

At this point it is suitable to introduce specific functions for $\alpha$ and f. Recall that the variation in electric field strength through an arc which is blown into a circular shape is given by

$$E(x, t) = E_0(t)/(1 + x/\rho)$$

Now presume further that the curvature is slight ($\rho$ large) so that one can write

$$\alpha(R, \xi) \cong C_1 E_0^{\,2} (\xi) \left[1 - 2 \left(r \cos \theta - r_0 \cos \theta_0\right)/\rho\right]$$

$$4\pi f(t_0) \cong C_2 E_0^{\,2} (t_0) \left(1 - 2 \, r_0 \cos \theta_0/\rho\right)$$

Here, in anticipation of further assumptions cylindrical coordinates have been introduced and as before the subscript ( )$_0$ on r and $\theta$ denotes source coordinates.

As was mentioned earlier it is now necessary to assume that Joule heat is produced only within a circle of radius "a" so that the limits of integration are from 0 to $2\pi$ for $\theta_o$ and from 0 to a for $r_o$. Introducing the necessary transformations one finds that the Green's function assumes the form:

$$e^{-\dfrac{U_o r_o \cos \theta_o}{2\lambda}} g(R,\tau) = \frac{e}{\tau} e^{-\frac{r^2}{4\lambda\tau}} \exp \left\{ -\frac{2\lambda A(\tau) r \cos \theta}{\rho} - \lambda \left[ \frac{\tau U_o^2}{4\lambda^2} - A(\tau) \right] \right.$$

$$\left. -\frac{r_o^2}{4\lambda\tau} - \left[ \frac{U_o}{2\lambda} - \frac{2\lambda A(\tau)}{\rho} \right] r_o \cos \theta_o + \frac{r r_o}{2\lambda\tau} \cos (\theta - \theta_o) \right\}$$

where $A(\tau) = \displaystyle\int_0^\tau C_1 E_o^2 (\xi)\, d\xi$. The required integration over the source coordinates is rather tedious and only the final results are presented here. The solution can be written as

$$\psi(r,\theta,t) = \mathscr{L}_1 + \mathscr{L}_2$$

where

$$\mathscr{L}_1 = \lambda C_2 \int_0^t dt_o E_o^2 (t_o) e^{-\frac{r^2}{4\lambda\tau}} \exp \left\{ -\lambda \left[ \frac{2A(\tau)}{\rho} r \cos \theta + \frac{U_o^2 \tau}{4\lambda^2} A(\tau) \right] \right\}$$

$$\times e^{\mu^2} [1 - J(\gamma^2, \mu^2)]$$

$$\mathscr{L}_2 = \frac{2\lambda C_2}{\rho} \int_0^t dt_o E_o^2 (t_o) e^{-\frac{r^2}{4\lambda\tau}} \exp \left\{ -\lambda \left[ \frac{2A(\tau)}{\rho} r \cos \theta + \frac{U_o^2 \tau}{4\lambda^2} - A(\tau) \right] \right\}$$

$$\times \frac{W}{Z} \left\{ a I_1 (Za) e^{-\frac{a^2}{4\lambda\tau}} - 2\lambda\tau e^{\mu^2} [1 - J(\gamma^2, \mu^2)] \right\}$$

(3-6)

31

There are several new relationships that must be defined:

$$\mu^2 = \frac{r^2}{4\lambda\tau}\left\{\left[\cos\theta - \frac{2\lambda\tau}{r}\left(\frac{U_o}{2\lambda} - \frac{2\lambda A(\tau)}{\rho}\right)\right]^2 + \sin^2\theta\right\}$$

$\gamma^2 = a^2/4\lambda\tau$ and $J(\gamma^2, \mu^2)$ is a function which has often been called the offset circle probability function. It is defined by the following equation:

$$\int_0^\gamma \nu e^{-\nu^2} I_o(2\mu\nu)\, d\nu = \frac{1}{2}e^{\mu^2}\left[1 - J(\gamma^2, \mu^2)\right]$$

wherein $I_o$ is the modified Bessel function of the first kind. Furthermore

$$W = \left\{\frac{r\cos\theta}{2\lambda\tau} - \left[\frac{U_o}{2\lambda} - \frac{2\lambda A(\tau)}{\rho}\right]\right\}$$

$$Z = \left\{\left[\frac{r\cos\theta}{2\lambda\tau} - \left(\frac{U_o}{2\lambda} - \frac{2\lambda A(\tau)}{\rho}\right)\right]^2 + \left(\frac{r\sin\theta}{2\lambda\tau}\right)^2\right\}^{\frac{1}{2}}$$

It would be quite superfluous to point out the extreme complexity of the above solution and it should be borne in mind that there yet remains an integration over the variable $t_o$ to be performed. It appears that this cannot be done in general but that some sort of asymptotic expansion for large t and large $U_o$ must be employed. An extreme simplification results when $\rho \to \infty$ or the arc does not bend in response to the flow. This situation has been rather exhaustively studied and it can be shown that there is no physical meaning connected with it except that it could result when $U_o = 0$. However, the present model displays a weakness in this instance because it provides no mechanism for thermal stabilization of the arc column. This is not too serious since even a small velocity provides a thermally stable arrangement and should yield reasonable results. The failure of the zero curvature case with non-vanishing velocity can be laid to the fact that

no intensification of field strength is provided to balance the convective cooling on the concave side of the arc. Hence the position of maximum temperature resides at the edge of the arc which gives a meaningless situation. Allowing for some curvature remedies this situation and, in fact, the radius of curvature, $\rho$, is determined by applying the condition that the value of S is a maximum at the origin.

The analysis has progressed no farther at this time but the next step will be to find the radius of curvature as a function of the most significant parameters and to find a perturbation solution which would allow an investigation of the stability of the blown arc by the method of small disturbances. It seems, however, that a complete solution to Equation (3-6) will have to be obtained with the aid of an electronic computer.

## B. THE DYNAMIC ARC IN AXIAL FLOW

An arc/flow arrangement of as much importance as the cross-flow situation is provided by a discharge through a well defined cylindrical tube through which gas is also flowing. In general, if one considers entrance effects, this is a very difficult problem and even when an arc is not present the fluid dynamics problem is rather formidable. Eventually, several tube diameters from the entrance, a fully developed Poiseuille flow is attained at which point the flow field and temperature field are decoupled. However, the velocity profile is still dependent upon the temperature distribution through the variable viscosity. Up to this point the energy and momentum equations must be solved simultaneously in order to arrive at the proper distribution of velocity and temperature.

Recently, Stine and Watson (6) have analyzed the DC arc in a tube and after making many simplifying assumptions arrived at a fairly simple relationship between the important parameters of the problem. Successive experimental investigations to test the validity of this analysis have shown it to be amazingly good

for a very wide range of conditions. This fact prompted a similar analysis of the AC arc column with the hope that certain salient features of the arc behavior would emerge.

In Reference 6 is presented a figure which serves to classify the various portions of the arc discharge and indicates what type of analysis applies to each part. This figure is reproduced herein as Figure 14. The region immediately adjacent to the electrode contains a space charge zone and there is no known analysis which could apply. As the arc begins to spread and fill the constricting tube, deviations from charge neutrality are slight but the fluid dynamics problem is very difficult. Chen (8) has performed an approximate analysis of this portion of the arc but it is applicable only to a continuously spreading arc and hence breaks down as the discharge approaches the wall. Shortly downstream of where Chen's model fails the model of Stine and Watson begins to be valid. Eventually, the so-called asymptotic column is attained and in the case of the DC arc many good analyses exist for this region. For the dynamic arc even the asymptotic column is not well understood but several crude analyses have been attempted. Herein is presented an approximate analysis of the transition region from the point where spreading stops to the asymptotic column position for an AC arc. Many of the same assumptions that Stine and Watson have used apply in this case as well as the further assumption that the arc is fed by a current source and is therefore stable. Briefly, one assumes that the electric potential is constant on planes normal to the flow direction, that axial conduction is small compared to convection, the arc has a constant radius, $\rho$, kinetic energy changes are small compared to static enthalpy changes, radiation is negligible, the electrical conductivity can be represented as a linear function of the heat flux potential, S, and the thermal diffusivity, $\lambda$, is constant. With these simplifications one obtains the following form of the Ebenbaas-Heller
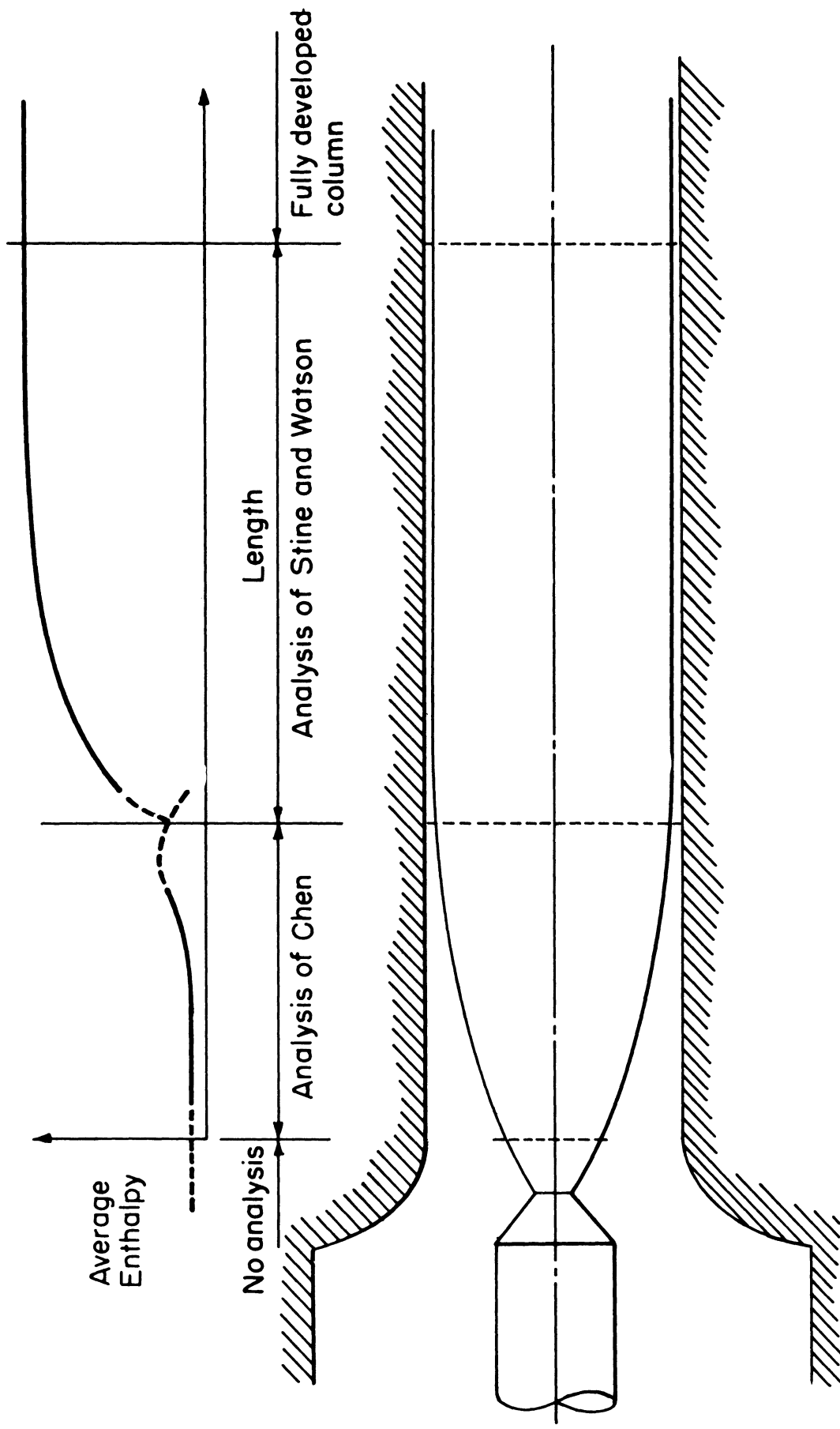
FIGURE 14. IMPORTANT REGIONS OF AXIAL ARC.

equation

$$\frac{1}{r}\frac{\partial}{\partial r}\left[r\frac{\partial S}{\partial r}\right] - \frac{U_o}{\lambda}\frac{\partial S}{\partial z} + \frac{I^2 S}{\left[4\pi^2 B\left[\int_0^\rho rS\,dr\right]\right]^2} = \frac{1}{\lambda}\frac{\partial S}{\partial t} \qquad (3-7)$$

Here $S = S_1 + \int \kappa\,dT$, $U_o$ is the flow velocity down the tube, I is the total current through the arc, and B is a constant which appears in the linear approximation to the electrical conductivity; $\sigma = B\,(S - S_1)$. The above equation can be solved by combining the techniques of separation of variables and the Laplace transformation. Equation (3-7) is valid in the domain $0 \leq r \leq \rho$, $t > 0$, $z \geq 0$ and has the boundary conditions that when $r = \rho$, $S = 0$ and $S(r, 0, t) = 0$. Then since the equation and its boundary conditions are homogeneous one can assume a solution of the form:

$$S\,(r, z, t) = P\,(z, t)\,R\,(r)$$

Inserting this form into Equation (3-7) one obtains

$$\frac{1}{r}\frac{(rR')'}{R} = \frac{1}{\lambda P}\frac{\partial P}{\partial t} + \frac{U_o}{\lambda P}\frac{\partial P}{\partial z} - \frac{I^2(t)}{\left[4\pi^2 B\left[\int_0^\rho r\,R\,dr\right]\right]^2}\cdot\frac{1}{P^2} = -\alpha^2$$

where $\alpha^2$ is a separation constant and $(\ )' = d/dr$. Then the above equation yields the two equations

$$(rR')' + \alpha^2 rR = 0 \qquad (3-8a)$$

$$\frac{1}{\lambda}\frac{\partial P^2}{\partial t} + \frac{U_o}{\lambda}\frac{\partial P^2}{\partial z} + 2\alpha^2 P^2 = \frac{I^2(t)}{\left[2\pi^2 B\left[\int_0^\rho r\,R\,dr\right]\right]^2} \qquad (3-8b)$$

36

Equation (3-8a) is easily solved in terms of Bessel functions and since the solution must be well behaved at r = 0 one obtains simply

$$R(r) = J_0(\alpha r)$$

Furthermore, since $S(\rho, z, t) = 0$ for all z and t one finds that

$$J_0(\alpha \rho) = 0$$

so that $(\alpha \rho)$ is the first zero of the Bessel function which shall be denoted by $\beta_1$. Finally

$$R(r) = J_0(\beta_1 \, r/\rho)$$

For use in Equation (3-8b) one evaluates the integral appearing therein as:

$$\int_0^\rho r \, R \, dr = \int_0^\rho r \, J_0\left(\beta_1 \frac{r}{\rho}\right) dr = \frac{\rho^2}{\beta_1} J_1(\beta_1)$$

Now for convenience introduce $W(z, t) = P^2(z, t)$ and consider the following partial differential equation:

$$W_t + U_0 W_z + \frac{2\lambda \beta_1^2}{\rho^2} W = \frac{\lambda \beta_1^2 \, I^2(t)}{2\pi^2 B \rho^4 J_1^2(\beta_1)} \tag{3-9}$$

This equation may be solved with the help of the Laplace transform with respect to t and since $S(r, z, o) = 0$ one obtains

$$p w(z, p) + U_0 \frac{d}{dz} w(z, p) + \frac{2\lambda \beta_1^2}{\rho^2} w(z, p) = k(p)$$

where

$$w(z, p) = \mathcal{L}[W(z, t)] = \int_0^\infty e^{-pt} W(z, t) \, dt$$

and

$$k(p) = \mathscr{L}\left[\frac{\lambda \beta_1^2 I^2(t)}{2\pi^2 B\rho^4 J_1^2(\beta_1)}\right] .$$

Now one is confronted with a simple, ordinary, first order differential equation for $w(z, p)$ where p is simply a parameter. Since $S(r, o, t) = 0$ one must set $w(o, p) = 0$ and obtain

$$w(z, p) = \frac{k(p)}{\left(p + \frac{2\lambda \beta_1^2}{\rho^2}\right)}\left\{1 - \exp\left[-\left(p + \frac{2\lambda \beta_1^2}{\rho^2}\right)\frac{z}{U_o}\right]\right\} \qquad (3\text{-}10)$$

Using the theory of the convolution integral one can invert Equation (3-10) and find

$$W(z, t) = \int_0^t e^{-\frac{2\lambda \beta_1^2}{\rho^2}(t - \tau)} K(\tau)\, d\tau - e^{-\frac{2\lambda \beta_1^2}{\rho^2 U_o}z}\int_0^t e^{-\frac{2\lambda \beta_1^2}{\rho^2}(t - \tau)} K\left(\tau - \frac{z}{U_o}\right) d\tau$$

where $K(\tau - z/U_o) = 0$ for $\tau < z/U_o$ and for convenience

$$K(\tau) = \frac{\lambda \beta_1^2 I^2(\tau)}{2\pi^2 B\rho^4 J_1^2(\beta_1)}$$

38

Recalling that $P \equiv W^{1/2}$ one can write the solution to Equation (3-7) as

$$S(r,z,t) = \sqrt{\frac{\lambda}{2B}} \frac{\beta_1 J_o\left(\beta_1 \frac{r}{\rho}\right)}{\pi \rho^2 J_1(\beta_1)} \left[ \int_0^t e^{-\frac{2\lambda\beta_1^2}{\rho^2}(t-\tau)} I^2(\tau) d\tau \right.$$

$$\left. - e^{-\frac{2\lambda\beta_1^2}{\rho^2 U_o}z} \int_0^t e^{-\frac{2\lambda\beta_1^2}{\rho^2}(t-\tau)} I^2\left(\tau - \frac{z}{U_o}\right) d\tau \right]^{1/2} \qquad (3\text{-}11)$$

Equation (3-11) is an expression which relates the internal structure (S distribution) of the arc to the nature of the gas which comprises it (through $\lambda$, B, and $S_1$), the geometry of the tube which encloses it, (through $\rho$) and the current which is imposed upon it. Although it is not necessary at this point to assume a current waveform (one could write a circuit equation and allow the current to determine itself), it will be instructive to assume the arc sees a current source of strength $I_o \sin \omega t$. First, however, notice that by using Ohm's Law,

$$2\pi BE \int_0^\rho rS(r,z,t) dr = I \quad ,$$

one can obtain an expression for the local electric field strength in the arc column. This is found to be:

$$\left|\frac{I}{E}\right|^2 = 2\lambda B \left[ \int_0^t e^{-\frac{2\lambda\beta_1^2}{\rho^2}(t-\tau)} I^2(\tau)d\tau - e^{-\frac{2\lambda\beta_1^2}{\rho^2}\left(\frac{z}{U_o}\right)} \int_0^t e^{-\frac{2\lambda\beta_1^2}{\rho^2}(t-\tau)} I^2\left(\tau - \frac{z}{U_o}\right)d\tau \right]$$

$$(3\text{-}12)$$

Then specializing to the asymptotic column $(z \to \infty)$ one obtains the expression

$$\frac{I^2}{E^2} = \frac{2\lambda BI_o^2}{\omega} \int_0^{\omega t} e^{-\frac{2\lambda\beta_1^2}{\omega\rho^2}\omega(t-\tau)} \sin^2(\omega\tau)\, d(\omega\tau)$$

Upon integrating this expression one obtains:

$$\sqrt{\frac{\lambda B\Theta}{2}}\, E = \frac{\sin \omega t}{\sqrt{1 - \sin\delta\,\sin(2\omega t + \delta)}} \tag{3-13}$$

where $\Theta = \rho^2/\lambda\,\beta_1^2$ and $\delta = \cot^{-1}(\omega\,\Theta)$. This function is plotted in Figures 15 through 18 for several values of $(\omega\,\Theta)$. One can think of $\Theta$ as being the time constant characteristic of the arc/tube system. If the product $\omega\Theta$ is very small, implying either a small applied frequency or a small time constant, the arc is able to follow all fluctuations without any appreciable lag and adjust its internal structure accordingly. As $\omega\Theta$ becomes larger there is a lag in the thermal behavior of the arc column with respect to the forcing function until the frequency, $\omega$, becomes so large that the arc cannot follow the current input at all. At this point the arc behaves as an Ohmic resistor and displays an E - I characteristic with the expected positive slope.

Unfortunately, the waveforms of instantaneous voltage across the arc do not correspond to reality at intermediate values of $\omega\Theta$. Consider Figure 19 which is an oscillogram of the column potential of an arc burning in nitrogen with an RMS current of about 30 amperes. The upper waveform is the arc current and it is immediately evident that the arc does not see a current source but is profoundly influencing the current in the circuit. Nevertheless, the voltage waveform is typical and one should notice particularly the two peaks which occur every half cycle. The one which occurs at the beginning of the cycle is called the reignition peak and arises due to the cooling of the arc column during the current zero passage. There is also an extinction peak occurring just before polarity reversal
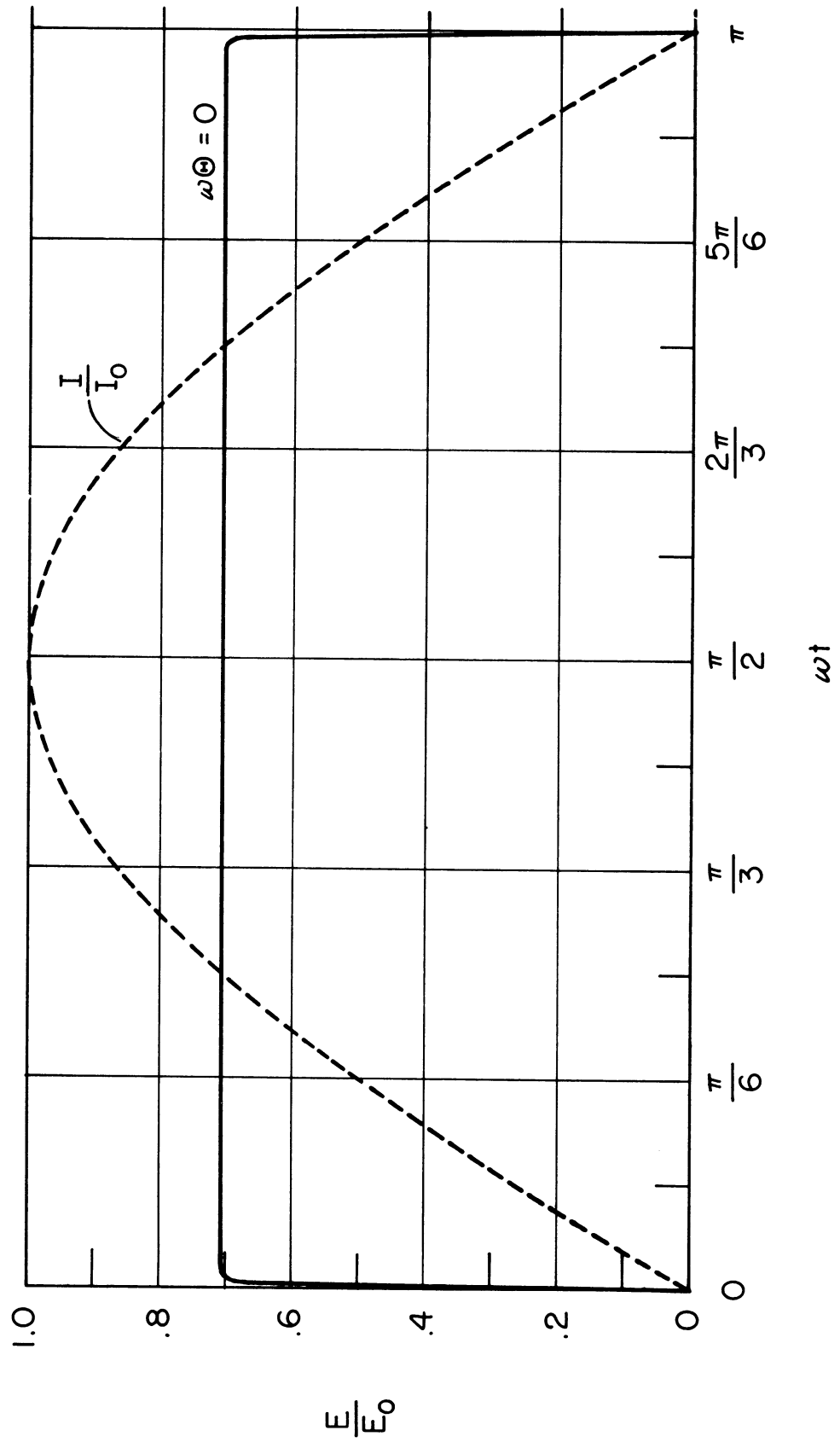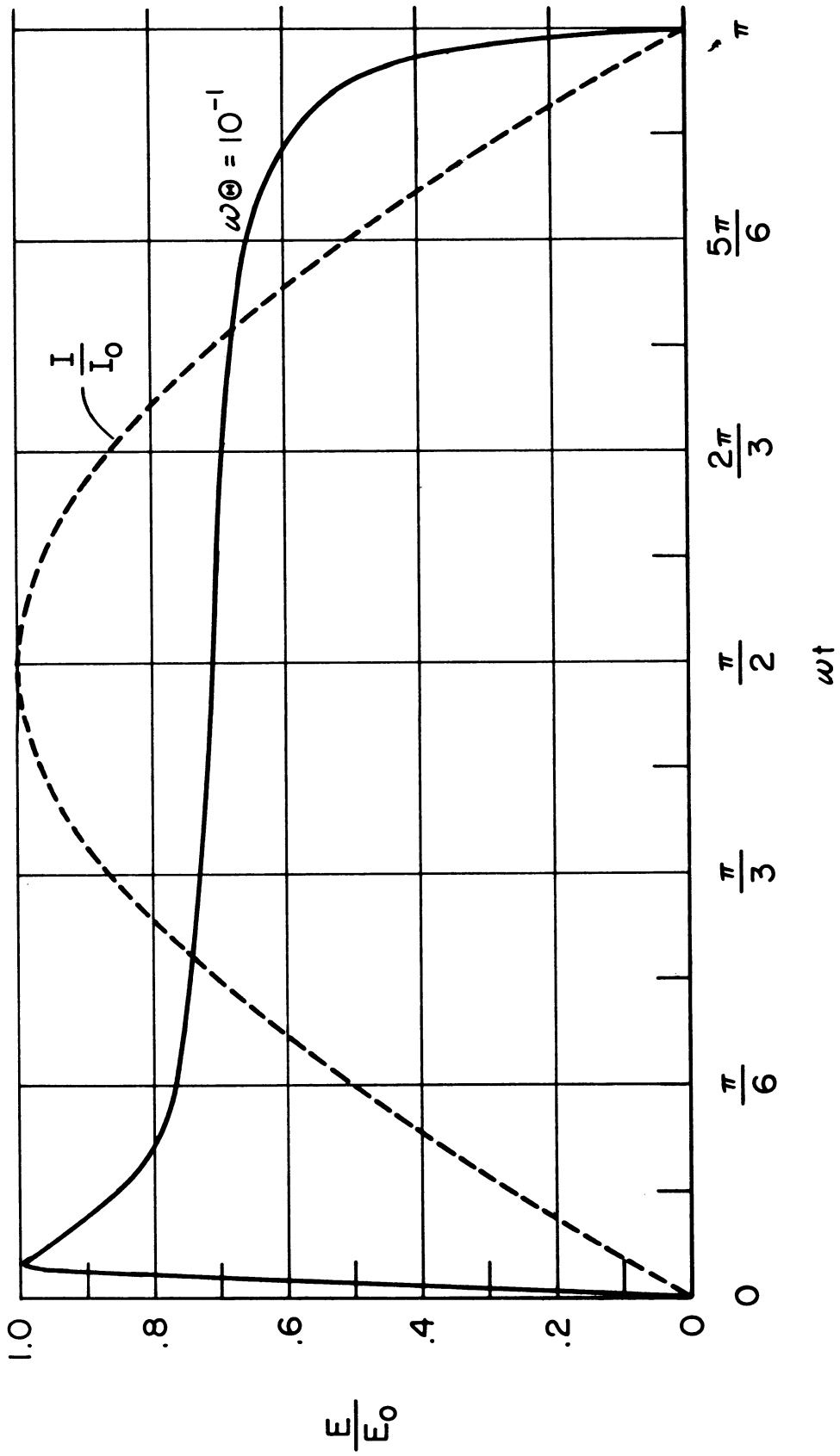
FIGURE I5. ASYMPTOTIC AC ARC COLUMN.

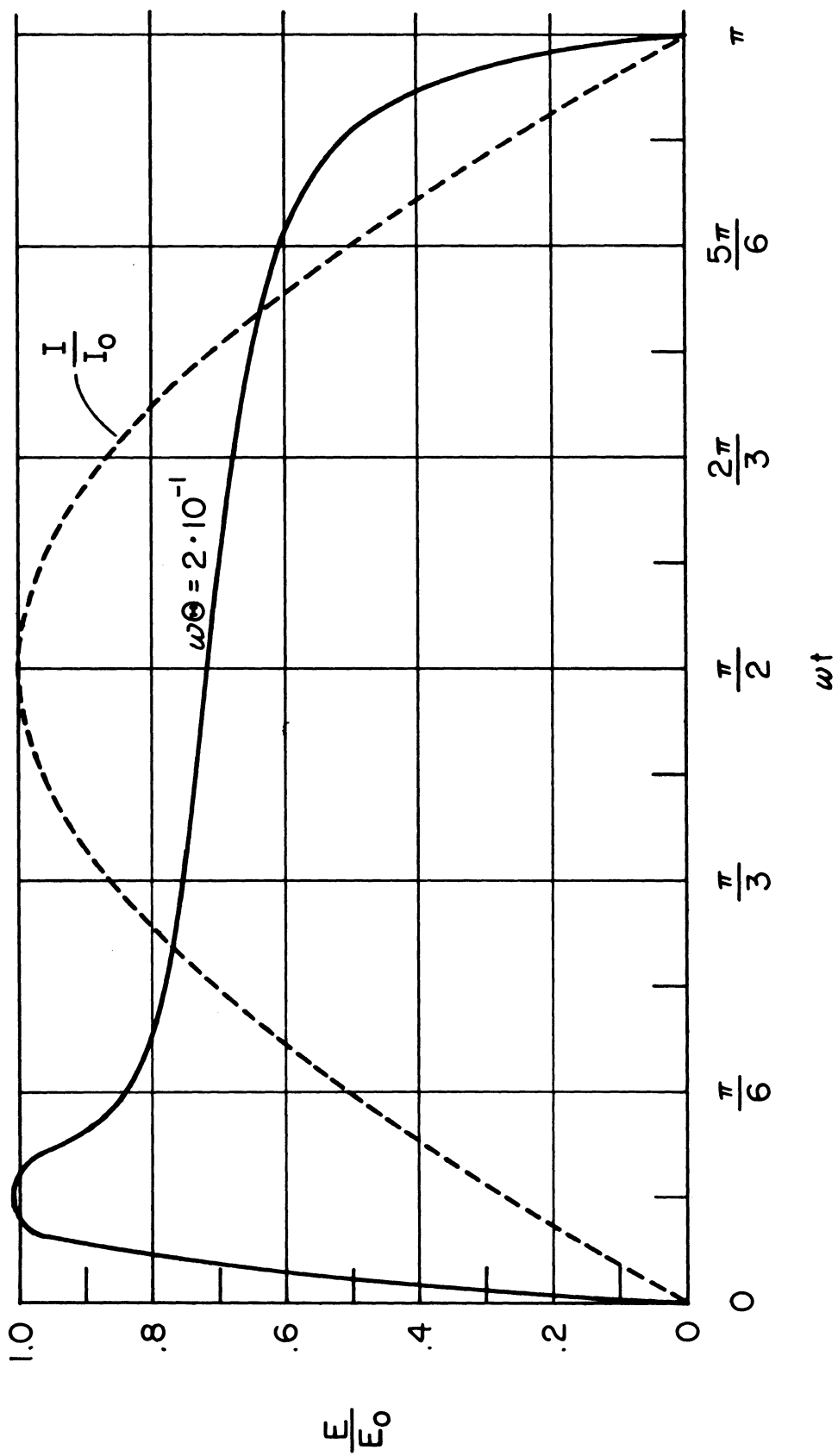FIGURE 16. ASYMPTOTIC AC ARC COLUMN.

42

FIGURE 17. ASYMPTOTIC AC ARC COLUMN.
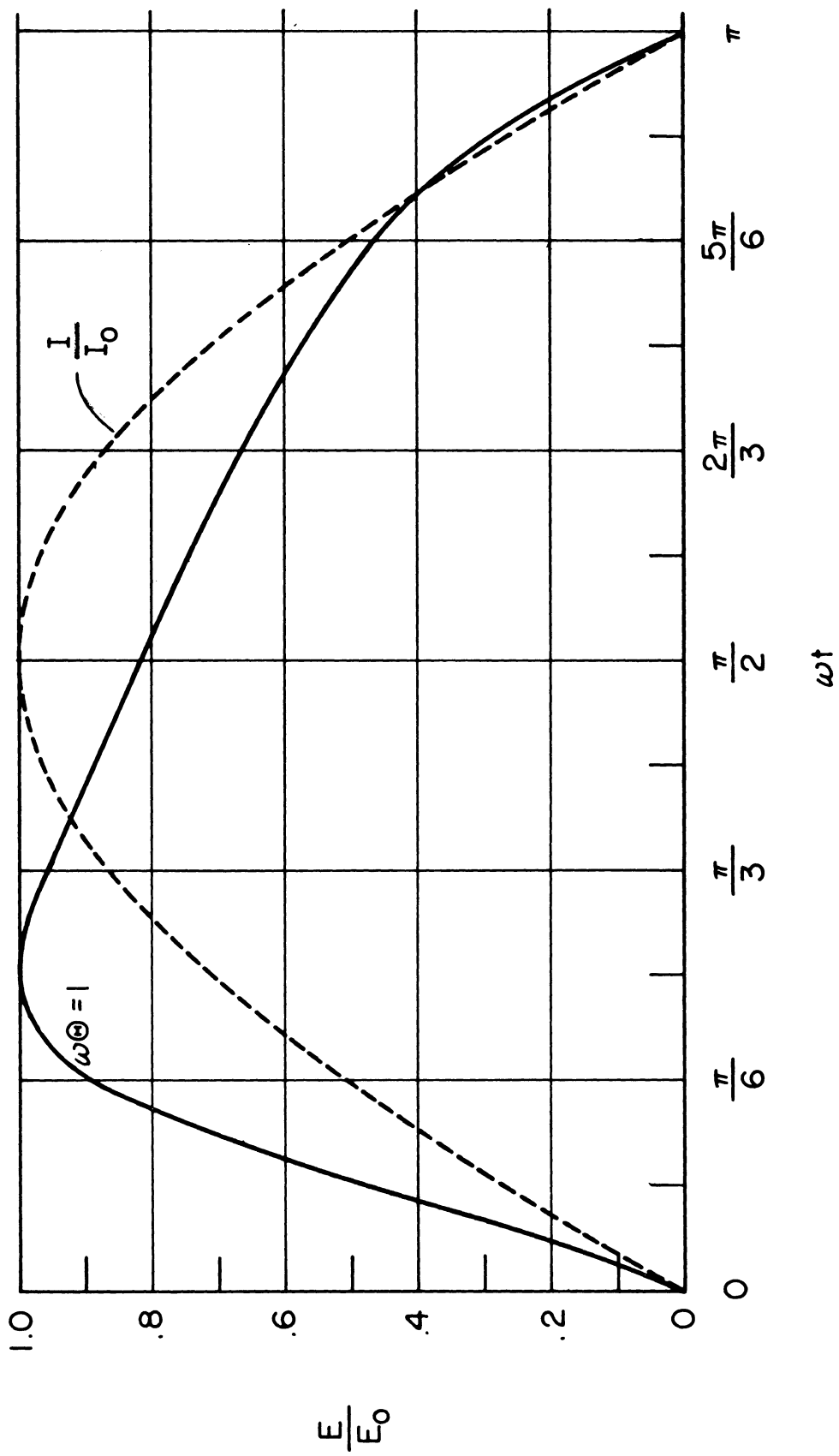
FIGURE 18. ASYMPTOTIC AC ARC COLUMN.
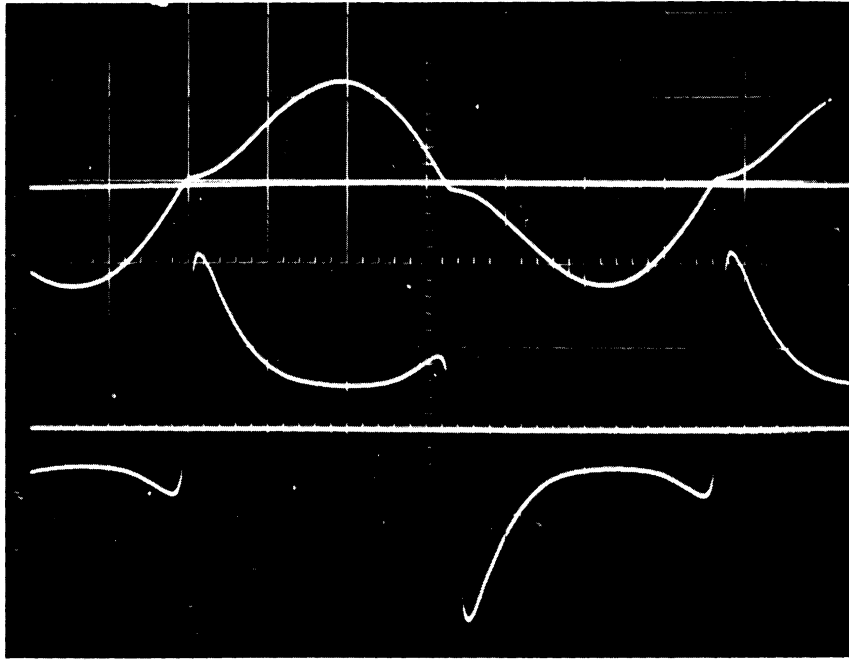
FIGURE 19. NITROGEN AC ARC WAVEFORMS.
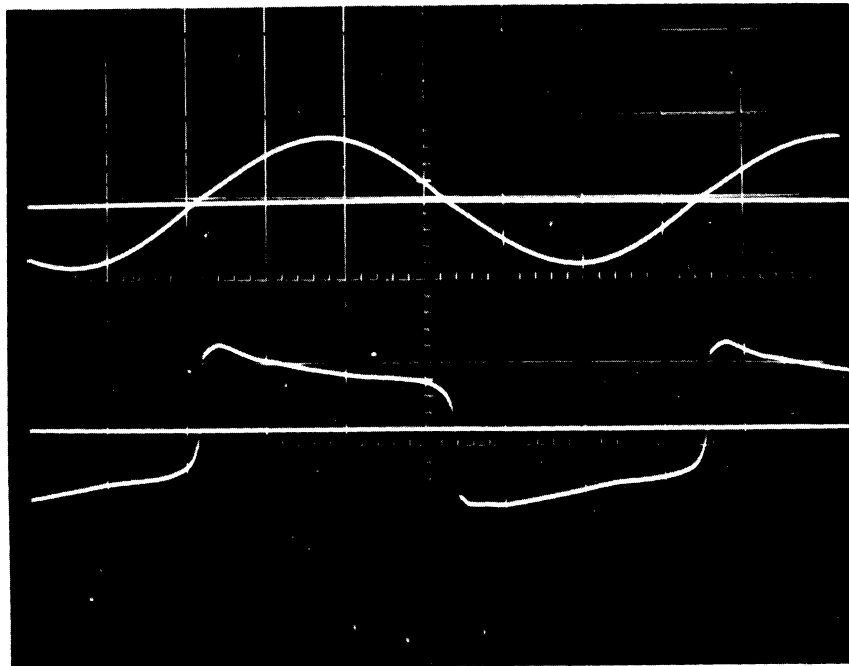


FIGURE 20. ARGON AC ARC WAVEFORMS.

45

and this likewise arises due to column cooling as the current input decreases.

It is evident that none of the analytical waveforms show the extinction peak and the reignition peak is not large enough relative to the plateau value to be a realistic description of a real arc. However, this analysis does predict trends due to changes in the transport properties of the arc gas (which is reflected in the thermal diffusivity, $\lambda$). Notice, for instance, a voltage waveform obtained under the same conditions as in Figure 19 but for argon rather than nitrogen and shown in Figure 20. Argon has a thermal conductivity which is lower by about a factor of 10 for the temperatures which prevail in these arcs. Then for the same applied frequency (60 cps in both cases) the product $\omega \Theta$ is about ten times larger than for nitrogen. The general differences are a much less severe reignition peak and no extinction peak at all and this trend is clearly shown in the analytical curves.

Further refinement of the theory is clearly necessary, however, and the next step is to include a variation of the arc radius with time. It is felt that this will provide voltage waveform predictions which are in much closer agreement with experiment, both qualitatively and quantitatively.

# IV. MAGNETOGASDYNAMIC ACCELERATOR

For some practical problems, the description of the motion of plasma from the microscopic point of view is too detailed to be useful. Even though the plasma is a mixture of various species; charged and neutral particles, in many practical cases, the variation of its composition is small and its effect is negligible. In such cases, the plasma may be considered as a single fluid of definite composition. Hence for these problems one postulates the fundamental equations for the dynamics of a plasma based on the continuum conservation laws of mass, momentum, energy and charge. In the dynamics of a plasma, one must consider both the electromagnetic forces as well as other gas dynamic forces.

With the above thoughts in mind one can introduce Maxwell's field equations and then show how these equations are coupled with the gas dynamic equations, and show in more or less a crude manner how the magnetogasdynamic equations arise. Then with the background established for magnetogasdynamic flow problems a cross-field plasma accelerator will be examined.

## A. INTRODUCTION OF MAXWELL'S FIELD EQUATIONS AND THE GASDYNAMIC EQUATIONS

It is postulated that at every ordinary point in space the field vectors $\vec{E}, \vec{B}, \vec{D},$ and $\vec{H}$ are subject to Maxwell's equations:

$$\nabla \times \vec{E} + \frac{\partial \vec{B}}{\partial t} = 0 \tag{4-1}$$

$$\nabla \times \vec{H} - \frac{\partial \vec{D}}{\partial t} = \vec{j} \tag{4-2}$$

where $\vec{E}$ is the intensity of the electric field

$\vec{H}$ is the intensity of the magnetic field

$\vec{D}$ is the electric displacement

$\vec{B}$ is the magnetic induction

$\vec{j}$ is the vector current density.

An ordinary point is one in whose neighborhood the physical properties of the medium are continuous.

Any ordered motion of charge constitutes a current. A current distribution is characterized by a vector field which specifies at each point not only the intensity of the flow but also its direction. The differential equation

$$\nabla \cdot \vec{J} + \frac{\partial \omega}{\partial t} = 0 \tag{4-3}$$

expresses the conservation of charge in the neighborhood of a point where $\omega$ is the charge density.

From Equation (4-1) it may be concluded that

$$\nabla \cdot \vec{B} = 0 \tag{4-4}$$

provided that in the past history the field has vanished, for example at the time of initial generation of the field. Likewise from Equations (4-2) and (4-3) one obtains

$$\nabla \cdot \vec{D} = \omega \quad . \tag{4-5}$$

Equations (4-4) and (4-5) are frequently included as part of Maxwell's system.

If the physical properties of a body in the neighborhood of some interior point are the same in all directions then, at every point in the isotropic medium

$$\vec{D} = \epsilon \vec{E} \tag{4-6}$$

$$\vec{H} = \frac{1}{\mu_e} \vec{B} \tag{4-7}$$

where $\epsilon$ and $\mu_e$ are scalar quantities. To Maxwell's equations there must now be added a third and last empirical relation between the current density and the field. This relation proves to be linear throughout a remarkably wide range of conditions in both solids and weakly ionized solutions.

$$\vec{J} = \sigma \vec{E} \tag{4-8}$$

where $\sigma$ is called the conductivity of the media.

In summary one is led to the following equations for an isotropic conducting media:

$$\nabla \times \vec{E} + \frac{\partial \vec{B}}{\partial t} = 0 \qquad \text{(a)}$$

$$\nabla \times \vec{H} - \frac{\partial \vec{D}}{\partial t} = \vec{j} \qquad \text{(b)}$$

$$\nabla \cdot \vec{j} + \frac{\partial \omega}{\partial t} = 0 \qquad \text{(c)}$$

$$\nabla \cdot \vec{B} = 0 \qquad \text{(d)}$$

$$\nabla \cdot \vec{D} = \omega \qquad \text{(e)}$$

$$\vec{D} = \epsilon \vec{E} \qquad \text{(f)}$$

$$\vec{H} = \frac{1}{\mu_e} \vec{B} \qquad \text{(g)}$$

$$\vec{j} = \sigma \vec{E} \qquad \text{(h)}$$

(4-9)

It is also easy to show that $\omega \vec{E}$ and $\vec{j} \times \vec{B}$ are quantities whose dimensions are those of force per unit volume and that

$$f = \omega \vec{E} + \vec{j} \times \vec{B} \qquad (4\text{-}10)$$

which is the sum of two force densities.

It is necessary for later use to extend Maxwell's theory for media at rest to moving media. If primed coordinates refer to a moving system and unprimed to laboratory coordinates one can find by the usual arguments

$$\vec{E}' = \vec{E} + \vec{V} \times \vec{B} \qquad (4\text{-}11)$$

By using similar arguments one finds

$$\vec{B}' = \vec{B} \qquad (4\text{-}12)$$

thus leading to what is usually called the generalized ohm's law

$$\vec{J} = \sigma \vec{E}' = \sigma(\vec{E} + \vec{V} \times \vec{B}) \qquad (4\text{-}13)$$

and to the Lorentz force

$$\vec{f}_L = \vec{J} \times \vec{B} \qquad (4\text{-}14)$$

where a neutral plasma has been assumed.

Now writing down the familiar equations of gas dynamics wherein the plasma is considered to be a single fluid one has:

$$P = \rho RT \qquad \text{Equation of State} \qquad (4\text{-}15)$$

$$\frac{\partial \rho}{\partial t} + \frac{\partial}{\partial x_i}(\rho u_i) = 0 \qquad \text{Conservation of Mass} \qquad (4\text{-}16)$$

$$\rho \frac{Du_i}{Dt} = -\frac{\partial P}{\partial x_i} + \frac{\partial \tau_{ij}}{\partial x_j} + f_{L_i} + F_{g_i} \qquad \text{Conservation of Momentum} \qquad (4\text{-}17)$$

where $P, \rho, u,$ and $T$ are the pressure, density, velocity, and temperature respectively.

Considering the fluid as a pure thermodynamic system with the electromagnetic effect entering only through the work done by the electromagnetic force and the joule heating, one must add to the energy equation $f_{L_i} u_i + J^2/\sigma$.

But note that

$$\vec{u} \cdot \vec{f}_L + \frac{J^2}{\sigma} = \vec{u} \cdot (\vec{J} \times \vec{B}) + \frac{J^2}{\sigma}$$

$$= \vec{u} \cdot (\vec{J} \times \vec{B}) + \vec{J} \cdot (\vec{E} + \vec{V} \times \vec{B})$$

$$= \vec{J} \cdot \vec{E}$$

Thus the conservation of energy equation becomes

$$\frac{\partial \rho e}{\partial t} + \frac{\partial \rho u_i e}{\partial x_i} = -\frac{\partial P u_i}{\partial x_i} + \frac{\partial u_i \tau_{ij}}{\partial x_i} + E_i J_i + \frac{\partial Q_i}{\partial x_i} \qquad (4\text{-}18)$$

50

## B. ORDER OF MAGNITUDE ANALYSIS AND APPROXIMATIONS TO BE EMPLOYED

Considering the plasma as a single fluid the fundamental equations are as follows:

$$P = \rho\,RT \tag{a}$$

$$\frac{\partial \rho}{\partial t} + \frac{\partial}{\partial x_i}\left(\rho\,u_i\right) = 0 \tag{b}$$

$$\rho\,\frac{Du_i}{Dt} = \frac{\partial P}{\partial x_i} + \frac{\partial \tau_j}{\partial x_j} + f_{L_i} + f_{g_i} \tag{c}$$

$$\frac{\partial \rho\,e}{\partial t} + \frac{\partial \rho\,u_i e}{\partial x_i} = -\frac{\partial Pu_i}{\partial x_i} + \frac{\partial u_j\,\tau_{ij}}{\partial x_i} + E_i J_i + \frac{\partial Q_i}{\partial x_i} \tag{d}$$

$$\nabla \times \vec{H} = \vec{J} + \frac{\partial \epsilon \vec{E}}{\partial t} \tag{e}$$

$$\nabla \times \vec{E} = -\frac{\partial \mu_e \vec{H}}{\partial t} \tag{f}$$

$$\nabla \cdot \vec{J} = 0 \tag{g}$$

$$J_i = \sigma\left[E_i + \mu_e\,(\vec{u} \times \vec{H})_i\right] \tag{h}$$

$$\nabla \cdot \vec{H} = 0 \tag{i}$$

$$\nabla \cdot \vec{E} = 0 \tag{j}$$

(4-19)

It will be convenient to introduce the following non-dimensional quantities:

$$x^* = \frac{x}{L}\ , \qquad \nabla^* = \nabla \cdot L\ , \qquad t^* = \frac{t}{t_o}$$

$$u^* = \frac{u}{U} \tag{4-20}$$

$$\vec{E}^* = \frac{\vec{E}}{E_o}\ , \qquad \vec{H}^* = \frac{\vec{H}}{H_o}\ , \qquad \vec{J}^* = \frac{\vec{J}}{\sigma \mu_e U H_o}$$

Then Equation (4-19e) in terms of the non-dimensional variables becomes

$$\frac{1}{R_\sigma} \nabla^* \times H^* = J^* + \frac{R_c R_E}{R_\sigma R_t} \cdot \frac{\partial E^*}{\partial t^*} \qquad (4\text{-}21)$$

where $R_t = \dfrac{t_o U}{L}$

      L = the characteristic length

      U = the characteristic velocity of the flow field

$$R_E = \frac{E_o}{\mu_e U H_o}$$

      $E_o$ = the characteristic value of the electric field

      $H_o$ = the characteristic magnetic field strength

$$R_c = \frac{U^2}{c^2} = U^2 \mu_e \epsilon$$

      c = velocity of light

It should be noticed that all the non-dimensional variables in Equation (4-20) are of the order of magnitude of unity. Under magnetogasdynamic approximations, $R_c R_E / R_t \ll 1$ in Equation (4-21) so that

$$\nabla \times \vec{H} = \vec{J} \qquad (4\text{-}22)$$

since the displacement current is negligibly small compared with the curl of the magnetic field.

From Equation (4-19h)

$$\vec{E} = \frac{\vec{J}}{\sigma} - \mu_e \, (\vec{u} \times \vec{H})$$

and substituting Equation (4-22) into this one obtains

$$\vec{E} = \frac{1}{\sigma} \, (\nabla \times \vec{H}) - \mu_e \, (\vec{u} \times \vec{H}) \qquad (4\text{-}23)$$

Thus all the electromagnetic variables may be expressed in terms of the magnetic field $\bar{\bar{H}}$.

Now consider the steady flow of plasma through a nozzle which is of major interest here. If the variation of the cross-sectional area of the nozzle is small, the flow may be considered one-dimensional so that all variables are functions of x only. For large Reynold's numbers assume that the uniform external applied magnetic field is in the z direction. The total magnetic field strength is then $H(x) = H_o + h(x)$ where $h(x)$ is the induced magnetic field due to the flow. Furthermore assume that the uniform external applied electric field is in the y direction. The total electric field is then $E(x) = E_o + e(x)$ where $e(x)$ is the induced electric field due to the flow.

The fundamental equations for this nozzle problem become:

$$\rho u A = \dot{m} \qquad\qquad \text{Equation of Continuity}$$

$$\rho u \frac{du}{dx} + \frac{dP}{dx} = - \mu_e H \frac{dH}{dx} \qquad\qquad \text{Equation of Motion}$$

$$\rho u C_p \frac{dT}{dx} + \rho u^2 \frac{du}{dx} = \mu_e \frac{dH}{dx} \left( \frac{1}{\sigma \mu_e} \frac{dH}{dx} - uH \right) \qquad\qquad \text{Equation of Energy}$$

$$\frac{duH}{dx} = \frac{d}{dx} \left( \frac{1}{\sigma \mu_e} \frac{dH}{dx} \right) \qquad\qquad \text{Equation of Magnetic Field}$$

or                                                                                                                          (4-24)

$$\frac{1}{\sigma \mu_e} \frac{dH}{dx} = uH + E_o$$

where $E_o$ is the constant of integration which depends on the external applied electric field, and

$$P = \rho R T \qquad\qquad \text{Equation of State}$$

The set of Equations (4-24) may be simplified even further depending upon the order of magnitude of the magnetic Reynolds number. This may be seen by the

following. Substitute Equation (4-23) into Equation (4-19f) and obtain

$$\nabla \times \frac{1}{\sigma} (\nabla \times \vec{H}) - \nabla \times \mu_e \, (\vec{u} \times \vec{H}) = - \frac{\partial \mu_e \vec{H}}{\partial t} \tag{4-25}$$

Besides the non-dimensional quantities of Equation (4-20), introduce one more non-dimensional quantity

$$(\sigma \mu_e)^* = \frac{\sigma \mu_e}{(\sigma \mu_e)_0}$$

The Equation (4-25) in terms of the dimensionless quantities with $R_t = 1$ becomes

$$\frac{\partial \vec{H}^*}{\partial t^*} = \nabla^* \times (\vec{u}^* \times \vec{H}^*) - \frac{1}{R_\sigma} \, \nabla^* \times \frac{1}{(\sigma \mu_e)^*} (\nabla^* \times \vec{H}^*) \tag{4-26}$$

where $R_\sigma = \sigma \mu_e UL$ = magnetic Reynolds number.

If the value of the magnetic Reynolds number is very small the first term on the right hand side of Equation (4-26) will be small compared to the second term. In this case the magnetic field $\vec{H}$ is practically independent of the flow motion. That is, for $R_\sigma$ small one can legitimately neglect the induced electromagnetic field components and consider $H(x)$ and $E(x)$ as the given external applied fields. Then for this case ($R_\sigma \ll 1$) Equations (4-24) reduce to:

$$\rho u A = \dot{m} \qquad\qquad\qquad \text{Conservation of Mass}$$

$$\rho u \frac{du}{dx} + \frac{dP}{dx} = \sigma E H - \sigma H^2 u \qquad\qquad \text{Conservation of Momentum}$$

$$\tag{4-27}$$

$$\rho u \, C_p \frac{dT}{dx} + \rho u^2 \frac{du}{dx} = \sigma E^2 - \sigma E H u \qquad \text{Conservation of Energy}$$

$$P = \rho R T \qquad\qquad\qquad \text{Equation of State}$$

## C. THEORETICAL STUDY OF A CROSS-FIELD PLASMA ACCELERATOR (STEADY FLOW)

Magnetogasdynamic accelerating nozzles or "ducts" can be envisaged which are designed for either; constant area, constant velocity, constant temperature, or constant pressure.

Some combination of these might also be effected by tailoring either the electric or magnetic field. However the use of the constant area design seems to be quite attractive. This has the advantage of being a constant area design for all operating conditions, while one of the other designs mentioned above is valid for only a particular condition.

For the case of the constant area duct; assuming frictionless flow without heat addition, small magnetic Reynolds number, etc.; and constant E and H; and for a first order approximation assume $\sigma$, $C_p$ and $C_r$ are constants also; then the magnetogasdynamic equations become:

$$\frac{d\rho u}{dx} = 0 \quad \text{or} \quad \rho u = \dot{m} \text{ (constant)} \qquad \text{Conservation of Mass}$$

$$\rho u \frac{du}{dx} + \frac{dP}{dx} = \sigma EH - \sigma H^2 u \qquad \text{Conservation of Momentum}$$

$$\rho u\, C_p \frac{dT}{dx} + \rho u^2 \frac{du}{dx} = \sigma E^2 - \sigma EHu \qquad \text{Conservation of Energy}$$

$$P = \rho RT \qquad \text{Equation of State}$$

Now one would like to solve for $u, \rho, P,$ and T in terms of the initial conditions and for a given $\sigma, E, H,$ and A. First, solve this set of equations for the velocity u.

Upon rewriting the conservation of momentum equation above, one obtains

$$\frac{dP}{dx} = \sigma EH - \sigma H^2 u - \dot{m} \frac{du}{dx} \qquad (4\text{-}28)$$

Similarly rewriting the equation of energy above yields

$$\frac{dT}{dx} = \frac{\sigma E^2}{\dot{m} C_p} - \frac{u}{C_p} \frac{du}{dx} - \frac{\sigma E H u}{\dot{m} C_p} \tag{4-29}$$

Now integrating the above two equations and substituting these expressions into the equation of state the following relation in u is obtained:

$$\int_0^x \left[ \sigma E H - \sigma H^2 u - \dot{m} \frac{du}{dx} \right] dx + P_i = \frac{\dot{m} R}{u} \int_0^x \left[ \frac{\sigma E^2}{\dot{m} C_p} - \frac{u}{C_p} \frac{du}{dx} - \frac{\sigma E H u}{\dot{m} C_p} \right] dx + \frac{\dot{m} R}{u} T_i \tag{4-30}$$

Or Equation (4-30) becomes

$$\sigma E x \left( Hu - \frac{RE}{C_p} \right) + \sigma H \left( \frac{RE}{C_p} - Hu \right) \int_0^x u\, dx + \dot{m} u^2 \left( \frac{R}{2 C_p} - 1 \right) + u \left( P_i + \dot{m} u_i \right)$$

$$= \dot{m} R \left( T_i + \frac{u_i^2}{2 C_p} \right) \tag{4-31}$$

which can be written as,

$$A x u + B x + (C u + D) \int_0^x u\, dx + E u^2 + F u + G = 0 \tag{4-32}$$

where A = $\sigma E H$

B = $- \sigma E^2 R / C_p$

C = $- \sigma H^2$

D = $\sigma E H R / C_p$

E = $\dot{m} (R / 2 C_p - 1)$

F = $(P_i + \dot{m} u_i)$

G = $\dot{m} R (T_i + u_i^2 / 2 C_p)$

For simplicity let

$$v = \int_0^x u\,dx \qquad \text{or} \qquad \frac{dv}{dx} = u \quad .$$

Then Equation (4-32) can be written as,

$$Ev'^2 + (Cv + Ax)\,v' + (Dv + Bx) + Fv' + G = 0$$

Now at this point it is important to note,

$$(Dv + Bx) = \frac{B}{A}\,(Cv + Ax) \quad .$$

Thus Equation (4-33) can be written as

$$Ev'^2 + (Cv + Ax + F)\left(v' + \frac{B}{A}\right) + G - \frac{B}{A}\,F = 0 \tag{4-34}$$

Now let $v = w + nx$ where n is a constant which will be determined shortly. Equation (4-34) becomes

$$E\,(w'^2 + 2nw' + n^2) + [\,C\,(w + nx) + Ax + F\,]\,\left(w' + n + \frac{B}{A}\right) + G - \frac{B}{A}\,F = 0 \tag{4-35}$$

Now let $n = -\dfrac{A}{C}$ to eliminate the variable coefficient and obtain

$$w'^2 + \alpha w' + \beta ww' + \gamma w + \epsilon = 0 \tag{4-36}$$

where $\alpha = \left|\dfrac{F}{E} - 2\dfrac{A}{C}\right|$

$\beta = C/E$

$\gamma = C/E\,(B/A - A/C)$

$\epsilon = F/E\,(B/A - A/C) + (A/C)^2 + G/E - F/E\,(B/A)$

Note that one is not really interested in v but rather $v'$ or u. Consequently one is interested in $w'$ not w. Thus solving for w in Equation (4-36) and differentiating the result one finds

57

$$w' = - \frac{(2w' + \alpha)\, w''}{(\beta w' + \gamma)} + \frac{(w'^2 + \alpha w' + \epsilon)}{(\beta w' + \gamma)^2} \cdot \beta w'' \quad . \tag{4-37}$$

Equation (4-37) can be written as

$$w' (\beta w' + \gamma)^2 + w'' [\beta w'^2 + 2\gamma w' + (\alpha\gamma - \epsilon\beta)] = 0 \tag{4-38}$$

Note: $\gamma = \beta\xi$ where $\xi = (B/A - A/C)$. Now Equation (4-38) can be immediately integrated to yield a relationship between x and w', i. e.,

$$\int_{w'_1}^{w'} \left[ \frac{1}{w'} + \frac{(\alpha\xi - \epsilon - \xi^2)}{w' (w' + \xi)^2} \right] dw' + \int_0^x \beta\, dx = 0$$

or

$$\ell n \frac{w'}{w'_1} + \left( \frac{\alpha\xi - \epsilon - \xi^2}{\xi} \right) \left[ \frac{1}{(w' + \xi)} - \frac{1}{(w'_i + \xi)} - \frac{1}{\xi} \ell n \left( \frac{w' + \xi}{w'_i + \xi} \cdot \frac{w'_i}{w} \right) \right] + \beta x = 0 \tag{4-39}$$

But note that $w' = u + A/C$ and $w' + \xi = u + B/A$ and that $\alpha\xi - \epsilon - \xi^2 = B/A\, (F/E - B/A) - G/E$ and also that $\beta = C/E$.

Thus Equation (4-39) becomes

$$-\frac{\frac{G}{E} - \frac{B}{A} \left( \frac{F}{E} - \frac{B}{A} \right)}{\left| \frac{B}{A} - \frac{A}{C} \right|^2} \left\{ \left| \frac{B}{A} - \frac{A}{C} \right| \left( \frac{1}{u_i + \frac{B}{A}} - \frac{1}{u + \frac{B}{A}} \right) + \ell n \left( \frac{u + \frac{B}{A}}{u_i + \frac{B}{A}} \right) \right\}$$

$$+ \left\{ \frac{\frac{G}{E} - \frac{B}{A} \left( \frac{F}{E} - \frac{B}{A} \right)}{\left| \frac{B}{A} - \frac{A}{C} \right|^2} - 1 \right\} \ell n \left( \frac{u + \frac{A}{C}}{u_i + \frac{A}{C}} \right) = \frac{C}{E} x \quad . \tag{4-40}$$

58

Now Equation (4-40) can be written in the form

$$-K_1\left\{K_2\left(1-\lambda_1^{-1}\right)+\ell n\,\lambda_1\right\}+(K_1-1)\,\ell n\,\lambda_2 = K_3 x \qquad (4\text{-}41)$$

which is the solution for the velocity in terms of x, and where

$$\lambda_1 = \frac{\dfrac{u}{u_i}-\dfrac{ER}{u_iHC_p}}{1-\dfrac{ER}{u_iHC_p}}$$

$$\lambda_2 = \frac{\dfrac{u}{u_i}-\dfrac{E}{u_iH}}{1-\dfrac{E}{u_iH}}$$

$$K_2 = \frac{\dfrac{E}{u_iH}\left(1-\dfrac{R}{C_p}\right)}{1-\dfrac{E}{u_iH}\cdot\dfrac{R}{C_p}}$$

$$K_3 = \frac{-\sigma H^2}{\dot{m}\left(\dfrac{R}{2C_p}-1\right)}$$

$$K_1 = \frac{1}{\left(\dfrac{R}{2C_p}-1\right)\left(\dfrac{E}{u_iH}\right)^2\left(1-\dfrac{R}{C_p}\right)^2} \times$$

$$\left[\frac{ER}{u_iHC_p}\left\{\frac{\gamma M_i^2+1}{\gamma M_i^2}+\frac{ER}{u_iHC_p}\left(\frac{R}{2C_p}-1\right)\right\}-\frac{1}{\gamma M_i^2}-\frac{R}{2C_p}\right]$$

Having solved for the velocity u one can determine the pressure P in terms of the velocity. From Equations of momentum and energy, one can easily obtain the following relation:

$$\frac{E}{H}\left(\rho u \frac{du}{dx} + \frac{dP}{dx}\right) = \rho u\, C_p \frac{dT}{dx} + \rho u^2 \frac{du}{dx}$$

or

$$\frac{E}{H}\frac{d}{dx}(\dot{m}u + P) = \frac{d}{dx}\left(\frac{C_p}{R}Pu + \dot{m}\frac{u^2}{2}\right) \tag{4-41a}$$

Now integrating Equation (4-41)

$$\frac{E}{H}[(\dot{m}u + P) - (\dot{m}u_i + P_i)] = \left[\left(\frac{C_p}{R}Pu + \frac{\dot{m}u^2}{2}\right) - \left(\frac{C_p}{R}P_i u_i + \frac{\dot{m}u_i^2}{2}\right)\right] \tag{4-42}$$

Dividing Equation (4-42) through by $P_i u_i$ and rearranging there results

$$\frac{P}{P_i}\left(\frac{E}{u_i H} - \frac{C_p}{R}\cdot\frac{u}{u_i}\right) = \gamma M_i^2\left[\frac{1}{2}\left(\frac{u^2}{u_i^2} - 1\right) - \frac{E}{u_i H}\left(\frac{u}{u_i} - 1\right)\right] + \left(\frac{E}{u_i H} - \frac{C_p}{R}\right)$$

or

$$\frac{P}{P_i} = \frac{\gamma M_i^2\left[\frac{1}{2}\left(\frac{u^2}{u_i^2} - 1\right) - \frac{E}{u_i H}\left(\frac{u}{u_i} - 1\right)\right] + \left(\frac{E}{u_i H} - \frac{C_p}{R}\right)}{\left(\frac{E}{u_i H} - \frac{C_p}{R}\cdot\frac{u}{u_i}\right)} \tag{4-43}$$

Now one can also very easily find the temperature ratio from the equation of state,

$$\frac{T}{T_i} = \frac{P}{P_i}\cdot\frac{u}{u_i}$$

60

It should be mentioned that the important parameters appear to be $R/C_p$, $E/u_i H$, and $\gamma M_i^2$ which should facilitate the mapping of the variables.

Before proceeding further into the analysis of this accelerator model examine the nature of the solution.

From Equation (4-41) one sees that the singularities which possibly exist are where $\lambda_1 = \infty$, and where $\lambda_2 = \infty$; that is, Equation (4-41) presents problems when $u_i = R/C_p \cdot E/H$ or when $u_i = E/H$. To investigate these two cases one should look at $du/dx$ as $u$ approaches either of the values just mentioned.

From Equation (4-38)

$$w'' = \frac{- \beta w' \, (w' + \xi)^2}{(w'^2 + 2\xi w' + \alpha \xi - \epsilon)} \tag{4-44}$$

but $w' = u - E/H$

and $w' + \xi = u - E/H \cdot R/C_p$

Thus Equation (4-44) becomes

$$\left[\frac{\frac{}{} + \sigma H^2}{\overset{\circ}{m}\left(\frac{R}{2\,C_p} - 1\right)}\right]^{-1} \frac{du}{dx} = \frac{\left(u - \frac{E}{H}\right)\left(u - \frac{E}{H} \cdot \frac{R}{C_p}\right)^2}{(w'^2 + 2\xi w' + \alpha \xi - \epsilon)} \tag{4-45}$$

In general, then, one concludes that for $u$ to approach either the value $E/H$ or $R/C_p \cdot E/H$, it must do so in an asymptotic manner due to the fact that $du/dx$ approaches zero as $u$ approaches either of these values. The two exceptions to this is where $(\alpha \xi - \epsilon)$, i. e., the initial conditions have certain values.

It is instructive to examine these two exceptions:

1) If $\alpha \xi - \epsilon = \xi^2$ (i. e., $K_1 = 0$)it is required that

$$\frac{E}{u_i H} \cdot \frac{R}{C_p}\left[\frac{\gamma M_i^2 + 1}{\gamma M_i^2} + \frac{E}{u_i H} \cdot \frac{R}{Cp}\left(\frac{R}{2\,C_p} - 1\right)\right] = \frac{1}{\gamma M_i^2} + \frac{R}{2\,C_p} \tag{4-46}$$

which determines the initial conditions for this special case.

Equation (4-44) now becomes

$$w'' = -w'\beta$$

or

$$\frac{du}{dx} = \frac{\sigma H^2}{\dot{m}\left(\frac{R}{2C_p} - 1\right)} \cdot \left(u - \frac{E}{H}\right) .$$

(4-47)

Thus one concludes, theoretically at least, that the flow will maintain smooth passage through $u = R/C_p \cdot E/H$ because $du/dx$ does not vanish there. The solution for this special case can be obtained immediately from Equation (4-47).

2) If $\alpha\xi - \epsilon = 0$ then

$$\frac{1}{\left(\frac{R}{2C_p} - 1\right)}\left[\frac{1}{\gamma M_i^2} + \frac{R}{2C_p} - \frac{E}{u_i H} \cdot \frac{R}{C_p}\left(\frac{1}{\gamma M_i^2} + 1\right)\right] = \left(\frac{E}{u_i H}\right)^2 \cdot \left(\frac{2R}{C_p} - 1\right)$$

(4-48)

i. e., Equation (4-48) determines the initial conditions for this special case.

Equation (4-44) now becomes

$$w'' = \frac{-\beta(w' + \xi)^2}{(w' + 2\xi)}$$

or

$$\frac{du}{dx} = \frac{-\beta\left(u - \frac{E}{H} \cdot \frac{R}{C_p}\right)^2}{\left[u + \frac{E}{H}\left(1 - \frac{2R}{C_p}\right)\right]}$$

(4-49)

62

Again, from a theoretical standpoint the flow will maintain smooth passage through u = E/H due to the fact that du/dx does not vanish. The solution for this special case can be obtained from Equation (4-48).

These two special cases are really the tunnel solutions that Resler and Sears originally pointed out in 1958 in Reference 9.

Figures 21 and 22 present numerical solutions for the above mentioned equations for several pertinent parameters. Of special interest are the following examples A and B which have been computed using parameters and physical constants appropriate to the 3-phase arc heater effluent.

Example A

    E = 150 volts/cm (Electric field)

    B = 10,000 Gauss (Magnetic field)

    $A = 2 \text{ in}^2$ (cross-sectional area of duct)

with

    $M_i$ = .414 (Mach number at entrance to duct)

    $u_i$ = 1640 ft/sec (initial velocity of flow)

    $\sigma$ = 1 mho/cm (conductivity)

    $\mathring{m}$ = .3 lb/sec (mass flow)

Then for a channel length of 13.65 in. one would have the following exit conditions:

$$M_{ex} = .541 \qquad \frac{T_{o_{ex}}}{T_{o_{in}}} = 8.512$$

$$u_{ex}/u_i = 3.80$$

$$\frac{P_{o_{ex}}}{P_{o_{in}}} = 2.37 \qquad \frac{P_{ex}}{P_{in}} = 2.218$$
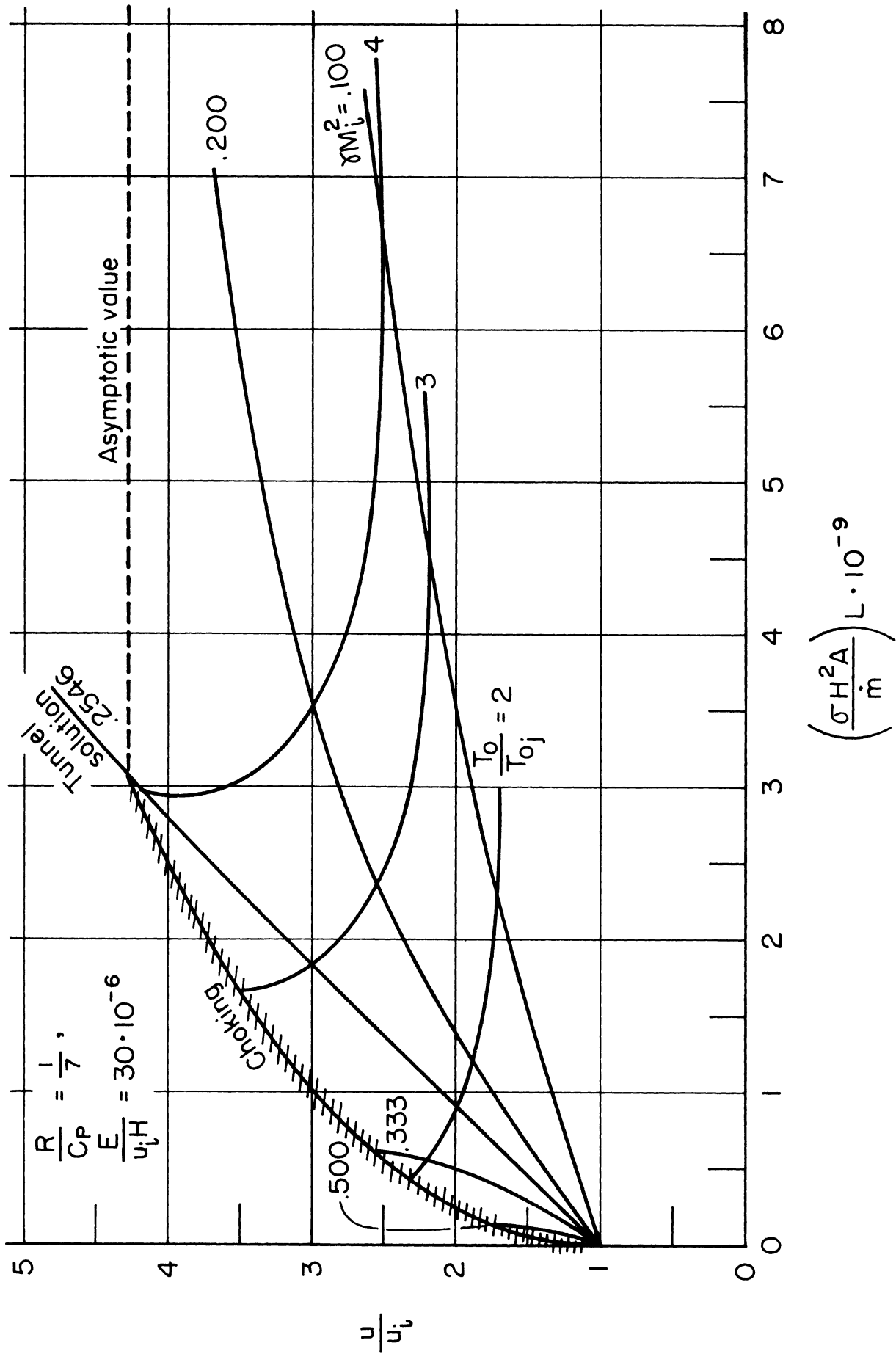
$$\frac{T_{ex}}{T_{in}} = 8.428$$
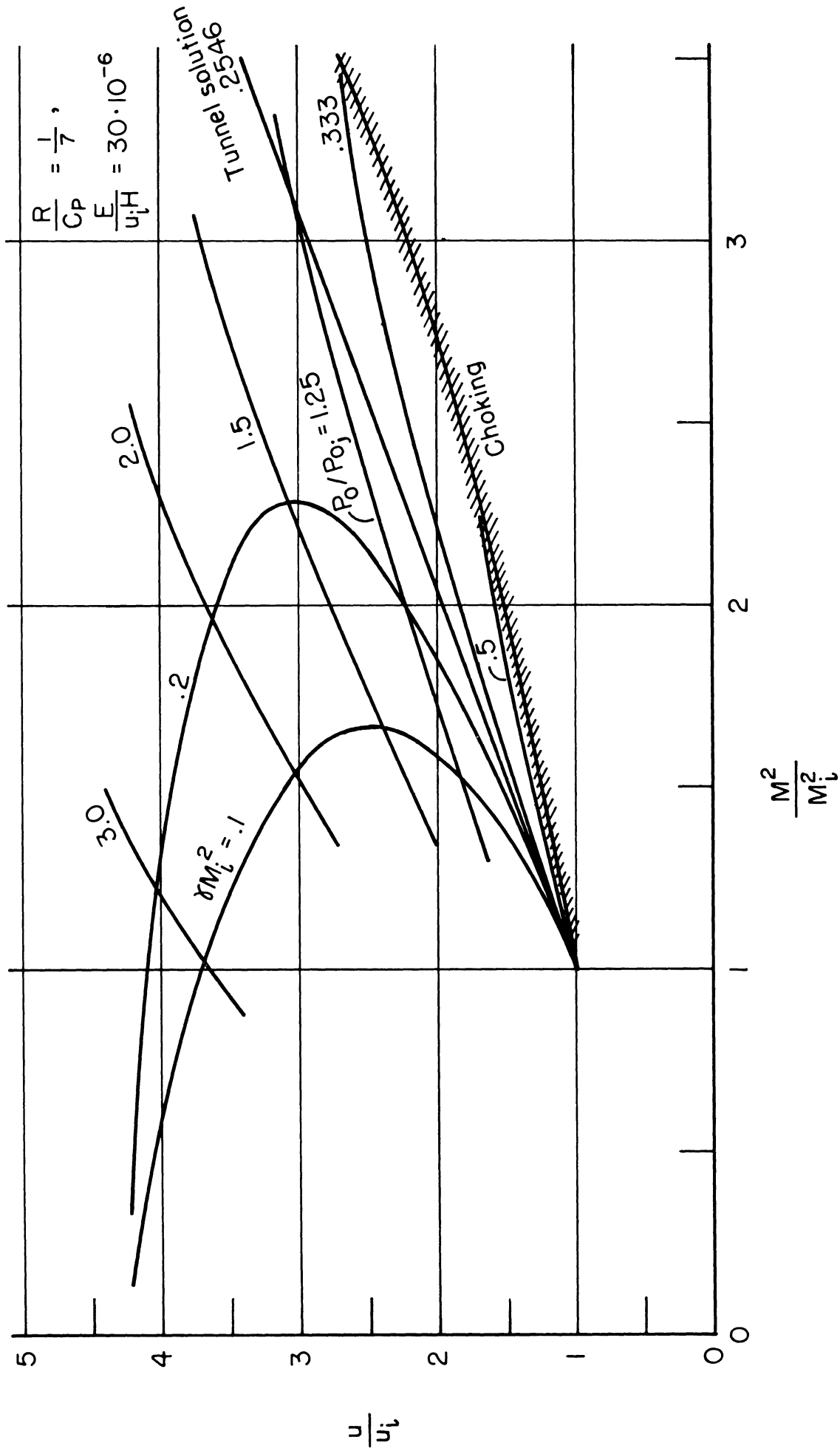
63

FIGURE 21a. SUBSONIC PERFORMANCE.
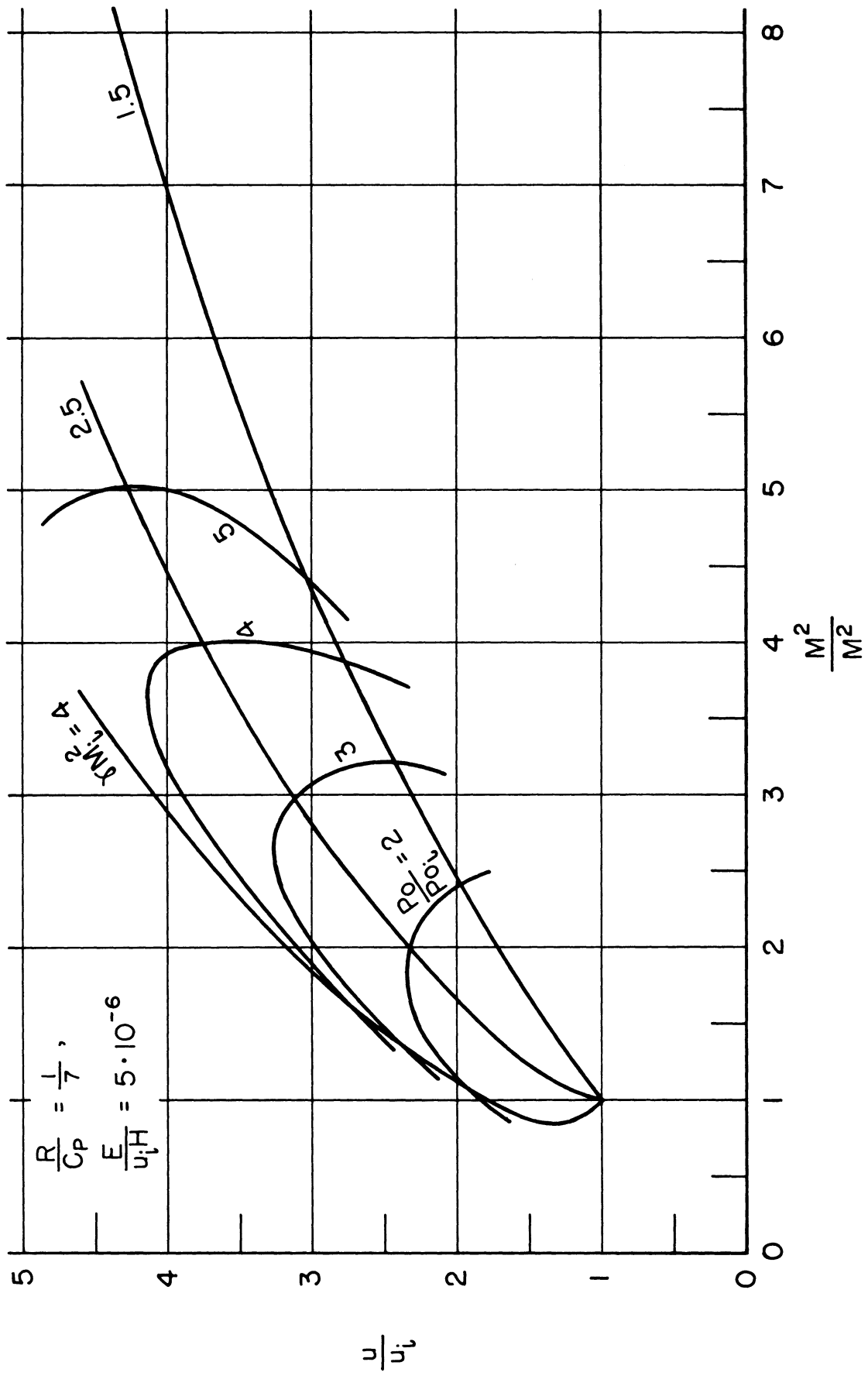
64

FIGURE 2lb. SUBSONIC PERFORMANCE.

FIGURE 22a. SUPERSONIC PERFORMANCE.
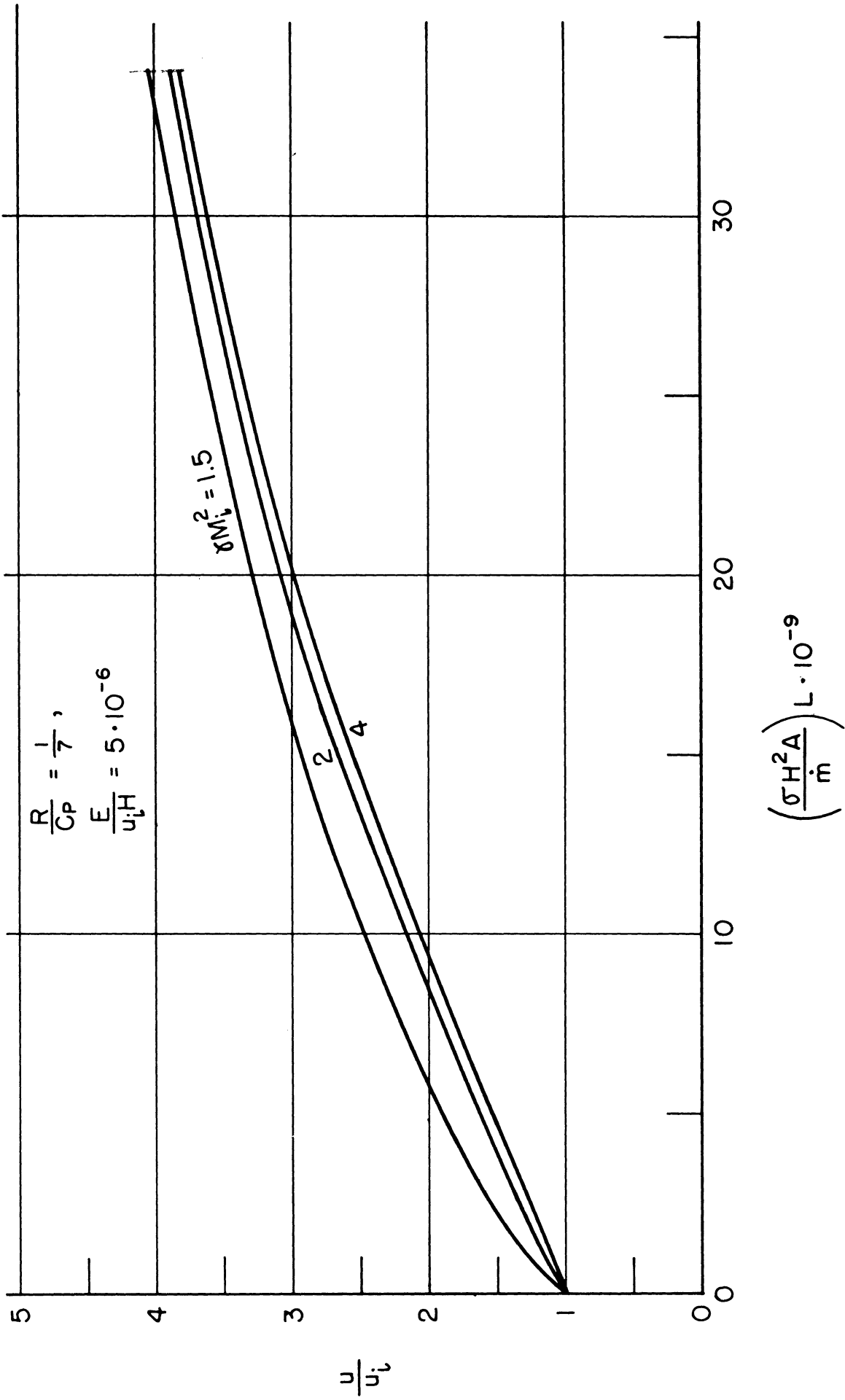
FIGURE 22b. SUPERSONIC PERFORMANCE.

Example B

$\quad$ E = 100 volts/cm

$\quad$ B = 15,000 Gauss

$\quad$ A = 4 in$^2$

with the initial conditions

$\quad$ $M_i$ = 1.47

$\quad$ $u_i$ = 4370 ft/sec

$\quad$ $\sigma$ = 1 mho/cm

$\quad$ $\overset{\circ}{m}$ = .3 lb/sec

then for a channel length of 13.10 in. one has the following exit conditions:

$\quad M_{ex}$ = 3.09

$\quad \dfrac{P_{o_{ex}}}{P_{o_{in}}}$ = 16.87

$\quad \dfrac{T_{o_{ex}}}{T_{o_{in}}}$ = 5.49

$\quad \dfrac{P_{ex}}{P_{in}}$ = .902

$\quad \dfrac{T_{ex}}{T_{in}}$ = 3.61

$\quad \dfrac{u_{ex}}{u_{in}}$ = 4.00

## D. CONCLUSIONS

W. R. Sears in response to a number of comments about the validity of the set of equations which have just been used in regard to the magnitude of the magnetic Reynolds number, makes this comment: The variables $P(x)$, $u(x)$, etc., were defined as average values of pressure, velocity, etc., for the cross sectional station, x. Thus, the current $J_y(x)$ is also the average value, and $J_y H_z$ the average body force at x. Maxwell's equations are not needed here, since the effects they describe do not enter explicitly in determining the above average quantities. The average value $H_z(x)$ is the same as the boundary value, i.e., the field strength at the walls of the channel.

The assumption of neglecting the induced part of the boundary values $H_z(x)$ is valid for nearly uniform slender channels; and for sufficiently slow variations of properties along the channel it is valid for any magnetic Reynolds number.

Sears shows that $h_z$ (the induced field) is of the order $(J_y \cdot \frac{ab}{L})$ over the middle portions of the duct. The approximations made in the derivation of the equations employed herein was to neglect terms of this order in comparison with the applied value of $H_z(x)$. This is justified if L is sufficiently large.
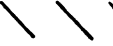
By contrast, the component $h_x$ is of the order $J_y \cdot a$ according to Amperes law. Up to now no mention has been of this component and it has significance for computation of the pinch effect.

The constant area accelerator model has been discussed quite thoroughly by Resler and Sears in Reference 9. Their general results are summed up quite concisely in Figure 23.

Just two of the regions (a and B) have been investigated in the analysis presented herein, then only rather sketchily. But here the general solution has been found. The conclusions which can be drawn from the consideration of these two regions is that the stagnation conditions can be increased quite considerably by this accelerator and this, of course, is of major interest. But perhaps of greater interest is the tunnel solution, i. e. , accelerating the flow through Mach number of unity, not from just a theoretical standpoint but from a practical one as well. For this operating condition seems to be an optimum situation in many respects. It seems to be the only solution which can accelerate a subsonic flow by the greatest amount in relatively short distances and at the same time increase the stagnation values considerably.

The tunnel solution, provided it is physically possible, should be a self-regulating operating condition if the channel is of sufficient length. Reference to Figure 23 indicates that by operating in the region A at too high an initial Mach

Code:

\ \ \ du/dx > 0
/ / / dM/dx > 0
∿ or △ Asymptote as x → ∞
⊸° "Tunnel"
≸ Choking
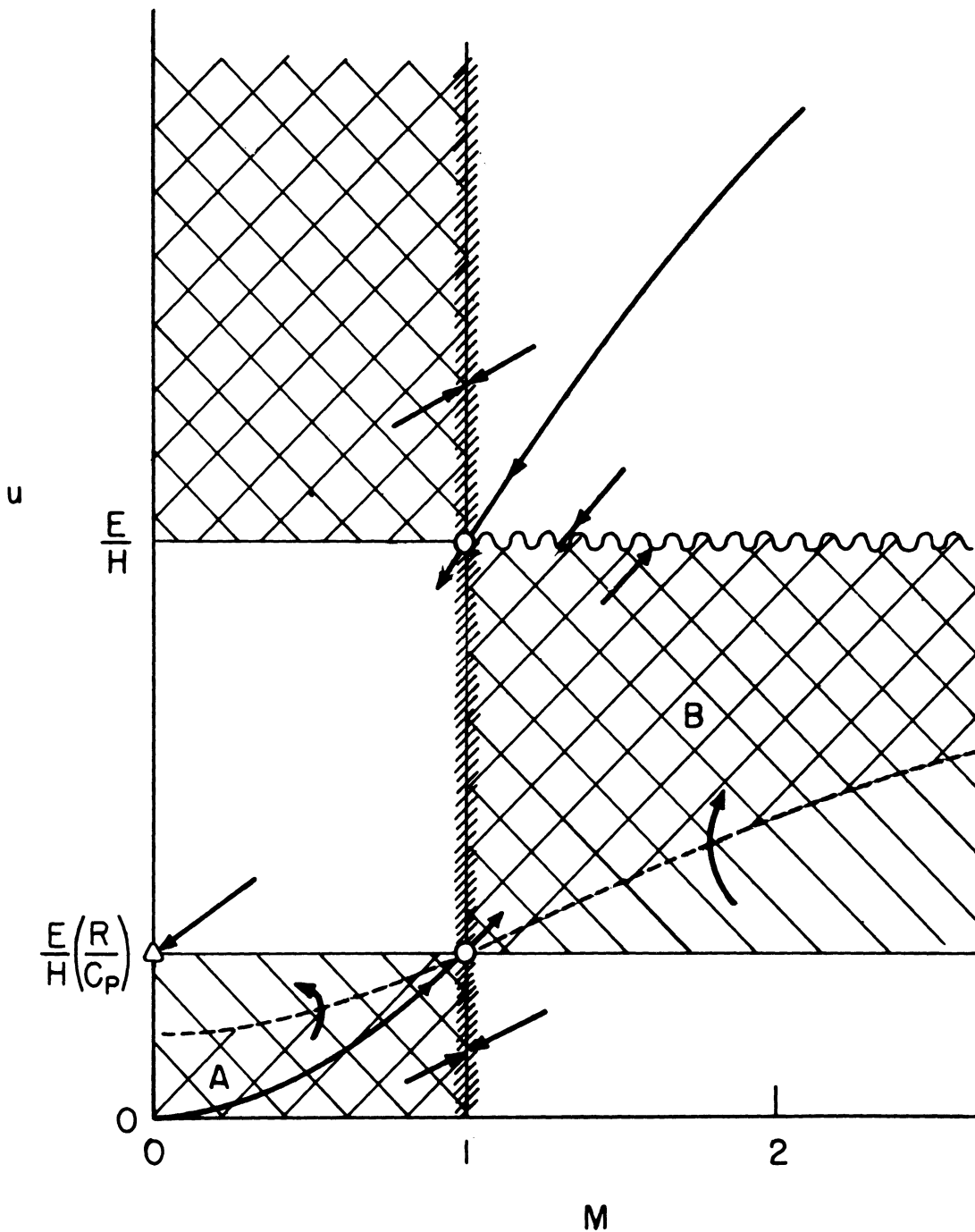


FIGURE 23. THE M-u MAP.

number would tend to choke the duct at some position. This of course means that the initial conditions are forced to change in such a manner so as to decrease the initial Mach number such that one would be operating the accelerator at the tunnel conditions. If this is not a physically possible situation then the asymptotic conditions would result provided the length of the channel were quite long. For short channels the accelerator could operate with the flow just choking at the exit of the duct.

Region B in Figure 23 shows great promise for accelerating a supersonic flow. As a matter of fact this region might be the only practical regime for operating a constant area plasma accelerator if one wishes to obtain a large increase in stagnation values, that is if the tunnel solution is not physically possible due to flow instability.

There are of course some very interesting problems which have not been considered:

1. Stability of the tunnel solution.
2. Pinch effect.

and 3. The interaction of the electromagnetic fields with the flow at the ends of the channel.

# V. PRESSURE VESSEL HEATING

## A. THE CONDUCTION PROBLEM

An important facet of the design of an arc heater facility is the prediction of the integrity of the chamber or pressure vessel. In general, one must determine two things; will the wall temperature of the chamber exceed that value which is allowable for the particular material from which it is fabricated and will the combined thermal and pressure stresses be too severe for reliable operation of the facility? There is no simple way of finding exact answers to these questions and even an attempt to provide approximate answers is quite complicated. First one must know with some certainty what is the thermodynamic and fluid dynamic state of the gas which is being contained by the pressure vessel. By the very nature of the arc heating process strong gradients in these properties exist within the chamber so that in order to obtain any answers at all one must assume the existence of some representative homogeneous state.

Next, one must determine the amount of energy being transferred to the chamber walls by the hot gas; a task which is complicated by the presence of significant radiative transfer at elevated temperatures and pressures. Having determined the heat flux to the chamber walls one must next solve the heat conduction problem in order to find the temperature distribution in the walls. This problem is not difficult for the steady state but if one is interested in the transient temperature distribution considerable complexity can be encountered.

Once all of the above steps have been completed one is in a position to find the combined stresses which will prevail in the confining walls of the chamber. Herein is presented a procedure for obtaining engineering estimates for the transient and steady state temperature distributions and for the determination of the heat fluxes which lead to these distributions. The stress analysis problem, while having been considered, will not be treated in the present report.

As stated above one must first presume the existence of some homogeneous gas state. By assuming reasonable flow rates and power dissipation capabilities of the arc one can arrive at a velocity, temperature, and pressure for the arc heated gas and it is assumed that these conditions prevail throughout the chamber. This procedure is straightforward and involves the consultation of appropriate charts and tables for the thermodynamic properties of high temperature gases. At this point the heat conduction problem will be discussed; the computation of the heat fluxes being deferred since the conduction problem dictates certain forms in which they can conveniently be expressed.

For a cylindrical geometry it is easily shown that if the thickness of the chamber walls is much less than the mean cylinder radius one can solve the infinite slab conduction problem and obtain results which are almost indistinguishable from those obtained by solving the much more difficult cylinder problem. Then consider a slab of thickness L which is of infinite extent and is being cooled at x = L by a flowing medium and being heated at x = 0 by the flowing hot gas. The appropriate form of the heat conduction equation is:

$$\frac{\partial \overline{U}}{\partial t'} = k \frac{\partial^2 \overline{U}}{\partial x^2} \qquad (0 \leq x \leq L, \qquad t' > 0)$$

Here k is the thermal diffusivity $K/\rho C$, the quotient of the thermal conductivity and the specific heat per unit volume, $\overline{U}$ is the temperature of the wall material, and t' is the time variable. Assuming Newton's law of heating and cooling is applicable one obtains the following boundary conditions:

$$k \frac{\partial \overline{U}}{\partial x} (0, t') = h'_1 [\overline{U}(0, t') - A']$$

$$k \frac{\partial \overline{U}}{\partial x} (L, t') = h_2' [B' - \overline{U}(L, t')]$$

Here $h'_1$ and $h'_2$ are the film coefficients on the hot and cold sides of the wall, respectively and A' and B' are the corresponding bulk stream temperatures. It is convenient to introduce the following simplifications:

$$h_1 = h'_1/k, \qquad h_2 = h'_2/k, \qquad t = kt',$$

$$U = (\overline{U} - T_0), \qquad A = (A' - T_0), \qquad \text{and} \qquad B = (T_0 - B'),$$

where $T_0$ is the initial uniform temperature of the chamber walls before heating begins. Then one has the following boundary value problem:

$$\frac{\partial U}{\partial t} = \frac{\partial^2 U}{\partial x^2} \quad,$$

$$U(x, 0) = 0 \qquad (0 \leq x \leq L, \qquad t > 0)$$

$$\frac{\partial U}{\partial x}(0, t) = h_1 [U(0, t) - A]$$

$$\frac{\partial U}{\partial x}(L, t) = h_2 [B - U(L, t)]$$

(5-1)

Introducing the Laplace transform

$$u(x, s) = \int_0^\infty e^{-st} U(x, t) \, dt$$

one obtains the following ordinary differential equation

$$\frac{d^2 u}{dx^2} - su = 0$$

along with the boundary conditions

$$\frac{d}{dx} u(0, s) = h_1 [u(0, s) - A/s]$$

$$\frac{d}{dx} u\,(L, s) = - h_2 \left[ u\,(L, s) - B/s \right]$$

The solution of this equation is found in a straightforward manner to be

$$u\,(x, s) = C_1 \cosh \sqrt{s}\, x + C_2 \sinh \sqrt{s}\, x \tag{5-2}$$

where

$$C_2 = h_1 s^{-\frac{1}{2}} (C_1 - \frac{A}{s})$$

and

$$sC_1 = \frac{h_2\, B \sqrt{s} + h_1\, A \sqrt{s} \cosh (\sqrt{s}\, L) + h_2 h_1\, A \sinh (\sqrt{s}\, L)}{(s + h_1 h_2) \sinh (\sqrt{s}\, L) + (h_1 + h_2) \sqrt{s} \cosh (\sqrt{s}\, L)} \tag{5-3}$$

Now for the transient problem one can facilitate the inversion of Equation (5-2) to the real plane by noting that only the temperature on the hot side (at $x = 0$) is really of interest since it will clearly be the highest value anywhere in the wall. In the steady state case the whole profile is easily found since the distribution must be linear. Then from Equation (5-2) one sees

$$u\,(0, s) = C_1$$

and one need only concentrate upon inversion of the coefficient $C_1$. The expression $sC_1$ has singularities whenever $s = 0$ or when

$$(s + h_1 h_2) \sinh (\sqrt{s}\, L) + (h_1 + h_2) \sqrt{s} \cosh (\sqrt{s}\, L) = 0$$

The latter condition can only be satisfied if $\sqrt{s}$ is a pure imaginary number so one sets $\sqrt{s} = i\alpha$ and finds that singularities occur when

$$\tan (\alpha_n L) = \frac{\alpha_n (h_1 + h_2)}{(\alpha_n^2 - h_1 h_2)} \tag{5-4}$$

75

In Equation (5-4), $n = 1, 2, 3 \ldots$ etc., since there are an infinite number of such singularities. The residue at $s = 0$ can be found by expanding $sC_1(s)$ in a Laurent series about the origin and finding the coefficient of the $s^{-1}$ term. One obtains in this manner the steady state value of $U(0, t)$

$$U_{ss} = \frac{h_1 A (1 + h_2 L) + h_2 B}{h_1 h_2 L + (h_1 + h_2)} \tag{5-5}$$

Since the roots of Equation (5-4) result in simple poles it is an easy matter to find the residues resulting therefrom. One can write the complete solution to Equation (5-1) as

$$u(0, t) = U_{ss} + \sum_{1}^{\infty} \rho_n(t) \tag{5-6}$$

where $\rho_n(t)$ are the residues due to the values of $s$ which cause the denominator of Equation (5-3) to vanish. One finds

$$e^{\alpha_n^2 t} \rho_n(t) =$$

$$\tag{5-7}$$

$$\frac{h_2 B \alpha_n + h_1 A \alpha_n \cos(\alpha_n L) + A h_1 h_2 \sin(\alpha_n L)}{\left[ h_1 h_2 - \frac{\alpha_n^2}{2} (h_1 L + h_2 L + 4) \right] \sin(\alpha_n L) + \frac{\alpha_n}{2} \left[ L (h_1 h_2 - \alpha_n^2) + 3 (h_1 + h_2) \right] \cos \alpha_n L}$$

The pertinent conduction problem is now solved but there remains the task of finding values for $h_1$ and A. The cold side film coefficient is easily obtained if one assumes no nucleate boiling exists in the cooling passages and for a conservative design this assumption is made. One proceeds now to find expressions for $h_1$ and A which include the effects of both convective and radiative heating.

Because of the low velocities which prevail in the arc chamber it was found that modified flat-plate incompressible relations could be used to predict the convective heat transfer to the interior walls of the chamber. More refined methods such as the reference enthalpy technique were explored but were found to yield no benefits in accuracy. Using the Colburn Prandtl number correction one writes for the convective heat transfer

$$\dot{q}_{con} = .332 \frac{\rho_\infty v_\infty}{\sqrt{Re_\infty}} (Pr_\infty)^{-\frac{2}{3}} C_{p_w} \left[ \frac{H_\infty}{C_{p_w}} - \overline{U}(0, t') \right] \tag{5-8}$$

Here the subscript $(\ )_\infty$ refers to conditions at the edge of the boundary layer and $\rho$, $v$, $Re$, and $Pr$ are the density, velocity, Reynolds number, and Prandtl number, respectively at those conditions. Furthermore $H_\infty$ is the stagnation enthalpy in the chamber and $C_{p_w}$ is the specific heat of the hot gas under the conditions which prevail at the wall. However, one must also take into account the radiative heating $\dot{q}_{rad}$ which is a function of the stagnation conditions and the chamber geometry. Determination of this flux can be quite involved particularly at very high pressures but presume for the moment it is known. Later more consideration will be given to this matter. Assuming that the total heat flux to the wall $\dot{q}_w$ can be written in an uncoupled manner

$$\dot{q}_w = \dot{q}_{con} + \dot{q}_{rad}$$

one finds

$$\dot{q}_w = .332 \frac{\rho_\infty v_\infty}{\sqrt{Re_\infty}} (Pr_\infty)^{-\frac{2}{3}} C_{p_w} \left[ \left( \frac{H_\infty}{C_{p_w}} + \frac{\dot{q}_{rad}}{.332 \frac{\rho_\infty v_\infty}{\sqrt{Re_\infty}} (Pr_\infty)^{-\frac{2}{3}} C_{p_w}} \right) - \overline{U}(0, t') \right] \tag{5-9}$$

Recall that the hot side boundary condition was written as

$$- K \frac{\partial \overline{U}}{\partial x} (0, t') = h'_1 [A' - \overline{U} (0, t)] = \dot{q}_w$$

so one can make the following identifications:

$$h'_1 = .332 \frac{\rho_\infty v_\infty}{\sqrt{Re_\infty}} (Pr_\infty)^{-\frac{2}{3}} C_{p_w}$$

and

$$C_{p_w} A' = \left( H_\infty + \frac{\dot{q}_{rad}}{.332 \frac{\rho_\infty v_\infty}{\sqrt{Re_\infty}} (Pr_\infty)^{-\frac{2}{3}}} \right)$$

(5-10)

One sees that the inclusion of $\dot{q}_{rad}$ has necessitated defining an effective bulk temperature so that radiation can be treated within the framework of Newton's linear law of heating. Now, fortified with sufficient thermodynamic data as well as the radiative properties of the gas in question, one can calculate a series of curves which indicate the steady state temperature distributions which will prevail in the walls of the pressure vessel as well as determining the time it requires to reach this steady state. It is interesting to note that the computations described above indicate that about 45-50 seconds will elapse before a steady distribution of temperature is attained in the walls of the arc chamber and experimental records indicate very nearly that value, 48 seconds almost independent of chamber conditions.

## B. RADIATIVE HEAT FLUX CALCULATIONS

It was mentioned above that the radiative heat flux to the walls of an enclosed vessel is dependent upon the geometry of the enclosure as well as the thermodynamic state of the radiating substance. It is no simple task to translate tabulated

radiation properties of gases into a heat flux which is suitable for use in Equation (5-10). Herein is presented the computations which lead from the basic radiative parameters of the hot gas to an engineering expression for $\dot{q}_{rad}$ for several common enclosure geometrics.

The volume element dV of gas radiating to an area element dA is in spherical coordinates (Figure 24(a))

$$dV = r^2 \sin\theta \, d\theta \, d\phi \, dr \qquad (5-11)$$

and in cylindrical coordinates (Figure 24(b))

$$dV = \rho \, d\rho \, dz \, d\phi \qquad (5-12)$$

The solid angle $d\Omega$ subtended by dA at distance r and angle $\theta$ away from the normal to dA is in spherical coordinates (Figure 24(c))

$$d\Omega = \frac{dA \cos\theta}{r^2} \qquad (5-13)$$

and in cylindrical coordinates

$$d\Omega = \frac{dA \, z}{\left(\rho^2 + z^2\right)^{3/2}} \qquad (5-14)$$

If N is the radiant intensity of the gas (the total energy radiated per second per $cm^3$ into $4\pi$ steradians), then the power passing through area dA from volume dV is given by

$$dP = \frac{N}{4\pi} d\Omega \, dV \, e^{-\alpha r} \qquad (5-15)$$

The last factor is included to account for the attenuation of the radiation leaving dV toward dA. The parameter, $\alpha$, is the absorbance per cm of path length. Since for a gas at equilibrium, the radiant emissivity per cm, $\epsilon$, equals the absorbance per cm by Kirchoff's law then
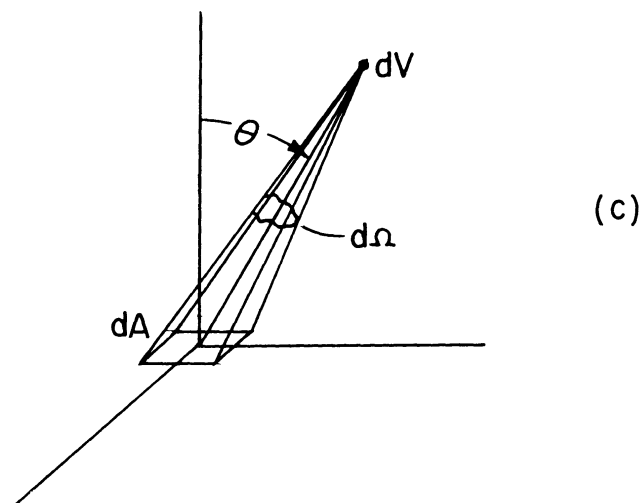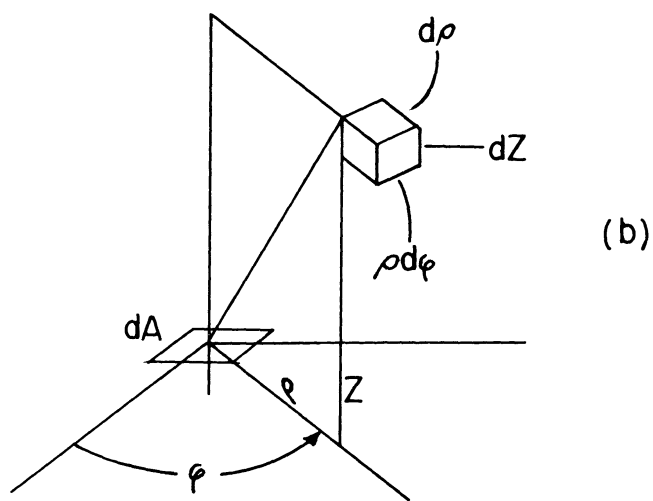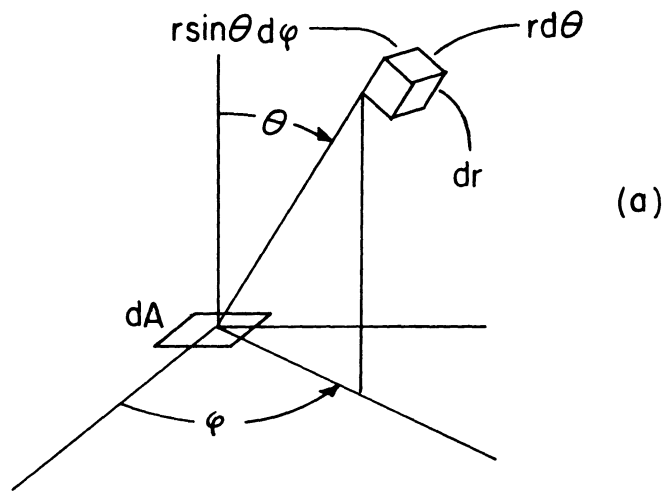
FIGURE 24. VOLUME ELEMENTS OF RADIATING GAS.

$$dP = \frac{N}{4\pi} d\Omega \, dV \, e^{-\epsilon r} \qquad (5\text{-}16)$$

Integrating over the entire volume of radiating gas we find in spherical coordinates

$$P = \frac{N}{4\pi} dA \iint_{r\,\phi\,\theta}\int \cos\theta \, \sin\theta \, e^{-\epsilon r} \, d\theta \, d\phi \, dr \qquad (5\text{-}17)$$

and in cylindrical coordinates

$$P = \frac{N}{4\pi} dA \iint_{z\,\rho\,\phi}\int \frac{\rho z \, e^{-\epsilon\sqrt{\rho^2 + z^2}}}{(\rho^2 + z^2)^{3/2}} \, d\phi \, d\rho \, dz \qquad (5\text{-}18)$$

In a large number of cases $\epsilon a << 1$, where a = characteristic dimension of the gas, so that the exponential can be neglected or expanded in a series. This is the case of an optically thin radiating gas.

Consider now the radiation from some simple gas volume geometries.

An important case is the radiation to an area element at the center of a hemisphere of radius a.

Equation (5-17) becomes

$$P = \frac{N \, dA}{4\pi} \int_0^a e^{-\epsilon r} \, dr \int_0^{2\pi} d\phi \int_0^{\pi/2} \sin\theta \, d\sin\theta$$

$$= \frac{N \, dA}{4} a \left( \frac{1 - e^{-\epsilon a}}{\epsilon a} \right) \qquad (5\text{-}19)$$

when $\epsilon a << 1$ one finds

$$P = \frac{N \, dA}{4} a \left[ 1 - \frac{\epsilon a}{2} + \frac{(\epsilon a)^2}{6} - \circ \circ \circ \right] \qquad (5\text{-}20)$$

and if $\epsilon a = 0$

$$P = \frac{N\ dA}{4}\ a \qquad (5\text{-}21)$$

Furthermore, for a slab of thickness $a$, with $\epsilon = 0$

$$P = \frac{N\ dA}{4\pi} \int\limits_{0}^{\pi/2} \int\limits_{0}^{a/\cos\ \theta} \int\limits_{0}^{2\pi} d\phi\ dr\ \sin\ \theta\ \cos\ \theta\ d\ \theta$$

or

$$P = \left(\frac{N\ dA}{4}\right) 2a$$

Comparison of the hemisphere when $\epsilon = 0$ to the nonabsorbing slab shows that the radiation from a slab of thickness $a$ is the same as the radiation from a hemisphere having radius $2a$. This is a special case of what is known as the shape factor S. See Reference 10.

In general the radiation from any shape of gas body to a specified point can be replaced by the calculation of the radiation from a non-absorbing equivalent hemisphere having radius $= Sa$ where a is a specified characteristic dimension of the actual body. For the non-absorbing slab $S = 2$ and for the absorbing hemisphere radiating to a point at its center,

$$S = \frac{(1 - e^{-\epsilon a})}{\epsilon a}$$

For an absoring slab of thickness $= a$ and $\epsilon \neq 0$ one finds (defining $\theta$ by the accompanying sketch)
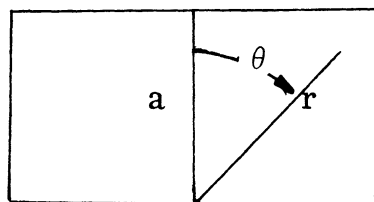
$$P = \frac{N\,dA}{4\pi} \int_0^{\pi/2} \int_0^{a/\cos\theta} \int_0^{2\pi} d\phi\; e^{-\epsilon r}\, dr\, \sin\theta\, \cos\theta\, d\theta$$

or

$$P = \frac{N\,dA}{4} \frac{2}{\epsilon} \left( \frac{1}{2} + \int_0^{\pi/2} \cos\theta\, e^{-\epsilon a/\cos\theta}\, d\cos\theta \right)$$

Let $z = 1/\cos\theta$ to transform the remaining integral and obtain

$$P = \frac{N\,dA}{4} \frac{2}{\epsilon} \left( \frac{1}{2} - \int_1^\infty \frac{e^{-\epsilon a z}}{z^3}\, dz \right)$$

Integrating twice by parts one finds

$$\int_1^\infty \frac{e^{-\epsilon a z}}{z^3}\, dz = 2e^{-\epsilon a} - 2\epsilon a e^{-\epsilon a} + 2(\epsilon a)^2 \int_1^\infty \frac{e^{-\epsilon a z}}{z}\, dz$$

and letting $u = \epsilon a z$

$$\int_1^\infty e^{-\epsilon a z}\frac{dz}{z} = \int_{\epsilon a}^\infty e^{-u}\frac{du}{u} = -\, Ei\,(-\epsilon a)$$

where Ei is the exponential integral function.

Thus

$$P = \frac{N\,dA}{4} \frac{2}{\epsilon} \left( \frac{1}{2} - \left\{ 2e^{-\epsilon a} - 2\epsilon a e^{-\epsilon a} + 2(\epsilon a)^2 \left[ -\, Ei\,(-\epsilon a) \right] \right\} \right)$$

Simplifying, one obtains

$$P = \frac{N \, dA}{4} \, 2a \left\{ \frac{1}{2\epsilon a} - \frac{2}{\epsilon a} \, e^{-\epsilon a} + 2e^{-\epsilon a} - 2\epsilon a \left[ - \text{Ei} \left( - \epsilon a \right) \right] \right\}$$

Thus

$$S = 2 \left\{ \frac{1}{2\epsilon a} - \frac{2e^{-\epsilon a}}{\epsilon a} + 2e^{-\epsilon a} - 2\epsilon a \left[ - \text{Ei} \left( - \epsilon a \right) \right] \right\}$$

for the absorbing slab of thickness a.

Next, consider a sphere of diameter a, radiating to a point on its inner surface with $\epsilon = 0$. Here one writes

$$P = \frac{N \, dA}{4\pi} \int_0^{\pi/2} \int_0^{a \cos \theta} \int_0^{2\pi} d\phi \, dr \, \cos \theta \, \sin \theta \, d\theta$$

so that

$$P = \frac{N \, dA}{4} \, a \, \frac{2}{3}$$

Therefore, $S = \frac{2}{3}$, the shape factor for the sphere.

For an __absorbing__ sphere of diameter a

$$P = \frac{N \, dA}{4\pi} \int_0^{\pi/2} \int_0^{a \cos \theta} \int_0^{2\pi} d\phi \, e^{-\epsilon r} \, dr \, \cos \theta \, \sin \theta \, d\theta$$

$$= \frac{N \, dA}{4} \, 2 \int_0^{\pi/2} \frac{1 - e^{-\epsilon a \cos \theta}}{\epsilon a} \cos \theta \, d \cos \theta$$

Transforming by letting $y = \cos \theta$ and integrating by parts we find

$$P = \frac{N \, dA}{4} \, a \left( \frac{1}{\epsilon a} \left\{ 1 + \frac{2}{(\epsilon a)^2} \left[ (\epsilon a + 1) \, e^{-\epsilon a} - 1 \right] \right\} \right)$$

84

so that

$$S = \frac{1}{\epsilon a} \left\{ 1 + \frac{2}{(\epsilon a)^2} \left[ (\epsilon a + 1) \, e^{-\epsilon a} - 1 \right] \right\}$$

As $\epsilon a \to 0$

$$S = \frac{2}{3} \left[ 1 - \frac{3}{8} \epsilon a + \frac{9}{80} (\epsilon a)^2 - \ldots \right]$$

Now consider the very pertinent case of a cylinder with height equal to the diameter (which equals a), $\epsilon = 0$, and radiating to a spot at the center of the end. Here one finds

$$P = \frac{N \, dA}{4\pi} \int_0^a \int_0^{a/2} \int_0^{2\pi} \frac{d\phi \rho z \, d\rho \, dz}{(\rho^2 + z^2)^{3/2}}$$

$$= \frac{N \, dA}{4} a \, (3 - \sqrt{5})$$

Therefore for a nonabsorbing cylinder with height equal to the diameter radiating to a spot at one end on the axis

$$S = 3 - \sqrt{5} = .764$$

Also for a cylinder with height equal to the diameter and $\epsilon = 0$ radiating to a spot at the edge of one end it can be shown

$$P = \frac{N \, dA}{4\pi} \int_{-\pi/2}^{\pi/2} \int_0^{a\cos\phi} \int_0^a \frac{z \, dz \, \rho d\rho \, d\phi}{(\rho^2 + z^2)^{3/2}}$$

$$= \frac{N \, dA}{4\pi} 2a \int_0^{\pi/2} (\cos\phi - \sqrt{\cos^2\phi + 1} + 1) \, d\phi$$

Now

$$\int_0^{\pi/2} \sqrt{\cos^2 \phi + 1} \; d\phi$$

$$= \sqrt{2} \; E\left(\frac{1}{\sqrt{2}}\right) = \sqrt{2} \; (1.35064)$$

where E is the complete elliptic integral of the second kind.

Thus

$$P = \frac{N \; dA}{4} \; a \left[\frac{2 - 2\sqrt{2} \; (1.35064) + \pi}{\pi}\right]$$

So that

$$S = \frac{2 - 2\sqrt{2} \; (1.35064) + \pi}{\pi} = .421$$

for a spot at the edge of the end of a nonabsorbing cylinder whose height equals the diameter. Recalling that for a spot at the center of the end of such a cylinder S = .764, we see the radiation flux falls in going from center to edge on the end of a cylinder.

Finally consider the case of a cylinder with height equal to the diameter, $\epsilon = 0$, radiating to a spot on the cylinder wall, midway between the ends. Proceeding in the usual manner

$$P = \frac{N \; dA}{4\pi} \int_{-\pi/2}^{\pi/2} \int_0^{a \cos \phi} \int_{-a/2}^{a/2} \frac{zdz \; \rho d\rho \; d\phi}{(\rho^2 + z^2)^{3/2}}$$

$$= \frac{N \; dA}{4\pi} \; 4a \left(1 + \frac{\pi}{4} - \frac{1}{2} \int_0^{\pi/2} \sqrt{4 \cos^2 \phi + 1} \; d\phi\right)$$

86

Now

$$\int_0^{\pi/2} \sqrt{4 \cos^2 \phi + 1} \; d\phi$$

$$= \sqrt{5} \; E\left(\sqrt{\frac{4}{5}}\right) = 2.64$$

where again E is the complete elliptic integral of the second kind. Thus

$$P = \frac{N \, dA}{2} \, a \quad (.702)$$

Therefore

$$S = .702$$

for a nonabsorbing cylinder radiating to a spot on the cylinder wall halfway between the ends.

It is instructive to consider the relation between $\epsilon/L$ (the emissivity per cm of a gas) and N, the radiant power per $cm^3$ radiated into $4\pi$ steradians.

The total power radiated to 1 square centimeter

$$P = \frac{N}{4} \, a \, S$$

where S = shape factor.

For a transparent slab of thickness a, S = 2. Therefore

$$P = \frac{Na}{2} \frac{watts}{cm^2}$$

Consider all the gas to be projected onto a hemisphere of radius = a. Then $\epsilon' = \frac{\epsilon}{L} \cdot d$ = apparent emissivity of the surface of the hemisphere where d = distance through the slab to the far side and is equal to $a/\cos \theta$. Therefore

$$\epsilon' = \frac{\epsilon}{L} \frac{a}{\cos \theta}$$

Now the radiation emitted from area dA' on the hemisphere into $2\pi$ steradian is

$$\epsilon' \sigma T^4 dA' \quad .$$

The solid angle subtended by a projected area $dA_n$ when viewed from a distance "a" at angle $\theta$ from the normal to area dA is

$$d\Omega = \frac{dA_n}{a^2}$$

and $dA_n = dA \cos \theta$. Therefore

$$d\Omega = \frac{dA \cos \theta}{a^2}$$

The fraction of the total radiation into $2\pi$ steradian, going into $d\Omega$ is

$$\frac{d\Omega}{2\pi}$$

Therefore the emission from area dA' on the hemisphere going into solid angle $d\Omega$, i. e. , the radiation that passes through area dA is

$$\epsilon' \sigma T^4 dA' \frac{d\Omega}{2\pi} = \frac{\epsilon}{L} \frac{a}{\cos \theta} \frac{\sigma T^4 dA'}{2\pi} \frac{dA \cos \theta}{a^2}$$

$$= \left(\frac{\epsilon}{L}\right) \frac{\sigma T^4}{2\pi a} dA' \, dA$$

Now as seen from dA, area dA' on the hemisphere subtends a solid angle $d\Omega$ given by

$$dA' = a^2 \, d\Omega'$$

88

The total power going through unit area dA from all dA' is

$$P = \int_{Hemi} \frac{\epsilon}{L} \frac{\sigma T^4}{2\pi} dA' = \frac{\epsilon}{L} \frac{\sigma T^4}{2\pi} \int_{Hemi} dA' = \frac{\epsilon}{L} \frac{\sigma T^4}{2\pi} a^2 \int_{Hemi} d\Omega' = \left(\frac{\epsilon}{L}\right) \sigma T^4 a$$

But

$$P = \frac{Na}{2}$$

so

$$N = 2 \left(\frac{\epsilon}{L}\right) \sigma T^4$$

The parameter $\epsilon/L$ for air is tabulated as a function of $\rho/\rho_o$ and T in Reference 11.

## TABLE II
### SUMMARY OF SHAPE FACTORS

| Shape | Characteristic Dimension, a | Nonabsorbing ε = 0 | Absorbing |
|---|---|---|---|
| Hemisphere radiating to center | radius | 1 | $\dfrac{1 - e^{-\epsilon a}}{\epsilon a}$ |
| Sphere, radiating to spot on surface | diameter | 2/3 | $\dfrac{1}{\epsilon a}\left\{1 + \dfrac{2}{(\epsilon a)^2}\left[(\epsilon a + 1)\,e^{-\epsilon a} - 1\right]\right\}$ |
| Slab | thickness | 2 | $2\left[\dfrac{1}{2\epsilon a} - \dfrac{2e^{-\epsilon a}}{\epsilon a} + 2e^{-\epsilon a} - 2\epsilon a\left[-\,\mathrm{Ei}(-\epsilon a)\right]\right]$ |
| Cylinder, diameter = height radiating to spot at center of end | diameter | .76393 | Not considered |
| Radiating to spot at edge of end | diameter | .42061 | " |
| Radiating to spot on cylinder wall halfway between ends | diameter | .70219 | " |

90

# VI. THE DESIGN OF A WATER COOLED SOLENOID

Since the use of an external magnetic field to induce arc rotation is of such importance in the successful operation of many plasma-jet facilities it behooves one to investigate the problems associated with the design of a high flux solenoid. In order to obtain field strengths of the order of 5000-10,000 gauss which are fairly uniform over volumes as large as 3000 $cm^3$ one must resort to rather high coil currents. Of course, only the total number of ampere-turns is of importance so high field strengths can be obtained by winding many turns around the volume of interest and passing only a small current through them. If the conductor is of a reasonable size, however, a large number of turns will require a power supply with an unreasonable open circuit voltage and, if to offset this, the conductor cross-section is increased the coil becomes unreasonably large. It is of interest, then, to examine the characteristics of a water cooled coil since one can then pass rather large currents through quite a small cross-section of copper with no undue heating. In fact, the coil which surrounds the present AC arc heater pressure vessel carries over 1200 amperes through a conductor cross-section of about 0. 60 $cm^2$. The temperature rise of the coil is at most about $5^o$F.

To be sure, the use of water cooled coils is nothing new but when one consults the literature one finds that the heat conduction problem which such a coil design presents is only imperfectly solved. Specifically it is assumed that at every point in the coil the coolant and the conductor are at the same temperature which is equivalent to assuming that the heat transfer coefficient of the coolant film is infinite. Herein is presented an analysis which shows that the effects of a finite heat transfer coefficient can indeed be significant. Since conservative coil design for research purposes is wasteful these differences were considered to be important.

As an analytical model consider a length of conductor in which Joule heat is being dissipated and through the middle of which exists a well defined passage to permit the flow of a coolant. The thin cross-section assumption is invoked; namely that there is no temperature gradient across either the conductor or coolant cross-sections. Then axial gradients are the only ones of importance. Furthermore the outside of the conductor is insulated so that all the Joule heat must be partially stored in the conductor and partially transmitted to the coolant. Finally, it is noted that since transient effects are unimportant in this case only the steady state is considered. The features of the model described above, are exhibited in Figure 25.

The following notation is used in the ensuing analysis:

$h$     Film coefficient of heat transfer

$p$     Perimeter of coolant passage

$\omega$     Cross-sectional area of conductor

$k$     Thermal conductivity of copper

$\rho$     Resistivity of the conductor

$I$     Current carried by the conductor

$\dot{w}$     Weight flow of coolant

$c$     Specific heat of coolant

$U$     Conductor temperature; function of x

$U_o$     Coolant temperature; function of x

The appropriate equations which govern the physics of the mathematical model described above are easily found to be:

$$\frac{d^2 U}{dx^2} - \frac{hp}{k\omega}(U - U_o) + \frac{I^2 \rho}{k\omega^2} = 0$$

(6-1)
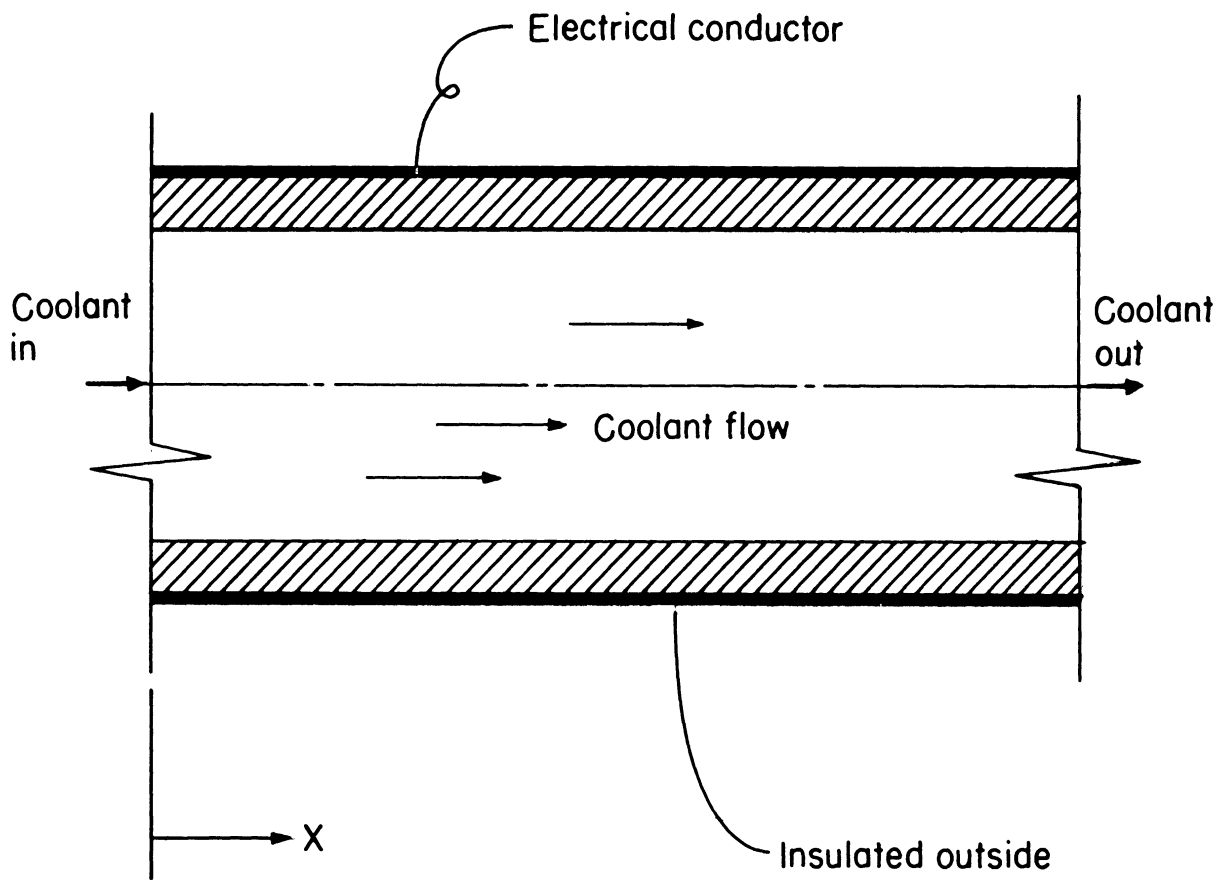
$$\frac{dU_o}{dx} - \frac{hp}{\dot{w}c}(u - U_o) = 0$$

FIGURE 25. MODEL FOR WATER COOLED COIL .

The system of Equations (6-1) simply states that all heat generated by the passage of current through the conductor is either conducted away from the element in which it was produced or transferred to the coolant. Of course the coolant temperature must rise in response to the heat which is added to it which in turn serves to limit the amount of heat which the film can pass.

Now the two equations in (6-1) can be combined to yield

$$\frac{d^2}{dx^2}(U - U_o) - \frac{hp}{k\omega}(U - U_o) + \frac{I^2\rho}{k\omega^2} + \frac{hp}{\dot{w}c}\frac{d}{dx}(U - U_o) = 0$$

Putting this equation in operator notation

$$\left(D^2 + \frac{hp}{\dot{w}c}D - \frac{hp}{k\omega}\right)(U - U_o) = -\frac{I^2\rho}{k\omega^2}\ ,\tag{6-2}$$

The characteristic equation for the homogeneous solution is easily found to be:

$$m^2 + \frac{hp}{\dot{w}c}m - \frac{hp}{k\omega} = 0$$

Upon solving the above the two roots of the characteristic equation are determined as:

$$m_1 = -a = \frac{1}{2}\left[\frac{hp}{\dot{w}c} + \sqrt{\frac{hp^2}{\dot{w}c} + 4\frac{hp}{k\omega}}\right]$$

$$m_2 = b = \frac{1}{2}\left[-\frac{hp}{\dot{w}c} + \sqrt{\frac{hp^2}{\dot{w}c} + 4\frac{hp}{k\omega}}\right]\tag{6-3}$$

The particular integral of Equation (6-2) is found by inspection and the complete solution may be written as:

$$(U - U_o) = C_1 e^{-ax} + C_2 e^{bx} + I^2\rho/hp\omega$$

In order to determine $C_1$ and $C_2$ certain boundary conditions must now be invoked. It seems reasonable to specify that at $x = 0$ there is no difference in the temperature of coolant and conductor and at $x = \ell$, where the coolant leaves the conductor, there is no gradient in their temperature difference. Mathematically this is expressed as

$$(U - U_0) = 0 \qquad \text{at} \qquad x = 0$$

$$\frac{d}{dx}(U - U_0) = 0 \qquad \text{at} \qquad x = \ell$$

Applying these boundary conditions one arrives at the following expression for $(U - U_0)$:

$$\frac{(U - U_0)}{I^2 \rho/hp\omega} = \left(1 - \frac{b\, e^{b\ell}\, e^{-ax} + a\, e^{-a\ell}\, e^{bx}}{a\, e^{-a\ell} + b\, e^{b\ell}}\right) \qquad (6\text{-}4)$$

One wishes to know, however, what the individual temperatures $U$ and $U_0$ are; not merely their difference. Recall

$$\frac{dU_0}{dx} = \frac{hp}{\dot{w}c}(U - U_0)$$

which upon being integrated yields

$$\frac{U_0 - U_i}{I^2 \rho/\dot{w}c\,\omega} = \left[x - \frac{\frac{a}{b}\, e^{-a\ell}\, (e^{bx} - 1) - \frac{b}{a}\, e^{b\ell}\, (e^{-ax} - 1)}{a\, e^{-a\ell} + b\, e^{b\ell}}\right]$$

where $U_i$ is the common initial temperature of coolant and conductor. Now since the temperature of both coolant and conductor will be a maximum at $x = \ell$ and since it is this temperature which determines the design of the coil one sets $x = \ell$ and obtains

$$\frac{U_o - U_i}{I^2 \rho \ell / \dot{w}c\omega} = \left[ 1 - \frac{\frac{a}{b}e^{-a\ell}(e^{b\ell} - 1) - \frac{b}{a}e^{b\ell}(e^{-a\ell} - 1)}{a\ell\, e^{-a\ell} + b\ell\, e^{b\ell}} \right]$$

(6-5)

$$\frac{U - U_o}{I^2 \rho / hp\omega} = \left[ 1 - \frac{(a + b)\, e^{-(a-b)\ell}}{a\, e^{-a\ell} + b\, e^{b\ell}} \right]$$

where one notices

$$(U - U_i) = (U - U_o) + (U_o - U_i)$$

For arbitrary values of a$\ell$ and b$\ell$ the equations have quite a complicated behavior but if one allows both of these quantities to become rather large much simpler relations are obtained and the following asymptotic formulae are easily obtained:

$$\frac{U_o - U_i}{I^2 \rho \ell / \dot{w}c\omega} \cong 1 + \mathcal{O}[(a\ell)^{-1}] \quad , \qquad (a\ell), (b\ell) \rightarrow \infty$$

$$\frac{U - U_o}{I^2 \rho / hp\omega} \cong 1 + \mathcal{O}(e^{-a\ell}) \quad , \qquad (a\ell), (b\ell) \rightarrow \infty$$

From the above expressions it is seen that as h becomes very large (which need not be implied by large a$\ell$ and b$\ell$) the difference between conductor and coolant temperatures goes to zero in which case the relations widely found in the literature apply. Specifically one then has

$$U_o = U = I^2 \rho \ell / \dot{w}c\omega$$

As was mentioned earlier, however, it will often be the case that $(U - U_o) \neq 0$ and the more exact expression will have to be considered. This is of importance since a knowledge of the coolant temperature alone is not sufficient for many coil designs. To be sure, one wishes to avoid coolant boiling but since the resistance

96

of the coil (and hence the coil current when connected to a constant potential power supply) is significantly affected by the conductor temperature it is this latter value which is of prime importance. It should be mentioned that the temperature effect upon resistivity could easily have been included in the initial set of equations (1) but the resulting characteristic equation is a cubic and not readily solvable in general.

The foregoing analysis has been used with considerable success in the design of the large solenoid surrounding the low-pressure arc heater and in several other less critical applications such as water cooled ballast resistors. Of course, there is more to the problem of final coil design such as that of determining the coolant flow rate, $\dot{w}$, when a certain pressure head is imposed on a selected length of conductor and determining the field strength which would result from a coil with a given number of ampere-turns and a given geometry. All of these considerations must be taken simultaneously in order to arrive at a suitable solenoid design but only the coil heating problem presents any unconventional aspects.

# VII. HIGH PRESSURE ARC-HEATER DESIGN

As previously discussed in Reference (12), the design of the high pressure arc heater will follow along the lines of the low pressure arc heater suggested in Section VIII.

Reiterating, its design will be approximately the same size as the above-mentioned unit, again using a Helmoltz pair for the DC magnetic field with the electrodes entering the arc-chamber between the field coils. The arc chamber will be flanged on the front to accept a nozzle and on the back to support an air inlet and baffling system.

As this unit will be the main tool for studies in high pressure arc-heater phenomenon, consideration is being given to the possibility of incorporating into its design, supporting devices for a radiation shield. Also the feasibility of placing a viewing port in the front or aft flange is being studied.

Because the new arc-heater will be subjected to both high temperature and high pressure, structural materials other than copper are being investigated. To date, it appears that the only material with the necessary thermal conductivity plus strength at elevated temperatures is a copper alloy. Both a copper-zirconium alloy and a copper-chromium alloy meet these specifications. Both are available in the billet form. However, it is anticipated that finding a company to fabricate the size chamber which is required, out of either of these materials, will be difficult. Therefore two concurrent structural and thermal analysis are being made. One, assuming that standard OFHC copper will be the structural material, the other assuming that copper-zirconium will be the structural material. Also, difficulties are anticipated in finding an electrode gland to withstand these pressures and temperatures.

Associated with the electrode gland problem is the effect on chamber stress concentrations created by having the six gland openings in the side of the chamber. This, of course, will be the weakest part of the chamber from the standpoint of both pressure stress and thermal stress. To help alleviate this problem, the possibility of supporting and supplying each electrode from only one gland is being studied. This will cut the openings into the side of the chamber down to three, spaced $120^{\circ}$ apart. This will require that each electrode leg will have to serve as both the water inlet and outlet. Figure 26 shows a sketch of one possible method for achieving this.

With the desirability of higher magnetic fields at high pressure arc-heater operations, it is quite apparent that the length of the chamber will be strongly governed by the DC field strength, i. e., the physical size of the field coils needed to produce the desired field. This is especially true of the front coil of the Helmoltz pair which governs the length between the front arc chamber flange and the location of the electrode glands. The aft closure on the chamber can be made anywhere along the axis of the back DC field coil. This could, however, locate the aft closure flange closer to the electrodes than the front closure, thereby increasing the thermal protection for the aft closure. This again may indicate a need for a baffle or injector system which would also serve to shield the aft closure. Also, if copper-zirconium is used as the structural material the maximum length of the chamber will be dictated by the length of billet of copper alloy available from the manufacturer, which is in the vicinity of thirty inches. Therefore, there will be a trade off between desired field strength, structural material, chamber size and chamber cooling.

The above should indicate that any one of a number of desired parameters could dictate the overall design of the remaining parameters. Therefore the influence of a number of these parameters on what can be called the desired high pressure arc-heater operation is being studied. It is felt that the final design and fabrication of the high pressure arc-heater should not be expedited until a number of the pertinent design parameters has been thoroughly investigated.
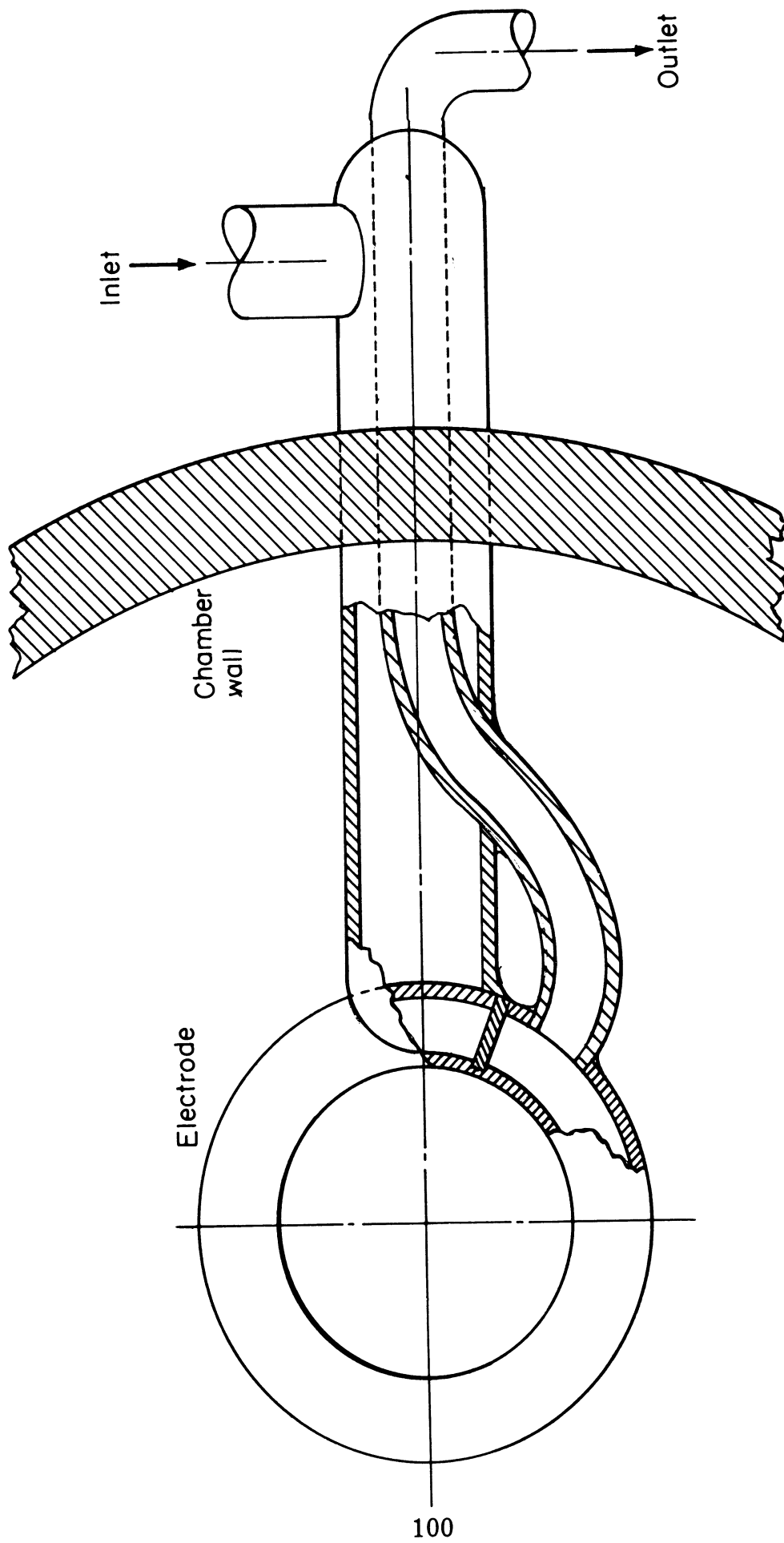
Outlet

Inlet

Chamber
wall

Electrode

100

FIGURE 26. UNITARY ELECTRODE.

# VIII. GENERAL DESIGN CONSIDERATIONS

In this section the design of a typical, low pressure, three phase, AC arc heater is presented. Since the design study was originally performed for a rather specific purpose, this section is quite self-contained.

## A. ARC-HEATER DESIGN

The arc-heater will consist of three major items; the arc-heater body, electrodes and magnetic field coils. Each of these items will be treated as a single unit and recommendations as to their design and operating characteristics will be given in the following paragraphs. Two possible starting techniques are presented.

### Arc-Heater Body

The arc-heater body will require; a main cylindrical body enclosing and supporting the electrodes, a converging nozzle to duct the hot air flow to the three inch inlet in the pebble bed heater, and an aft closure flange, housing the air inlet and supporting an air baffle. See Figure 27.

For ease in arc-heater construction and monitoring of cooling water temperature it is felt that each of these units should have its own cooling water inlet and exit. It is quite conceivable however that the inlets could have a common supply and a common drain.

The arc heater main body consists of a copper inner shell, cooling passage and outer copper shell. A typical cross section of the chamber body is shown in Figure 28. The arc-heater body shown is to be properly flanged top and bottom to accept the aft closure flange and the converging nozzle. By necking the arc-heater body into the aft closure flange, the removal or replacement of the magnetic field coils will be greatly simplified.
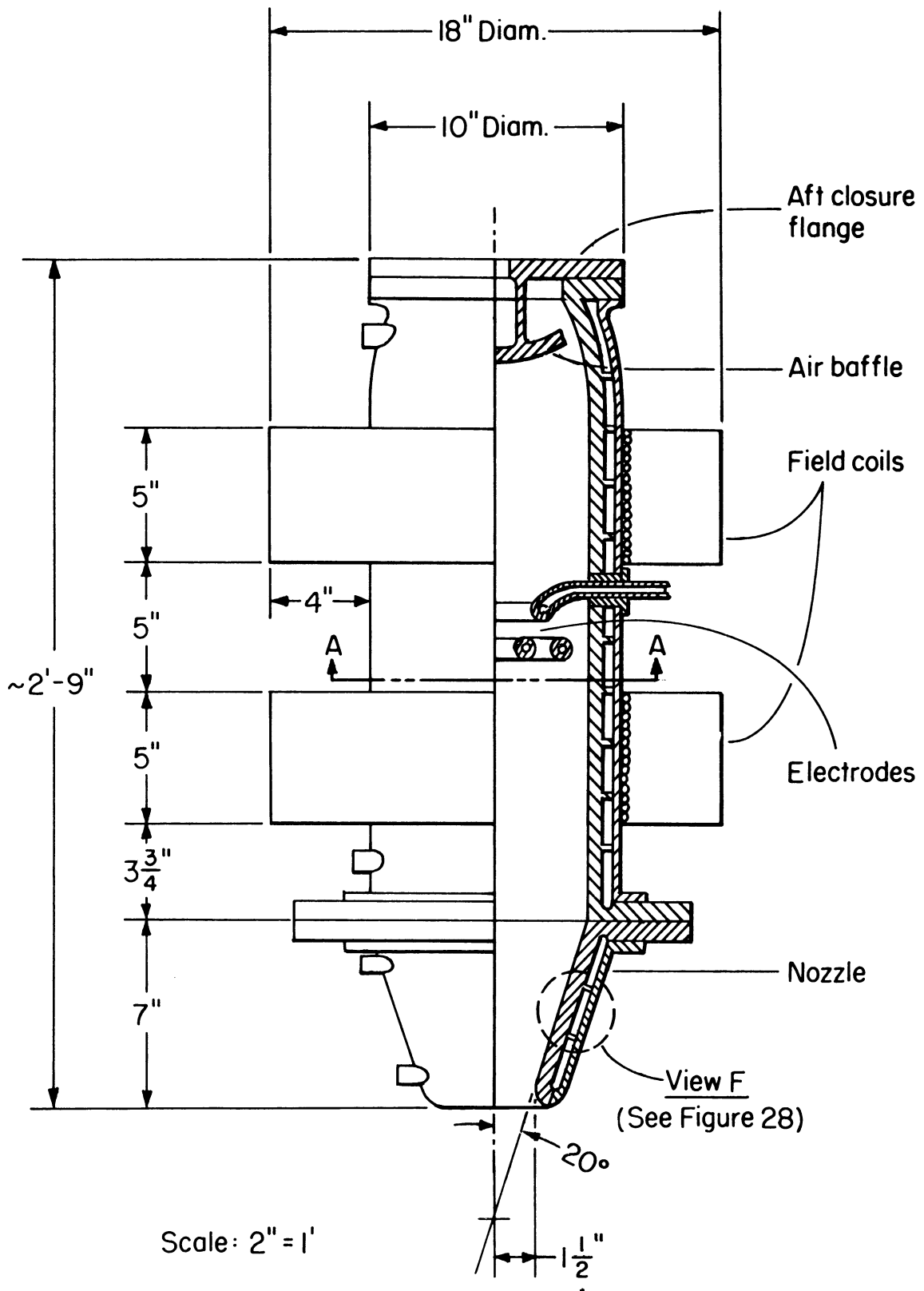
101

FIGURE 27. ATMOSPHERIC PRESSURE ARC-HEATER.

Arc-heater
center line (Ref.)

2"

$\frac{5}{8}$"

$\frac{3}{8}$"

$\frac{1}{4}$"
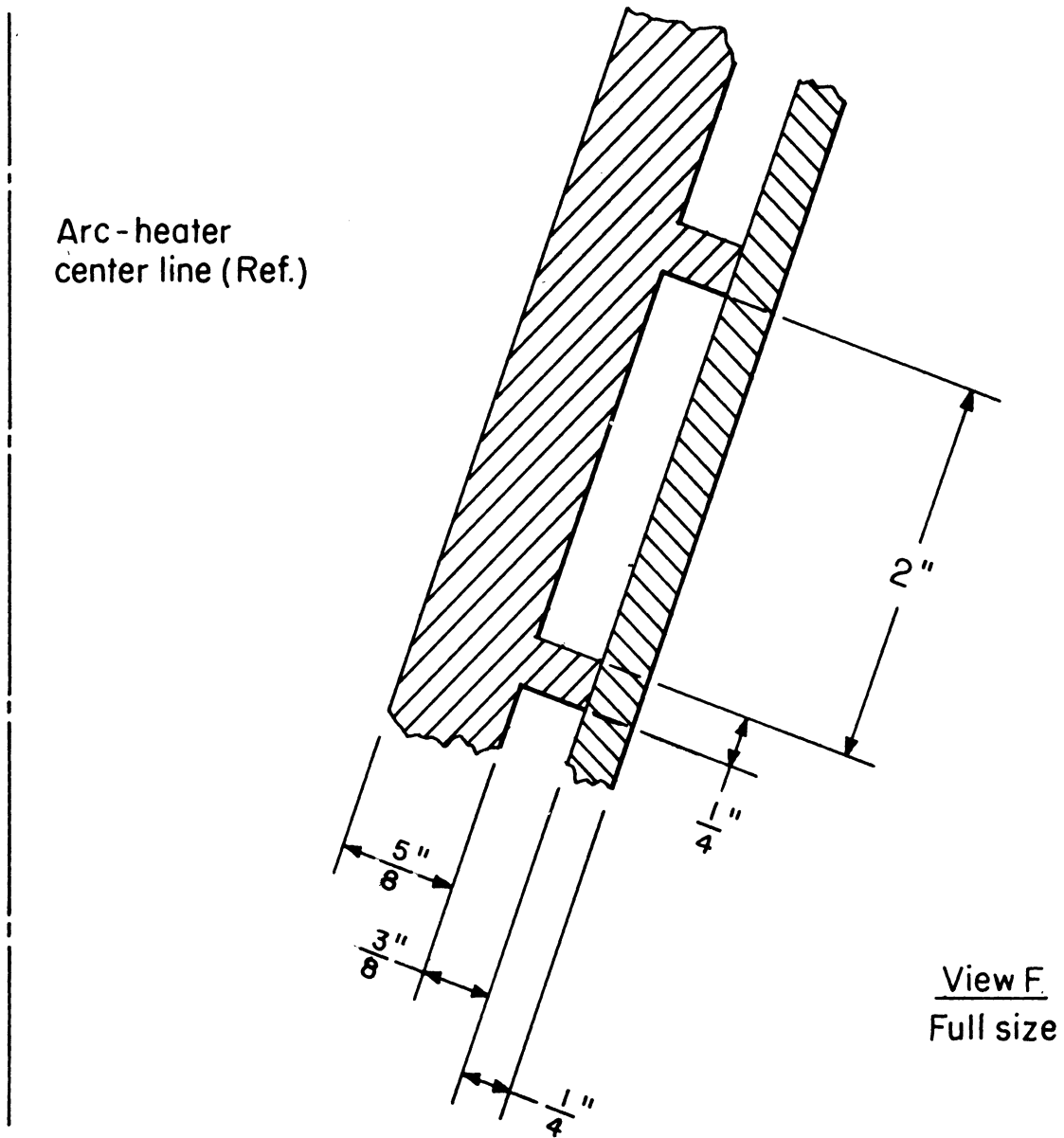
$\frac{1}{4}$"

View F.
Full size

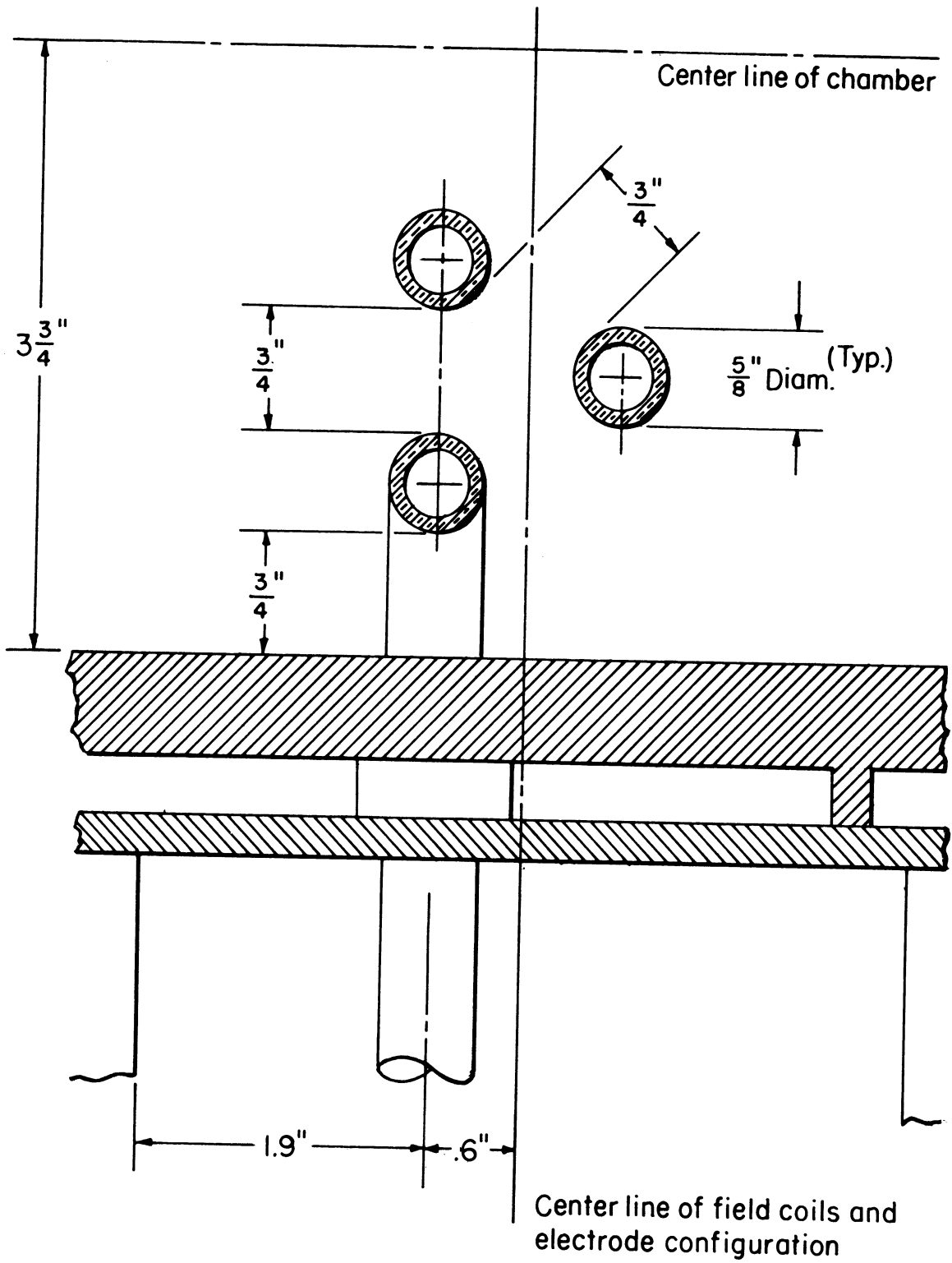FIGURE 28. CROSS SECTION VIEW OF ARC-HEATER BODY.

103

By using a Helmholtz pair for field coils it (as well as producing a more uniform magnetic field) will leave an open area directly over the electrodes. This area will be used for installation of electrode glands. These glands will support and position the electrodes and starting system. As each electrode has two supporting legs, through which cooling water and AC power pass, there will be a need for three pairs of electrode glands. Each pair should be spaced $120^O$ around the circumference of the arc-heater body, with the starting gland located half way between the aft most pairs $(60^O)$. Spacing of the electrode and starter glands axially between the field coils is shown in Figures 30 through 33. It is felt an electrode gland similar to that made by the Conax Corporation in Buffalo, New York, could be adapted to this configuration. Sufficient room will be needed between the lower field coil and the lower arc-heater flange to allow for a cooling water inlet and its necessary connections.

Adequate chamber cooling can be realized by supplying the cooling passage with the "house" water supply through a one inch inlet. The cooling configuration recommended is a spiraling rectangular passage beginning at the water inlet above the lower flange and ending at the water outlet below the aft closure flange.

The type of arc-heater construction used in our three phase arc-heater facility could also be used in this design. This would be to (1) centrifugally cast the inner shell with the cooling passages as an integral part of it, (2) centrifugally cast the outer shell with sufficient tolerance to be able to slide the outer shell over the inner shell forming the body and cooling passages in two pieces. Joining would be at the upper and lower flanges. A pressure tap into the arc-heater chamber should also be provided.

Nozzle

Because the only means of introducing the arc-heated gases into the pebble bed will be through the existing inlet, a converging nozzle is required on the arc

Center line of chamber

$3\frac{3}{4}''$

$\frac{3}{4}''$

$\frac{3}{4}''$

$\frac{3}{4}''$

$\frac{5}{8}''$ Diam. (Typ.)

1.9"   .6"

Center line of field coils and
electrode configuration

Scale: Full size

FIGURE 30.   ELECTRODE SPACING AND SUPPORT
(Section B-B, Figure 29).

105

Center line of chamber

$3\frac{3}{4}''$

$\frac{3''}{4}$

$1\frac{1}{16}''R.$

$\frac{3''}{4}$

Center line of field coils and
electrode configuration

$\frac{7''}{8}$
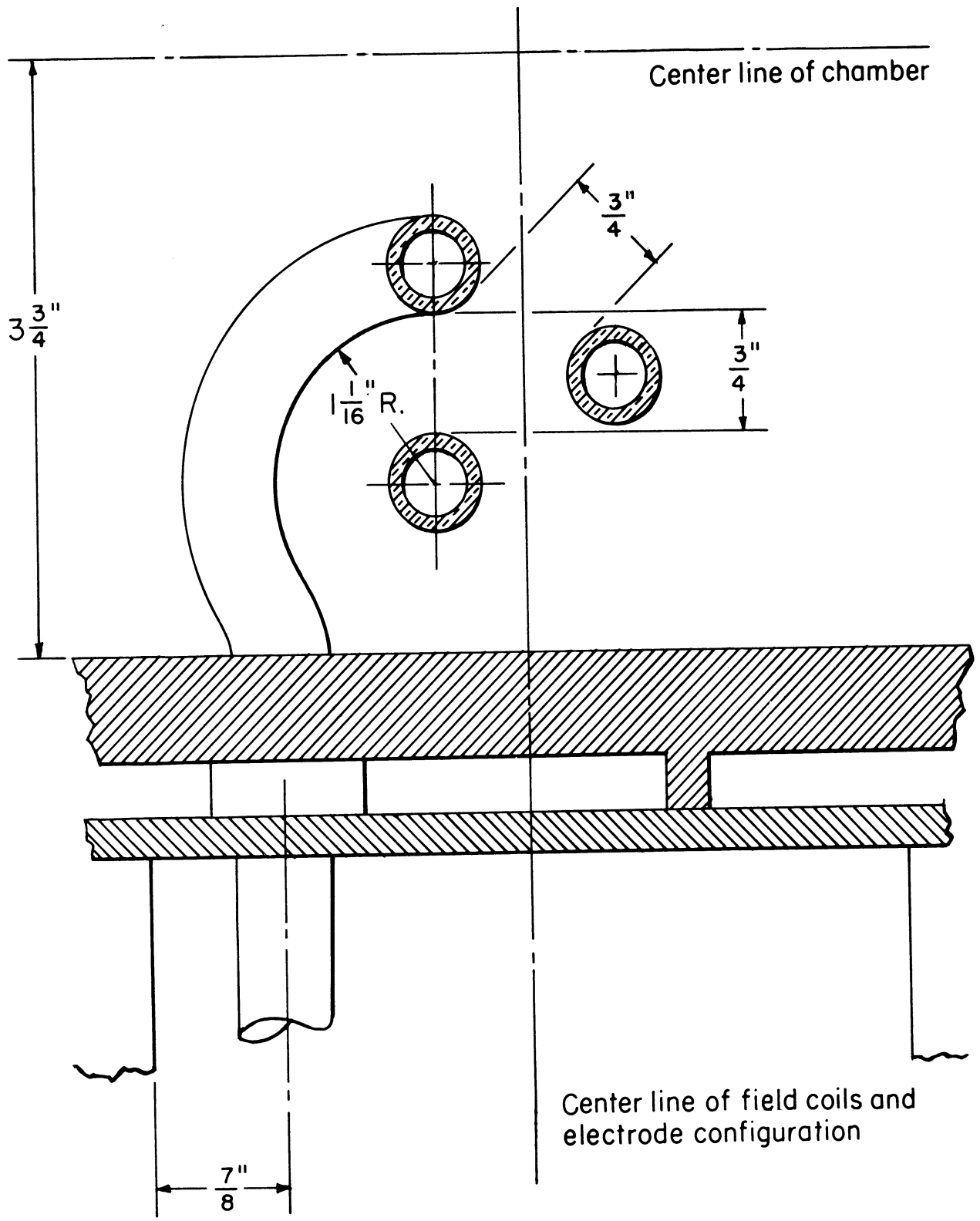
Scale: Full size

FIGURE 31.  ELECTRODE SPACING AND SUPPORT
(Section C-C, Figure 29).

106

Center line of chamber

$3\frac{3}{4}''$

$\frac{3}{4}''$

$\frac{11}{16}''$ R.

Center line of field coils and electrode configuration

$\frac{7}{8}''$
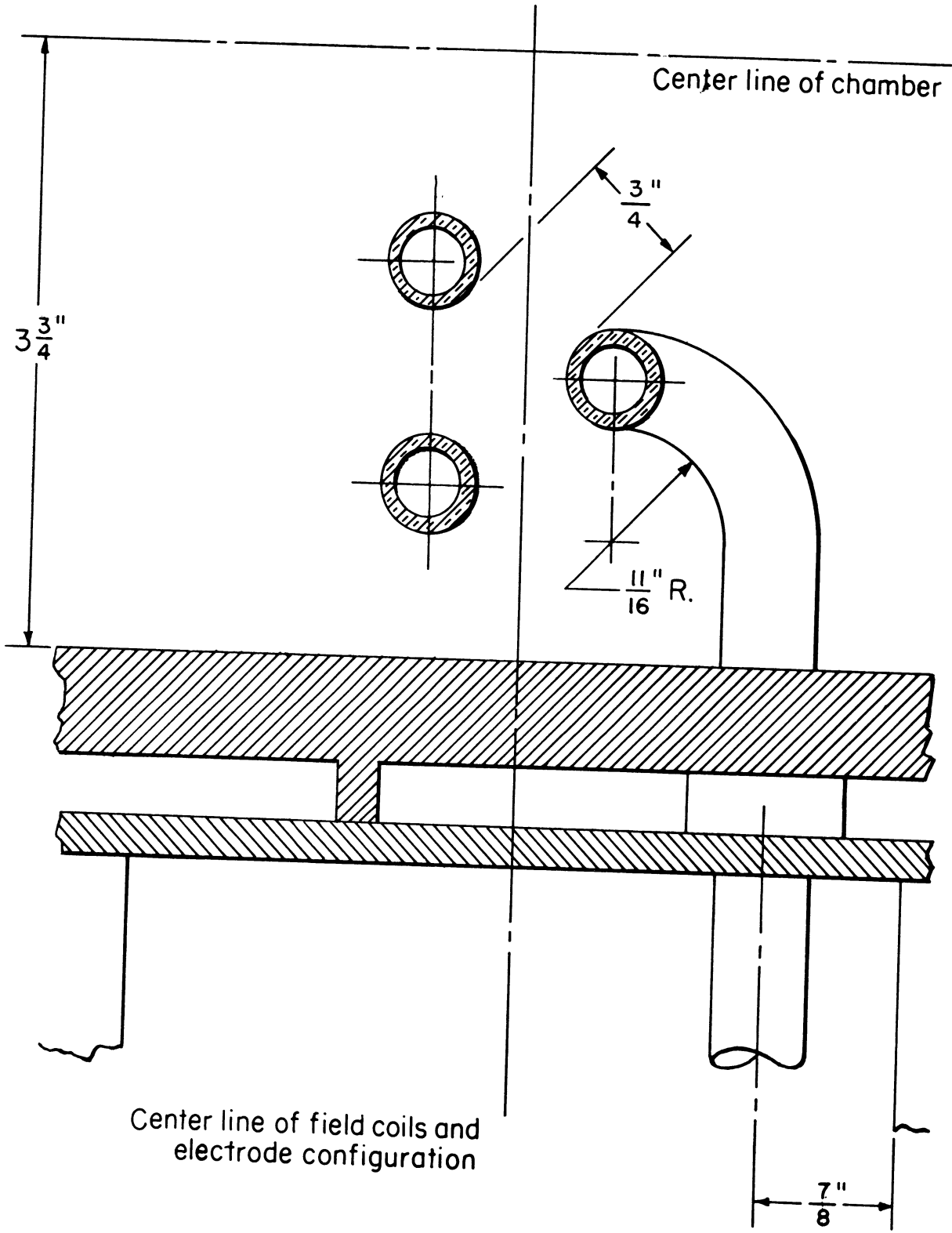
Scale: Full size

FIGURE 32. ELECTRODE SPACING AND SUPPORT
(Section D-D, Figure 29).

107

Center line of chamber

$3\frac{3}{4}''$

60°

$\frac{1}{2}''$

Center line of starter

Center line of field coils and
electrode configuration
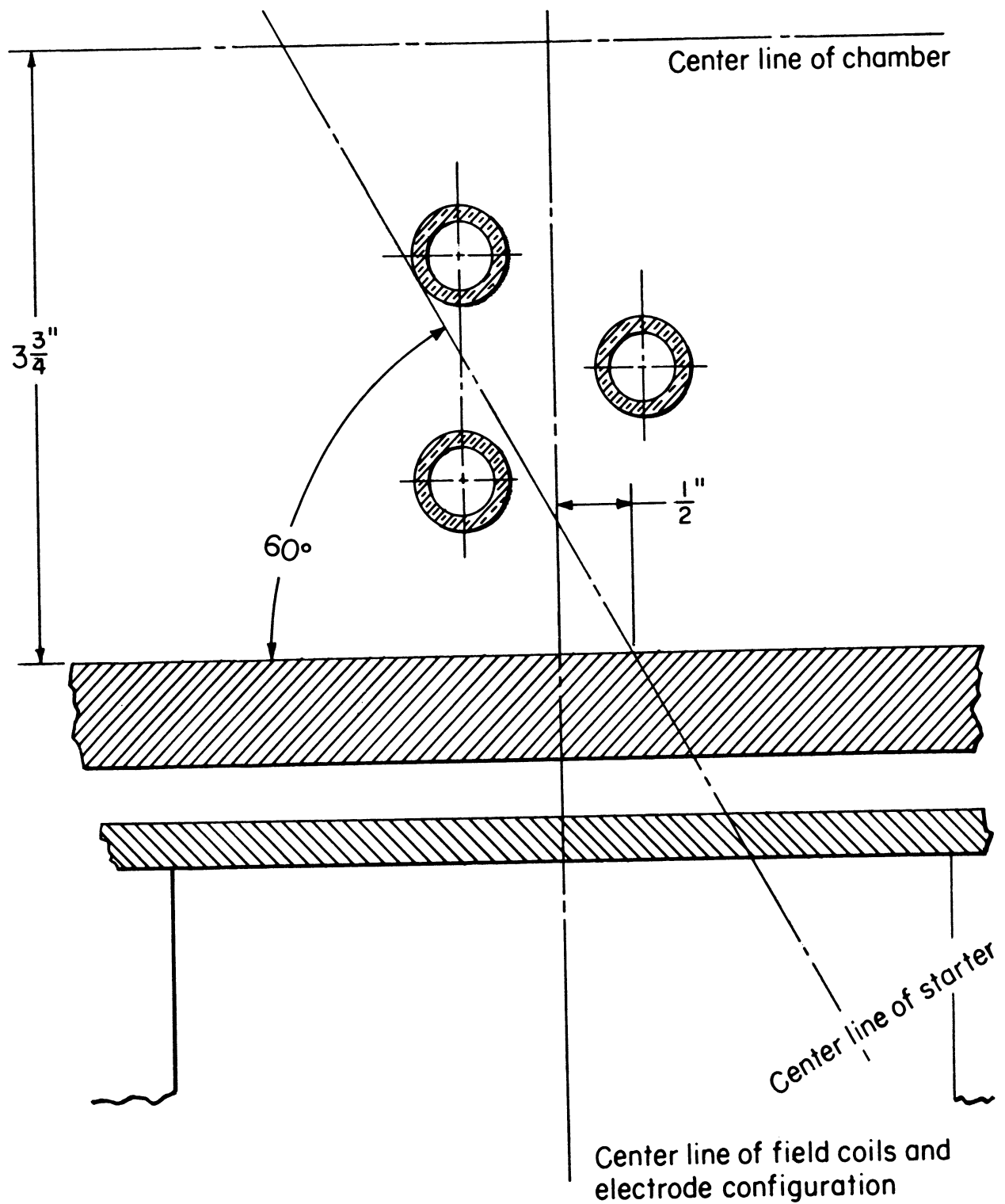
Scale: Full size

FIGURE 33. STARTER REFERENCE
(Section E-E, Figure 29).

108

heater. The nozzle recommended is conically shaped with a half angle of $20^{\circ}$.
It will reduce the I. D. of the arc heater from 7 1/2 inches to the required
3 inches; Figure 27.

The converging nozzle, as in the case of the arc heater body would consist
of a copper inner shell with cooling passages and a copper outer shell. The noz-
zle body cross-sectional dimensions will be the same as those for the arc heater
body; Figure 28.

Nozzle cooling will be identical to that used in the main arc heater body with
the same type and size of cooling water inlets, passages and outlets.

Centrifugal castings can also be used for the nozzle components. Again the
cooling passages and inner shell can be made as one casting. In the construction
of the nozzle body, provisions should be made, for a pressure tap and thermo-
couple tap near the nozzle exit.

Aft Closure Flange

Although it was first suggested that the arc heater be open in the back, with
the pressure vessel and arc heater sharing one air source, this arrangement will
create serious flow and control problems. Therefore, an aft closure flange is
needed. The aft closure flange will create a unit with its flow control completely
separate from the one used by the pressure vessel. This flange would also be
made of copper. It would house the arc heater air inlet and provide the means
for supporting the baffle system. Provision for cooling the flange should also
be incorporated.

Air Baffle System

The air baffling system should be designed to destroy most of the axial veloc-
ity component of the incoming air. The one shown is dish shaped, allowing the
air to pass through an annular opening between the baffle and the inner chamber
wall. It is suggested that it be supported by the aft closure flange and constructed
of either Boron Nitride or copper. If made of copper it must be water cooled.
It could get its cooling water from the aft closure flange with the baffle supporting

legs serving as water inlets and outlets. The axial location of the baffle will depend on the final baffle design, material used, and the arc stability at high mass flows.

## Electrode Design

The electrode configuration for the arc heater is shown in Figures 29 through 33. It consists of three circular hollow copper rings so arranged in the axial plane to form an equilateral triangle. This gives the best arc current to magnetic field orientation. The electrode spacing is 3/4 inch.

Each electrode consists of a hollow ring and two supporting legs made of 5/8 inch O. D. general purpose temper copper tubing with approximately .1 inch wall thickness. These legs will support each electrode as well as provide the means for cooling the electrode and supplying it with AC power. The electrode is closed off internally between the supporting legs to give a cooling water flow in one direction, thereby making one of the legs a water inlet and the other the outlet. All electrode configurations to date, used in our three phase arc heater facility, have had the AC power connections on the cooling water inlets.

To date, the most successful method of fabricating the electrodes has been to make each supporting leg and electrode ring a continuous series of bends, free of any intermediary joints or corners. The only joints would be where the legs join the electrode ring and where the electrode ring closes on itself. It is recommended that this closure be between the points where the electrode legs fasten to the ring. The internal closure, previously mentioned should be made in this area also. The only successful method of making the leg to ring joints has been to use heli-arc welding. This method leaves the joint free of leaks and internal flaws. All joint surfaces should be smooth and free of protuberances or indentations.

As the consistancy of the electrode spacing is somewhat critical the electrodes should be held circumferentially to within .050 inches.
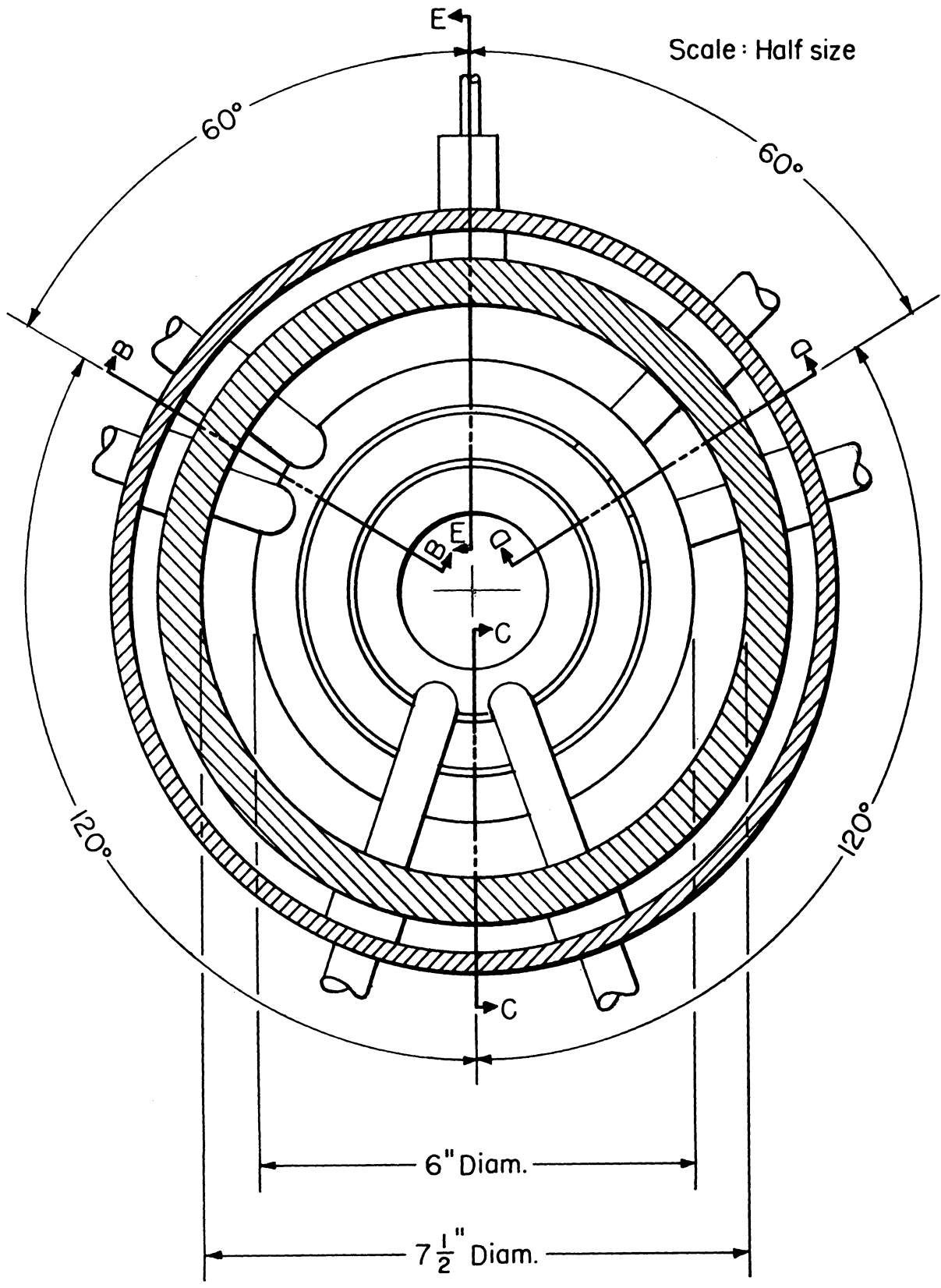
FIGURE 29. ELECTRODE CONFIGURATION
(Section A-A, Figure 27).

111

Approximately 50 gpm at 300 psig should adequately cool all three electrodes. Seeing that the water inlet and AC power connection are one in the same, it would be desirable to have a type of cable which would bring in both power and water in the same unit. Such a unit is commercially available. Although the name of the supplier is not known, the Plasmadyne Corporation does use this type of power-cooling water cabling on their Plasmatron units.

## Magnetic Field Coils

The recommended field coil configuration is that type normally referred to as a Helmholtz pair. Strictly speaking, a Helmholtz coil is a pair of identical solenoids separated by a distance equal to their mean radius. The advantage of this arrangement is that a very homogeneous magnetic field is produced in the space between the solenoids. In addition, this intervening space can be used to facilitate the insertion and withdrawal of water and power leads to the arc-heater electrodes.

The proposed coils are made from standard wall 1/4 inch copper tubing which has a nominal conductivity of 85% of IACS. Naturally, the tubing chosen must have some type of insulation to prevent a turn-to-turn short circuit. There are three alternative ways of providing this insulation.

The first way would be to buy the bare copper tubing and insulate it by 50 foot lengths with a product known as "Scotchtite" heat reactive tubing made by 3-M. This is a vinyl tubing which is shipped in diameters substantially larger than that attained after shrinking by the application of heat. It has a dielectric strength of 950 volts per mil and can operate at temperatures up to $105^{\circ}$C. This method of insulation, however, is rather clumsy and time consuming. The closest representative is in Cincinnati at 4835 Para Drive.

Another method would be to buy the bare copper tubing and have it coated with "Formvar" or "Nyclad." The advantage of this coating is that it is extremely abrasion resistant and can be applied in thin layers; about .003 inch.

Finally, there is available a copper tubing which is already covered by about
.020 inch of polyvinlychloride. This is sold by the Crescent Insulated Wire and
Cable Company, Trenton, New Jersey. Use of this product would probably afford
the simplest means of winding the coils.

It is suggested that the coil be fabricated by forming 50 foot lengths of the
insulated tubing into co-planar spiral "pancakes." The inside diameter of each
"pancake" will be slightly larger than the O. D. of the copper liner and will have
about an 18 inch outside diameter. Each half of the Helmholtz pair will consist
of 20 such "pancakes" placed side by side and connected electrically in series.
The coils should be cooled from a common manifold which supplies fresh cooling
water for every 100 feet of tubing length. That is, while all 20 pancakes are con-
nected electrically in series, only two pancakes may be series connected for water
flow. The computations supporting this statement may be found in Appendix A.
The multiple pancake method of coil fabrication offers many advantages over con-
ventional solenoid construction. In the event that an accidental overload should
occur in the coil circuit only that portion of the coil (perhaps one or two pancakes)
which has been damaged need be replaced rather than rewinding a whole coil.
Various series-parallel electrical hook-ups can be devised to vary the coil im-
pedance and the magnetic field geometry and strength. Finally, the coil can
easily be added to should higher field strengths become necessary.

As shown in Figure 27, each half of the Helmholtz pair will have a rectangular
cross-section of about 4 x 5 inches. For a coil current of 540 amperes the mag-
netic field strength at the electrode location will be somewhat greater than 4800
gauss.

Magnetic Field Strength

To determine the field strength that will result from the coil design, one can
consult the NASA report of Callaghan and Maslen (Reference 13). Knowing the
total number of ampere-turns in the coil, the field due to each solenoid is added

to obtain the total field at the electrode location. Each pancake will contain about 15 turns so that each half of the Helmholtz pair will provide about 81,000 ampere turns at the lower current and 162,000 ampere turns at the higher level (see Appendix A). The corresponding field strengths at the electrode location are about 2400 gauss and 4800 gauss respectively. Based upon the experience gained at this laboratory, even the lower field strength should insure a rather long electrode life.
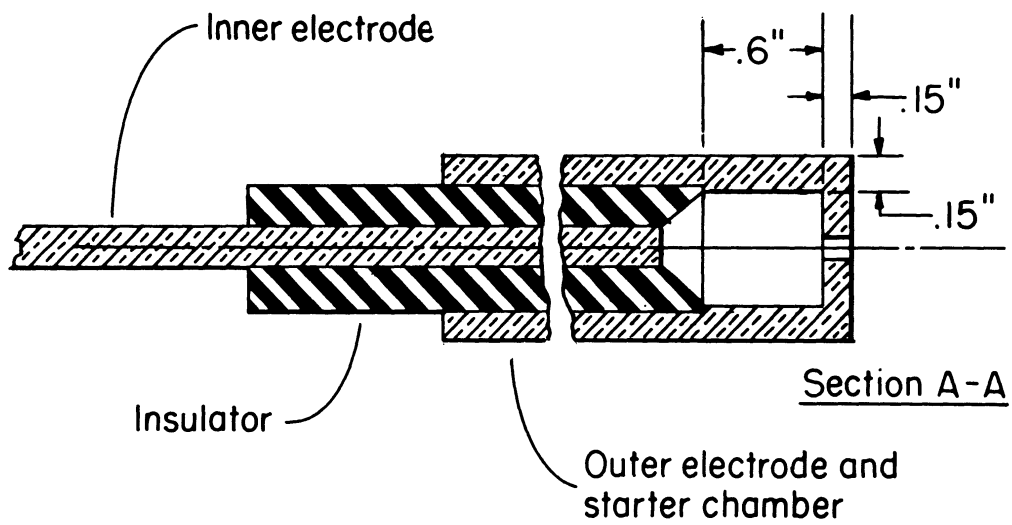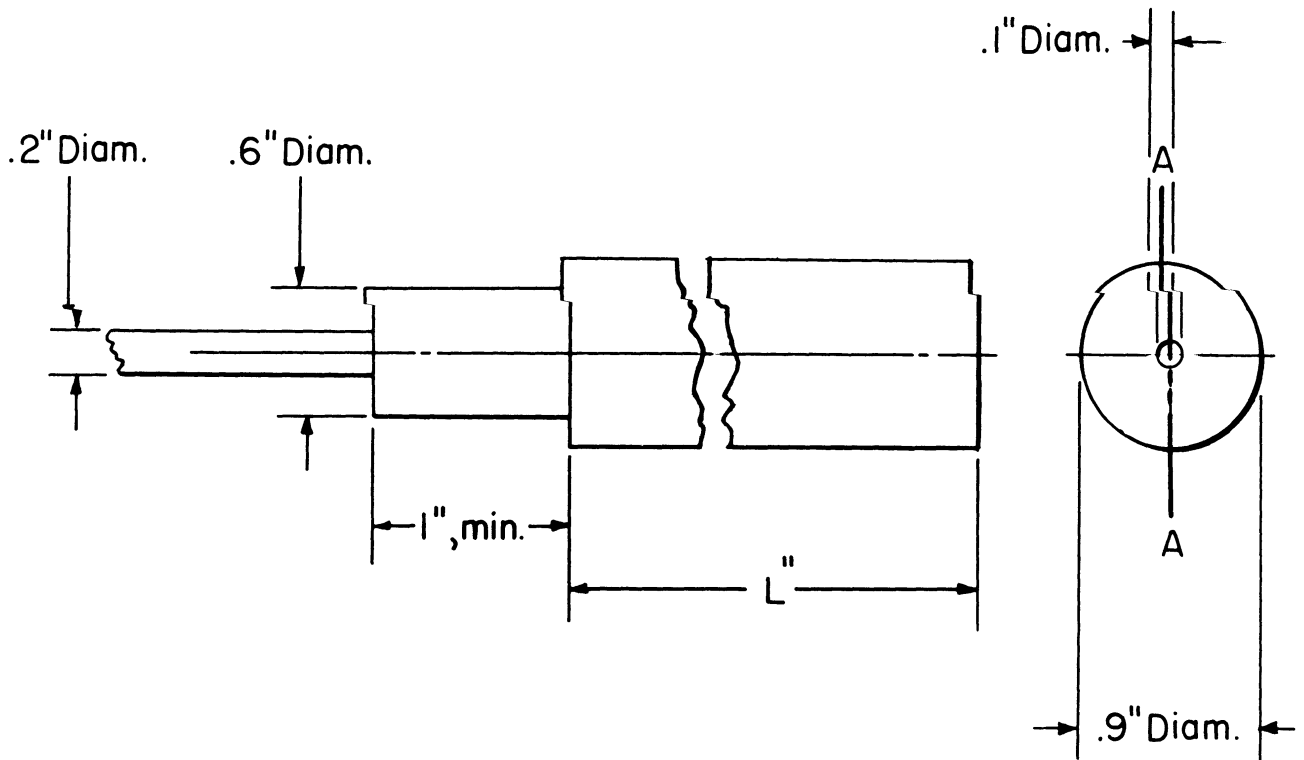
## Starting Techniques

Described herein will be two arc heater starting techniques, either of which can be easily adapted to the starting gland. Both starters use the same phenomena for initiating an arc across two electrodes, namely shorting across them with a gaseous conductor. Only the means of creating the conductor is different. Both methods will lend themselves to automatic control and operation.

One method would be to create a plasma, by discharging a high energy source in an enclosed chamber with a small nozzle at one end; Figure 34. The heating of the gas and its associated expansion would drive the plasma out the small nozzle. Upon striking two of the arc heater electrodes, it would initiate the main arcs.

A starter using this method was designed, built and tested for use in our three phase arc heater facility. The energy source was a bank of capacitors with a storage capability of 2700 joules. The capacitors were charged to between 20 kv and 30 kv. This would, for the configuration shown, produce a plasma column from 3 to 6 inches long. This device has successfully started our small test arc. Due to the difficulties of physically installing the unit in our large arc heater it has not been tested in that specific application. A schematic diagram of the necessary circuitry is shown in Figure 35.

The second method would be to use a oxy-acetylene torch, with the plasma thereby created serving the same purpose as mentioned above. This would

.2"Diam.    .6"Diam.

.I"Diam.

|← I",min. →|

L"

.9"Diam.

Inner electrode

.6"

.I5"

.I5"

Section A-A

Insulator

Outer electrode and
starter chamber

Electrodes material : Copper

Scale : Full size
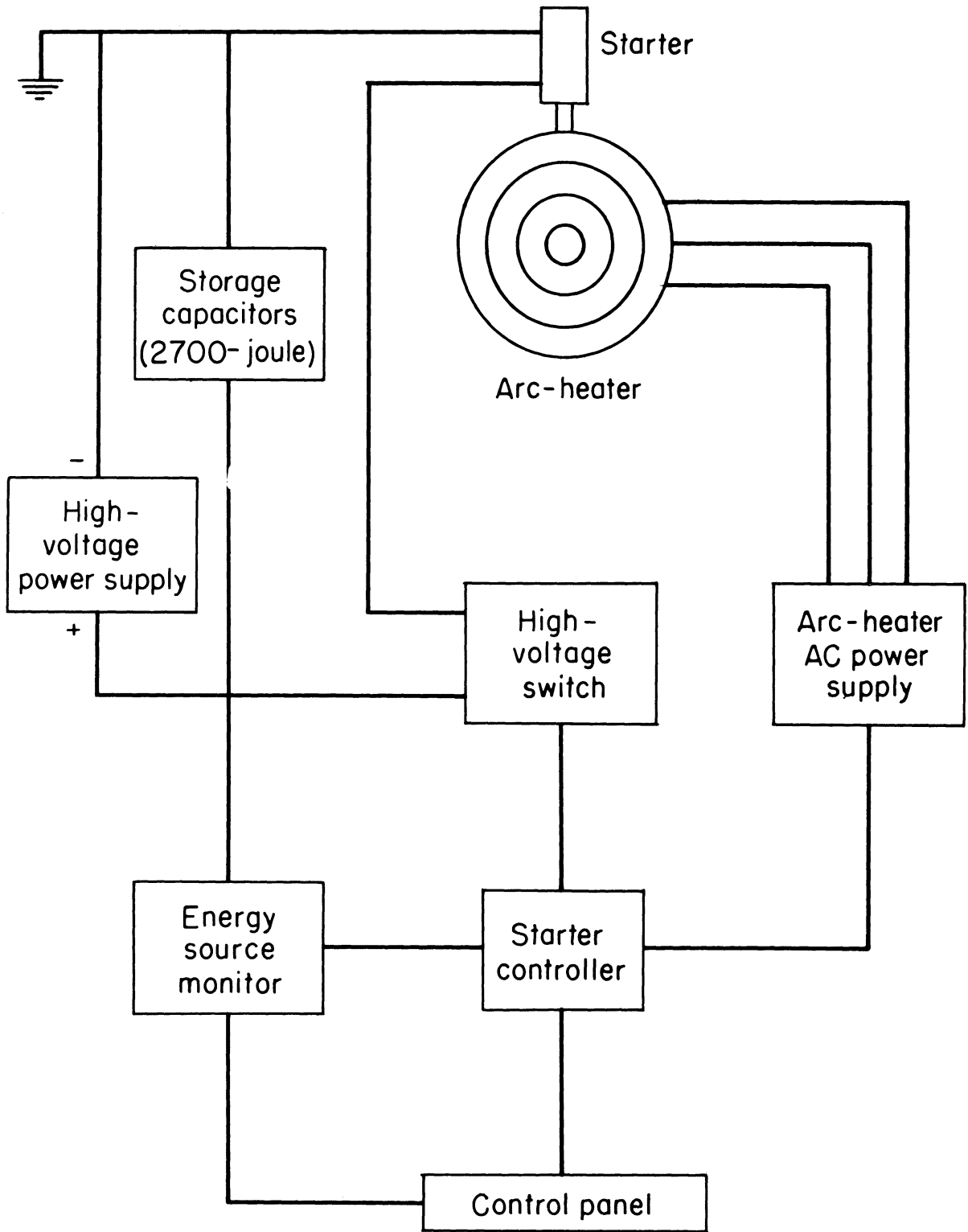
FIGURE 34. CAPACITIVE STARTER.

FIGURE 35. SCHEMATIC DRAWING OF CAPACITIVE STARTING.

116

require a dual gas system, oxygen and acetylene, introduced into a small mixing chamber, ignited, and the flame directed across the electrodes. Ignition of the gaseous mixture can be accomplished by using a small spark plug. A schematic for this starter is shown in Figure 36. This method also has successfully started our test arc, but for the reason mentioned above has not been used in our large arc heater.

As mentioned earlier, either system can be installed in the area of the arc heater body shown for the starter. If so desired, either one can be made as an integral part of the arc heater body rather than using a gland to position and support it.

## B. RECOMMENDED INSTRUMENTATION AND STARTING PROCEDURE

There are certain basic instruments and controls which have been found to be essential to the operation of an arc heater facility of the type described herein. First, of course, one must have the common electrical switchboard instruments which indicate line current and line voltage. Suitable potential and current transformers should be utilized in conjunction with these instruments with one side of their secondaries grounded. In addition, the cases of the instruments are normally grounded.

A recording kilowatt-meter has been found to be quite useful since it is a sensitive indicator of the conditions prevailing within the arc chamber. By hooking the voltage coils of this instrument directly across the electrodes one can measure only arc power and exclude the copper losses associated with the external circuit. A dual recording KW meter and KVAR meter is used at this laboratory since the power factor of the circuit can be determined from these two readings.

In order to monitor the flow of the cooling water to the various cooled components several rather good flow meters will be required. It will be
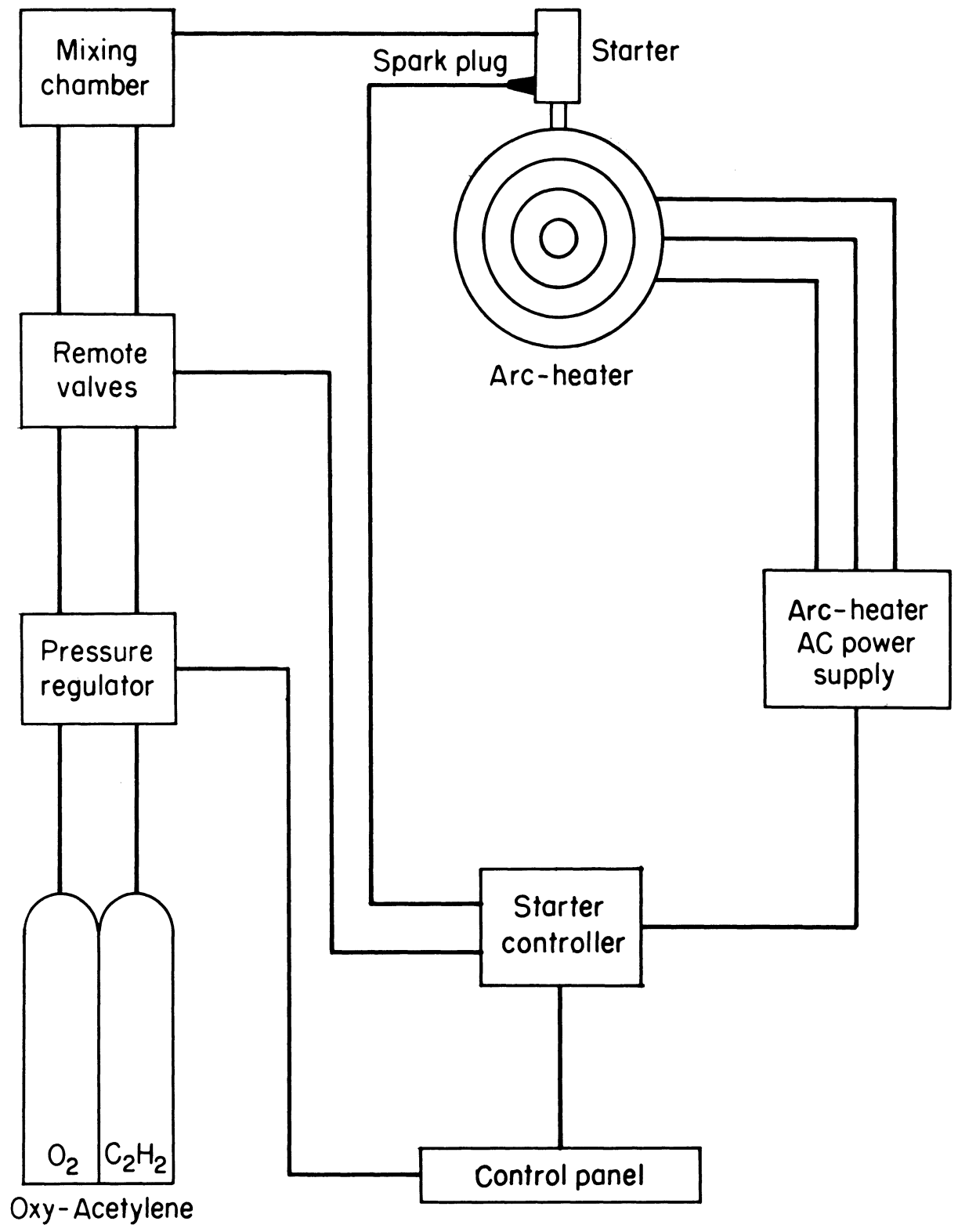
FIGURE 36. SCHEMATIC DRAWING OF OXY-ACETYLENE STARTING.

118

helpful if each of these flow meters is equipped with a microswitch such that the power to the arc will be interrupted should the flow rate fall below some specified value. The closing of the microswitch could activate some type of lock-out relay which would then have to be reset after it opened the main circuit.

In order to determine the system efficiency it will be necessary to monitor the inlet and exit temperature of the cooling water for each component. A multiple station thermistor system (as made by Fenwal) would be ideal for this purpose. The cooling water temperature rise coupled with an appropriate flow rate can indicate the approximate power loss to that particular item. When all power losses have been accounted for one can reasonably assume that the balance of that power read on the KW meter is in the arc heater effluent.

The air supply system for the arc heater should include the following components: (1) a Grove pressure regulator which delivers a flow at a preset downstream pressure, (2) a throttling valve downstream of the Grove which acts as a sonic orifice to prevent pressure fluctuations in the arc chamber from influencing the mass flow and (3) a reliable flow meter for measurement of arc heater mass flow. A recommended installation scheme for this equipment is shown in Figure 37. The throttling valve should be electrically actuated so that flow adjustments can be made remotely during operation.

The instrumentation and control requirements for the magnetic field coil are slight. While it will not be necessary to monitor the rate of cooling water flow through the coils there should be a pressure or flow switch in the system which will turn off DC power in the event of a loss of cooling water. Since the arc should not continue to run without the presence of a magnetic field the same signal which turns off the DC power should interrupt the main power to the arc. Again, this is a matter of a simple relay system. It would be quite useful to bury one or two thermistors in the magnetic field coil, which upon
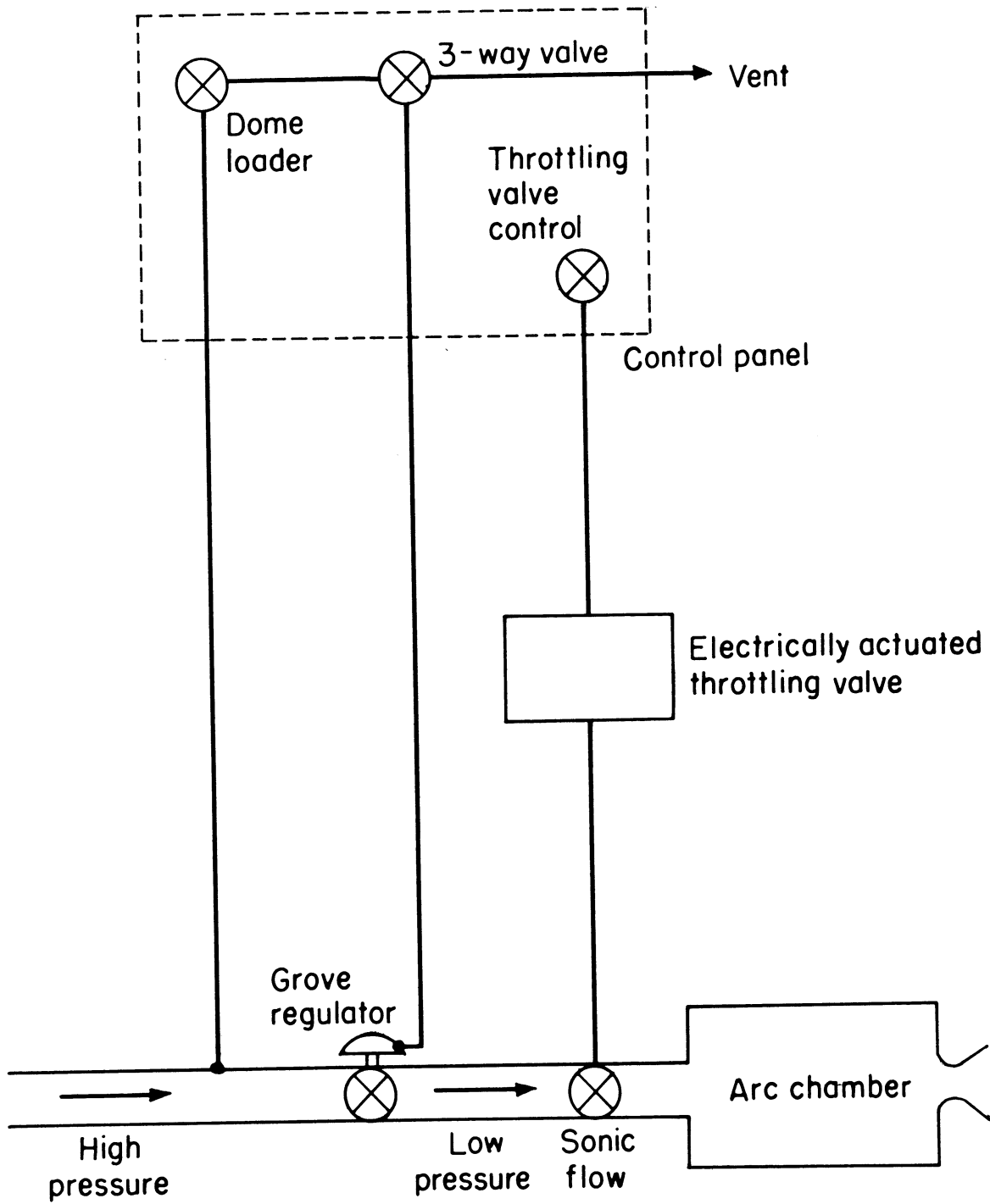
119

FIGURE 37. SCHEMATIC DRAWING OF PRIMARY AIR FLOW.

120

sensing an over-temperature would trigger the same chain of events as the flow switch described above. Finally, a means of varying the coil current should be provided as well as a DC ammeter.

The arc-heater itself will require one or two pressure transducers to monitor arc-chamber pressure and nozzle exit pressure. Either the signal indicating chamber pressure or chamber mass flow should be integrated into the control system. This should interrupt the main power to the arc in the event of a loss in arc-heater air flow.

As there is to be a mixing of arc-heater air with secondary air, there will be a need for pressure and temperature instrumentation on the secondary air flow. This information coupled with arc-heater nozzle exit flow conditions and a temperature measurement near the pebble bed inlet should give a good control over pebble bed inlet temperature.

Starting Procedure

As a first step the flow of water through all components requiring cooling must be established. The instruments previously described will prevent initiation of the arc in the absence of cooling water. Next, the flow of air through the arc-heater should be set at no more than 0.01 lbs/sec. It will start at higher flow rates but starting will be facilitated if there is only a little flow initially. Next, the DC field coil should be actuated and provision should be made which will prohibit application of the main AC power unless there is current flowing through the coil. The AC voltage may now be applied to the electrodes and the starting device triggered. If the unit fails to start the AC power should be turned off while the starter is readied for another try.

When turning off the unit it is important to leave the magnetic field on until the arc is fully extinguished. That is, they should not be turned off "simultaneously" since the operation of the arc with no field for only a small fraction of a second can result in electrode burn-out.

121

## C. OPERATING CURVES AND CONDITIONS

In this section a series of operating and design curves are presented which are a product of the theoretical predictions developed during the arc heater development contract. The expressions from which the curves were drawn are given in Appendix B so that operating conditions other than those requested can be considered. Two sets of curves are presented; one corresponding to the stand-by condition with $3000^O$R air entering the pebble bed and one pertaining to the rapid heat-up condition where $6000^O$R air leaves the arc heater. The weakest step in the computations which led to these curves was the need to assume an overall efficiency for the arc heater unit. Since the design of the present heater is not the same as the one which has been operated at this laboratory it is not possible to predict accurately the efficiency level. Therefore it is suggested that the following curves be treated as design guides and that the actual operating curves be determined by bench testing the final unit. Since an efficiency close to 30% is highly likely all computations were made assuming that value. In addition, atmospheric pressure has been assumed to prevail throughout the entire heating process.

For a given value of exit temperature a series of curves are given for required inductance per phase, line current, arc power, and KVA, with the total mass flow (primary air plus secondary air) as the independent variable. These appear as Figures 38 to 45.

Upon consulting these figures it will be seen that the voltage ratio $e_a/V_\ell$ appears as a parameter. This denotes the ratio of the mean arc voltage to the RMS line voltage (750 volts in this case). Depending upon the mass flow through the arc heater this ratio will vary from about 0. 3 to 0. 4. Again, the actual variation will have to be determined by experimentation.

It can be determined from Figure 38 that the variable inductance in each phase must be capable of providing at most 1. 2 ohms of inductive reactance. Reference
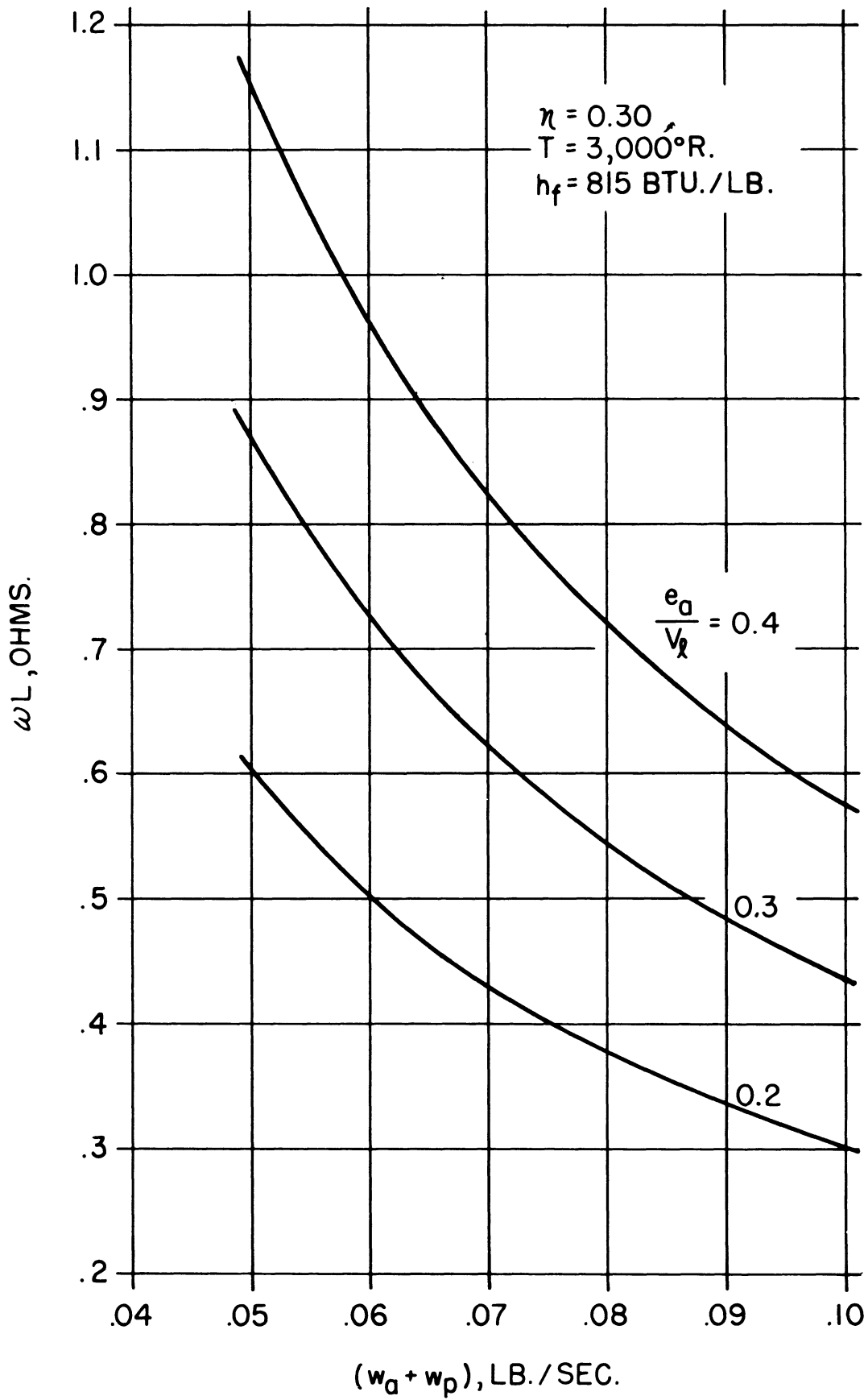
122

FIGURE 38. INDUCTANCE VS. MASS FLOW.

The figure plots $\omega L$, OHMS. (vertical axis) versus $(w_a + w_p)$, LB./SEC. (horizontal axis), with conditions $\eta = 0.30$, $T = 3{,}000°R.$, $h_f = 815$ BTU./LB. Curves are shown for $\dfrac{e_a}{V_\ell} = 0.4$, $0.3$, and $0.2$.
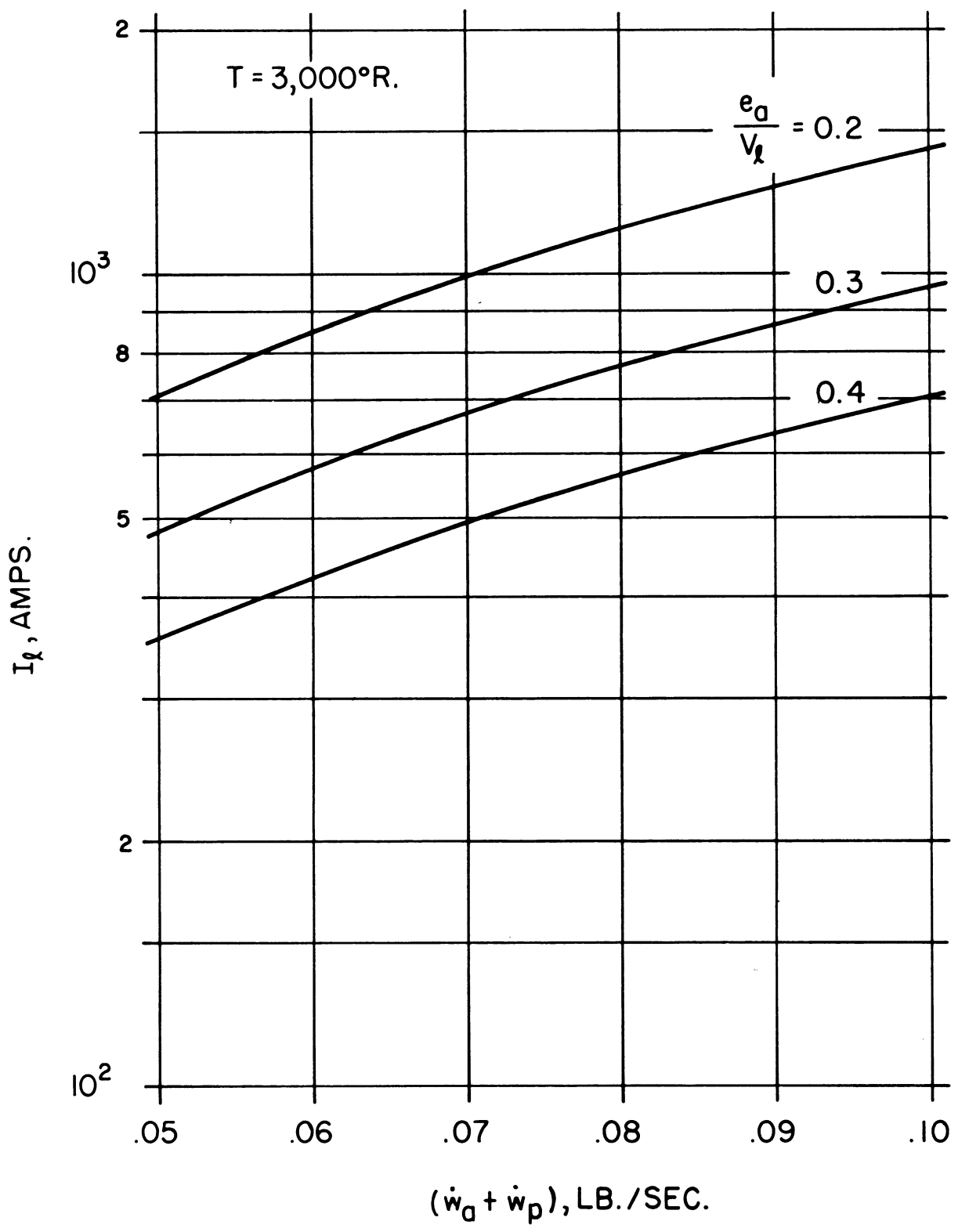
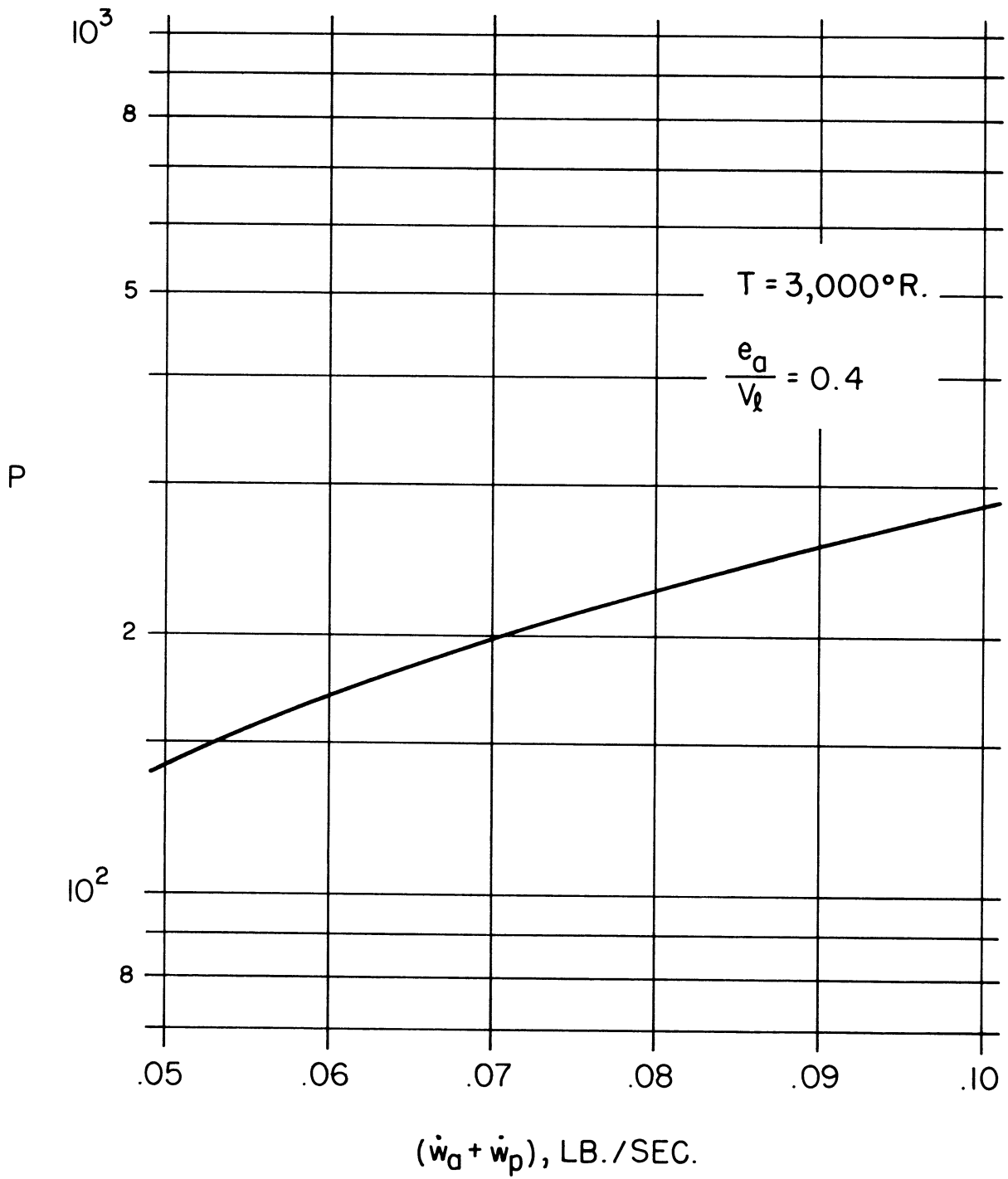FIGURE 39. CURRENT VS. MASS FLOW.

FIGURE 40. POWER VS. MASS FLOW.
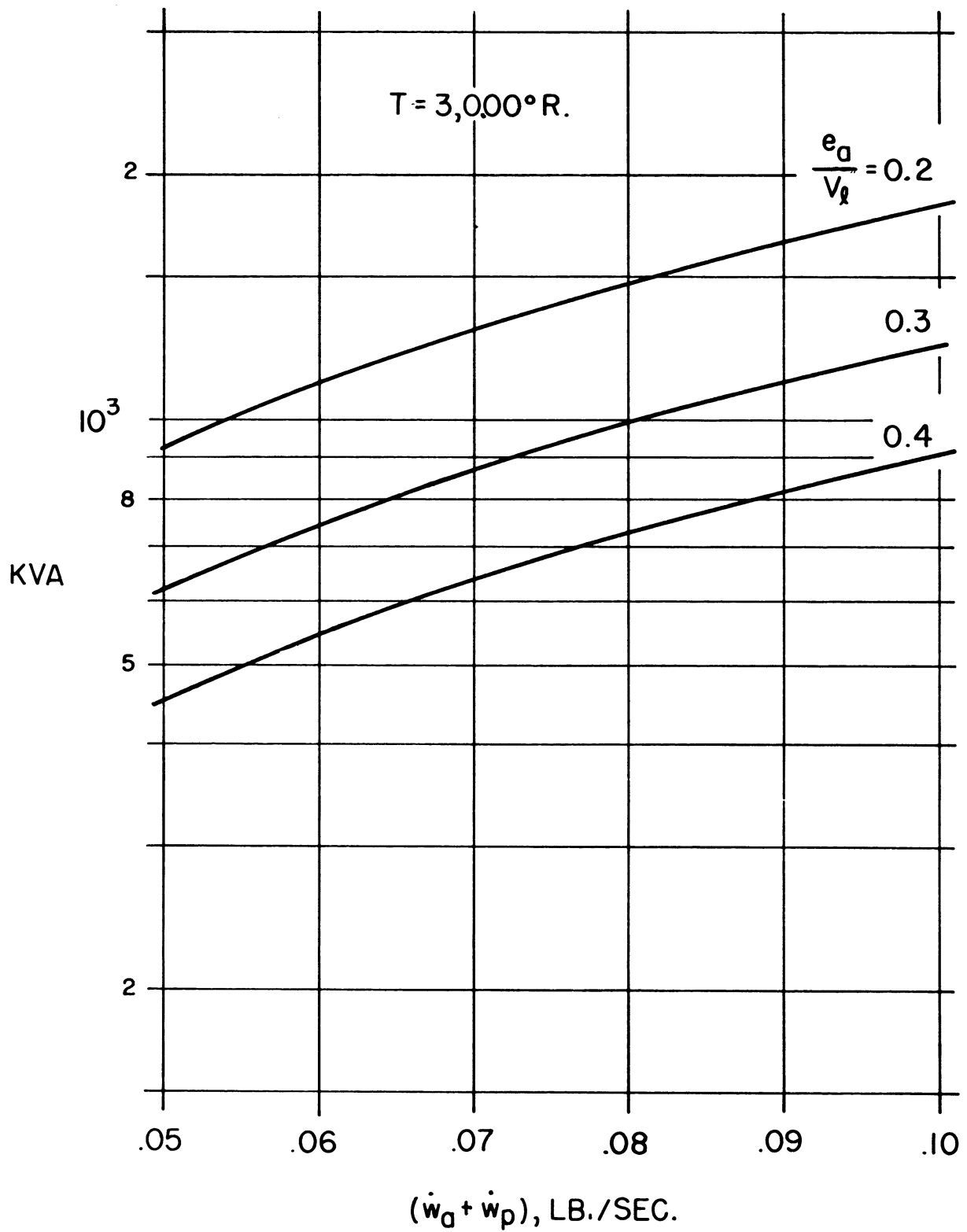
FIGURE 41. KVA VS. MASS FLOW.
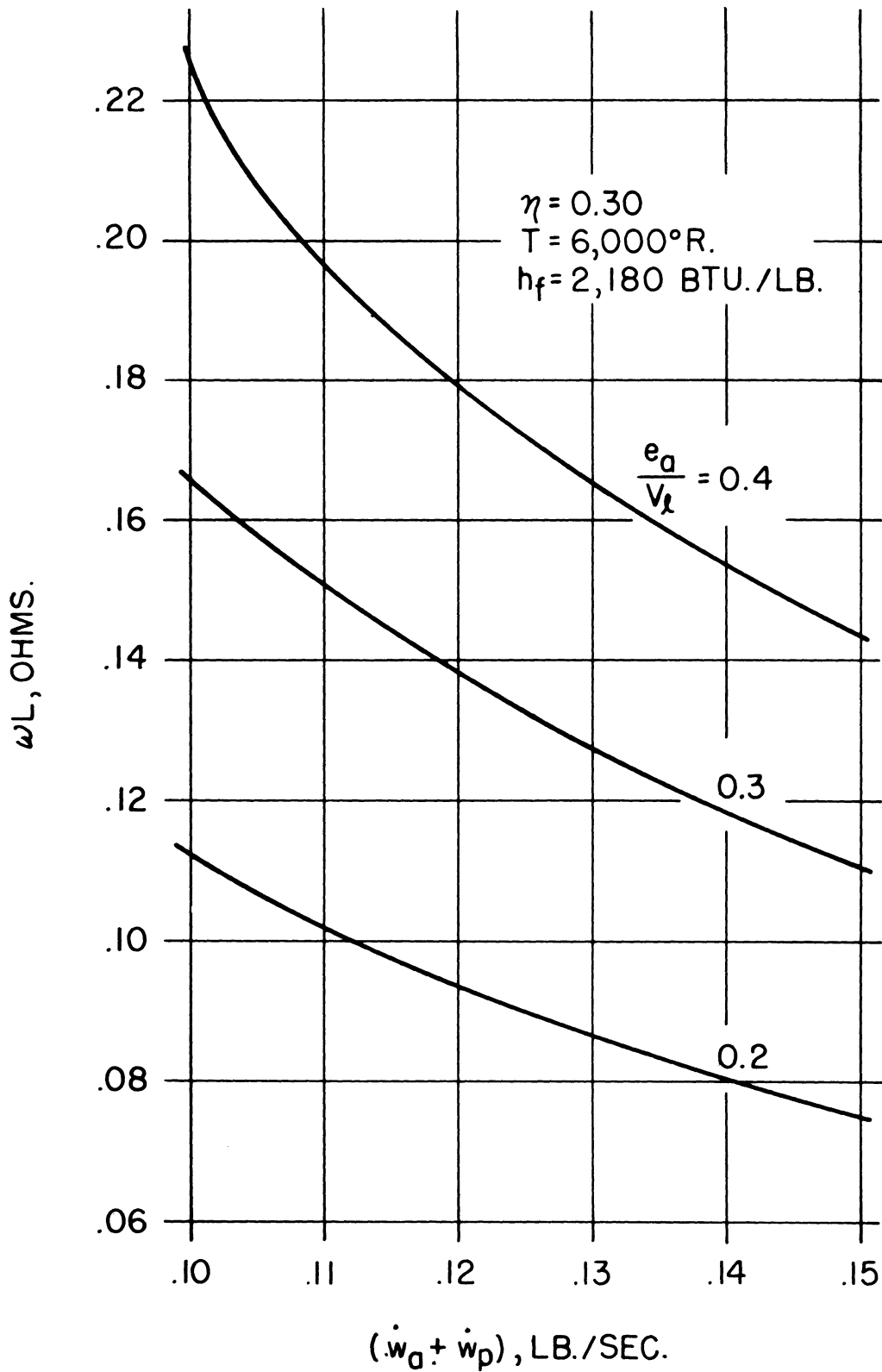
FIGURE 42. INDUCTANCE VS. MASS FLOW.

The figure shows curves of $\omega L$, OHMS. (vertical axis) versus $(\dot{w}_a + \dot{w}_p)$, LB./SEC. (horizontal axis).

Conditions noted on the chart:

$\eta = 0.30$
$T = 6{,}000°R.$
$h_f = 2{,}180$ BTU./LB.

Curves labeled $\dfrac{e_a}{V_\ell} = 0.4$, $0.3$, and $0.2$.

127
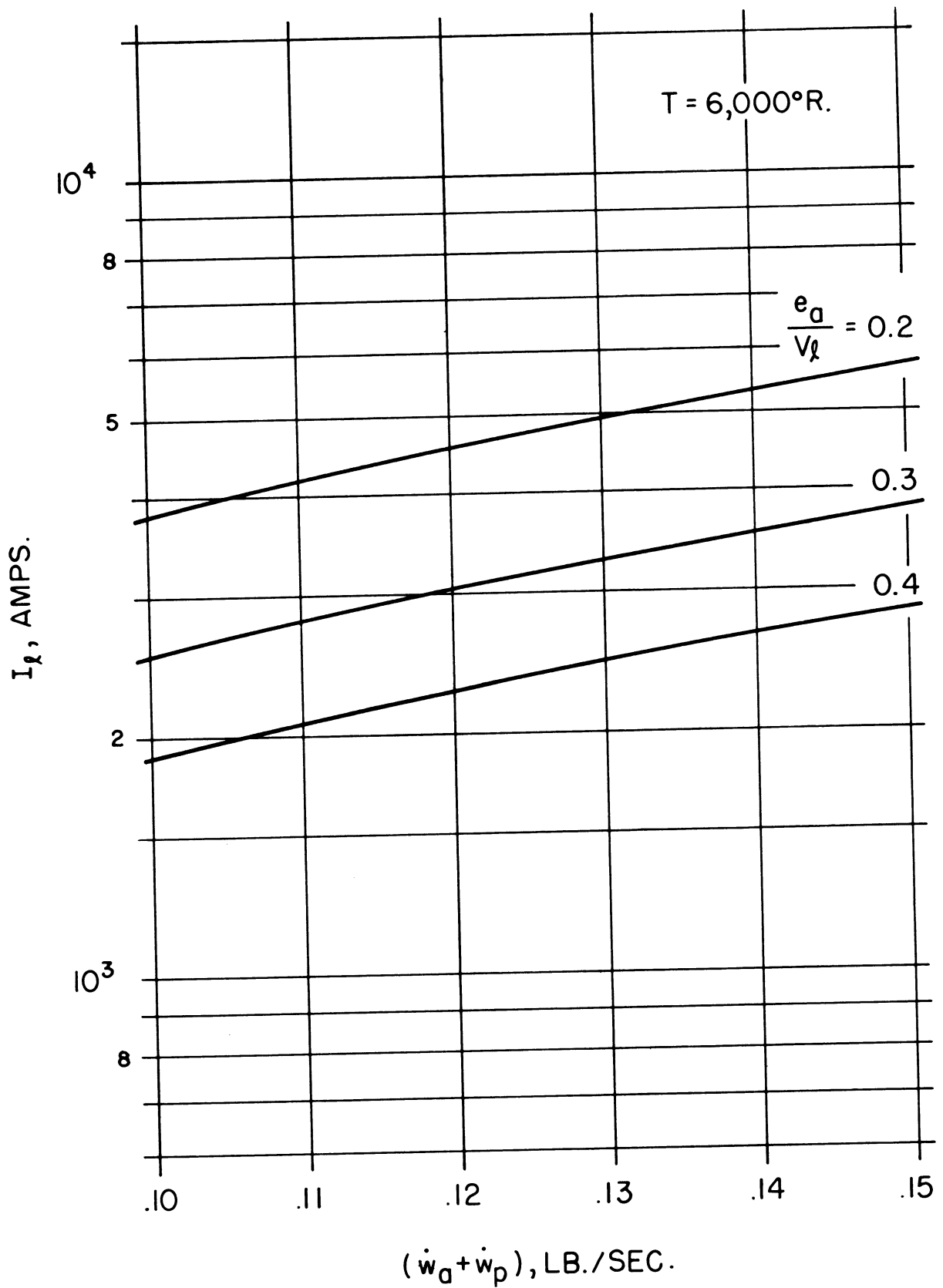
FIGURE 43. CURRENT VS. MASS FLOW.
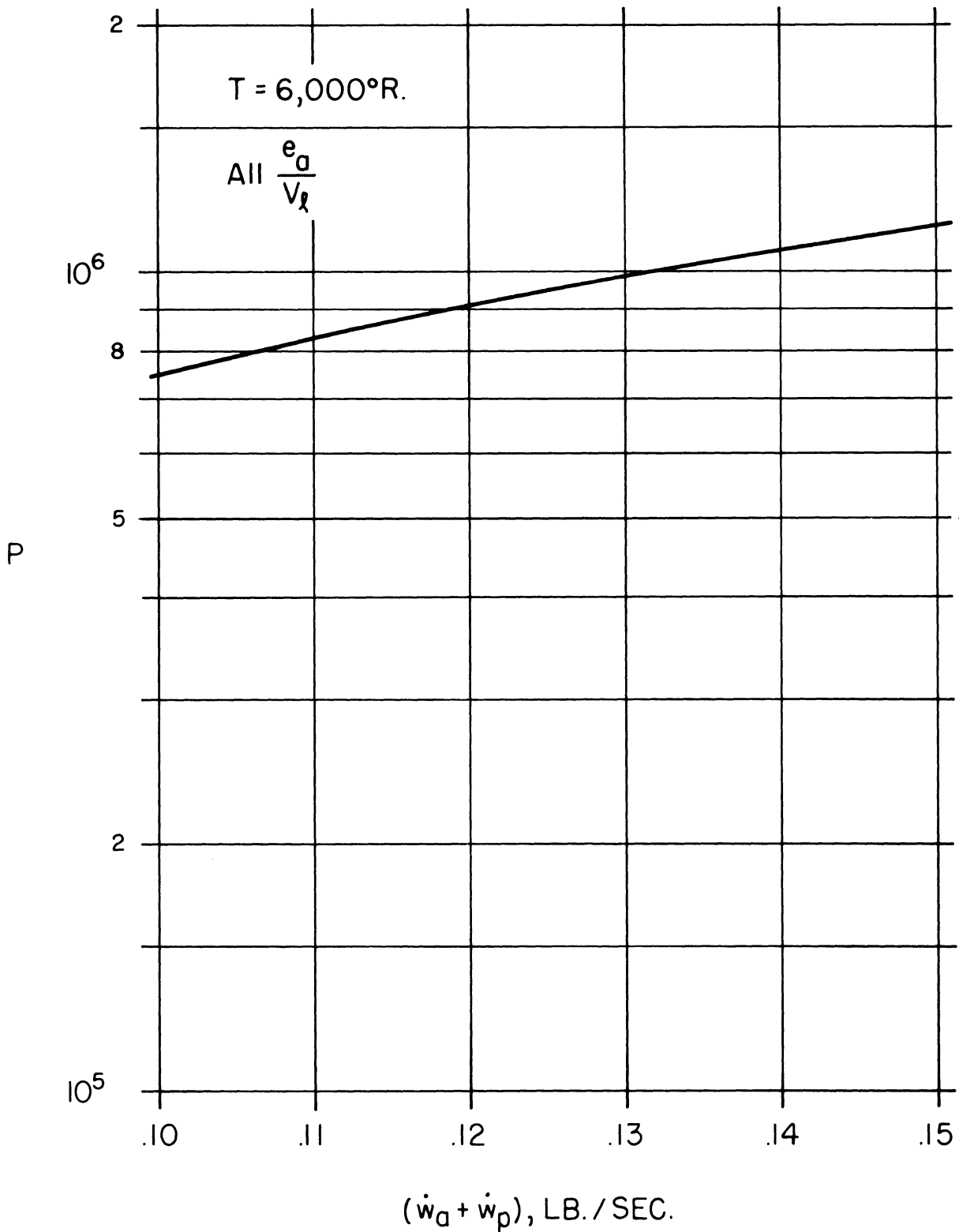
FIGURE 44. POWER VS. MASS FLOW.

FIGURE 45. KVA VS. MASS FLOW.

Graph axes and labels:

- Vertical axis: KVA, logarithmic scale from $10^3$ to $2 \times 10^4$, with gridlines at 2, 5, $10^4$, 8, 2 (×$10^3$)
- Horizontal axis: $(\dot{w}_a + \dot{w}_p)$, LB./SEC., from .10 to .15

$T = 6{,}000°R.$

$\dfrac{e_a}{V_\ell} = 0.2$

0.3

0.4
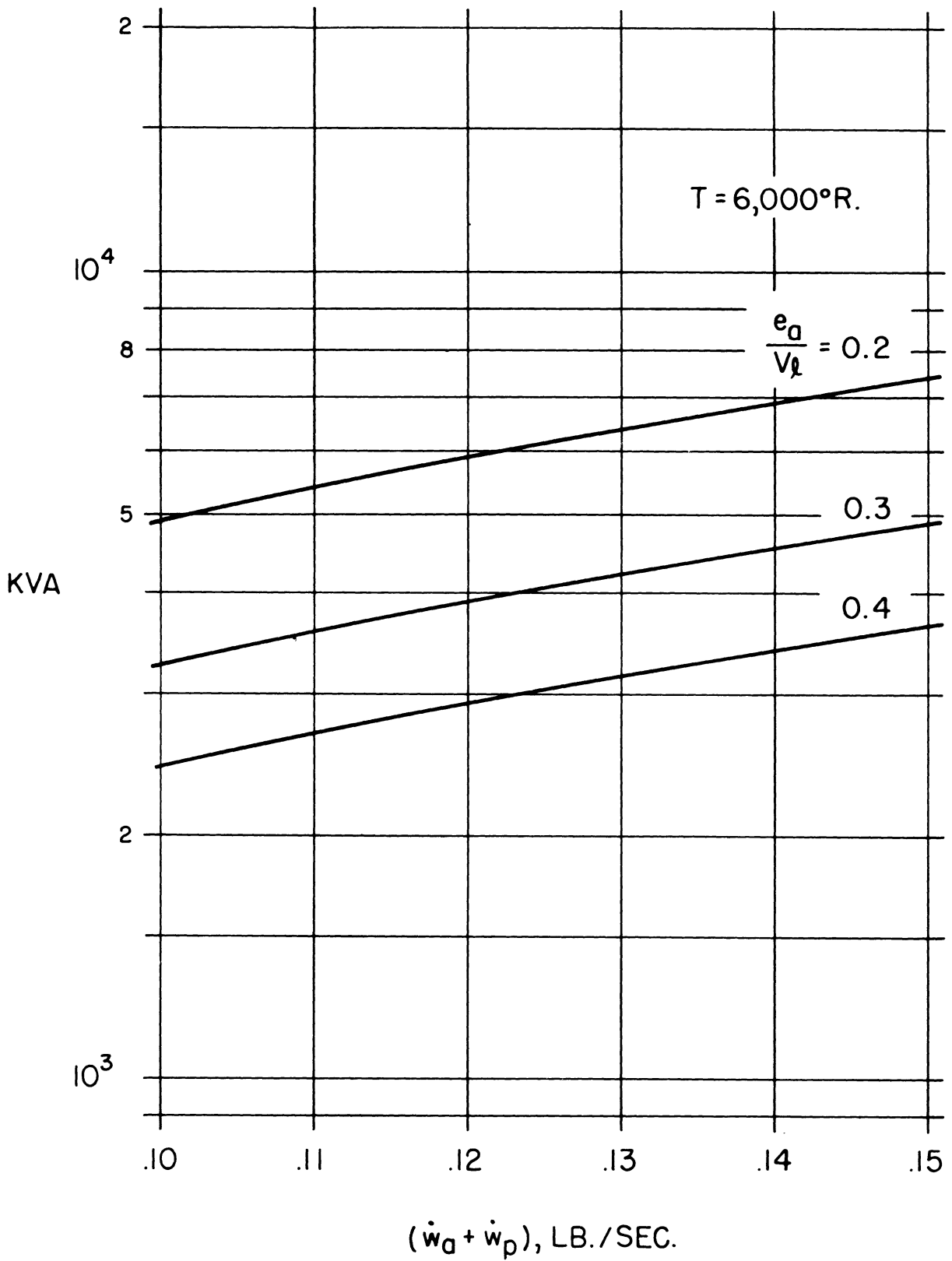
130

to Figures 39 and 43 shows that the inductors should be capable of carrying a maximum current of about 3500 amperes and must have an inductive reactance variable down to about 0.12 ohms.

It will be noted that the abscisca of all graphs is the total weight flow in pounds per second. That is the sum of the primary air, that which is directly heated by the arc, and the secondary air, that which is mixed with the arc heater effluent. Now if one neglects the enthalpy of the secondary air compared to the primary effluent enthalpy it can be shown that (theoretically) it should make no difference in the final enthalpy whether all the flow is primary flow or is divided between primary and secondary flow in any proportion. Of course, this assumes a constant arc power, uninfluenced by mass flow at either extreme. This is not the case over the whole range of mass flows being considered and the proper ratio of secondary to primary air must be determined during actual heater operation. Up to the maximum mass flow of 0.15 lb/sec the arc heater stability should not be impaired so that secondary air need be added only to provide a cooler final flow for heating the pebble bed.

It may also be that operation of the whole unit will be simplified by always running the arc heater with a fixed mass flow and varying the mass flow and gas temperature entering the pebble bed by adding secondary air. Again referring to the figures, it is seen that the KVA to be supplied to the arc heater varies between 500 and 5000 KVA. The arc power ranges from 150 KW to 1200 KW.

Again, all computations are based upon an overall efficiency of 30%. Reference should be made to Appendix B to determine unit performance for other efficiencies. It is strongly recommended that the electrical circuit be designed extremely conservatively to allow for any operational anomalies of the unit.

Electrical Circuit

The external circuit, i.e., exclusive of the arcs, for which all computations have been made is a three phase, three wire system with a variable inductance

in each line of the transformer secondary. The power transformer used in this application should utilize a wye-connected secondary with a floating (ungrounded) neutral point. The only solid ground in the system should occur at the arc chamber; both the inner shell and the pressure vessel. Of course, the necessary current-limiting inductance can be placed in the transformer primary if the values given herein are suitably adjusted according to the turns ratio of the transformer. While the required inductance would be higher, the copper losses of the coils would be lower by the square of the line current; a feature that may prove desirable in view of the high secondary currents which are required. Finally, the ratio of the total secondary resistance per phase (bus bars plus inductance coils) to the secondary inductive reactance per phase should not exceed 0. 10. This limitation is imposed for arc stability purposes since a resistive ac arc current tends to be destabilizing.

## D. ARC HEATER—PRESSURE VESSEL INSTALLATION

To facilitate the operation of the arc heater in conjunction with the pebble bed unit, the following method is presented for installing the arc heater in the 3000 psi pressure vessel. This method aims at a simple way to align and support the arc-heater in the pressure vessel, while at the same time supply it with the necessary electrical and plumbing connections. It does not make any conclusions as to the structural capabilities that must be met. Also the support system would be appropriate only if the arc-heater and pressure vessel were mounted vertically.

Figure 46 is a sketch showing the method for mounting the arc-heater in the pressure vessel. The support of the arc-heater is through a ring and leg system attached to the pressure vessel top flange. This would allow for the alignment of the arc-heater in the pressure vessel to be dependent only on the alignment of the top flange bolt pattern. It would also allow for easy installation or removal of the arc-heater. By routing all air leads, instrumentation leads,

132

cooling water leads and AC and DC power leads, through the top flange, the arc-heater can be installed and removed as a complete unit. This allows the arc-heater to be checked out independent of the pressure vessel. It is believed, that a most desirable procedure would be to run the arc-heater outside the pressure vessel, thereby checking out or trouble shooting the arc-heater plus its associated systems.

Figure 46 also shows a copper water cooled nozzle mounted on the top flange of the pebble bed. This plus the arc-heater nozzle could form an injector, thereby facilitating the mixing of the arc-heater air with the secondary pressure vessel air. Instrumentation placed in this area could be used to insure that the pebble bed air inlet temperature did not exceed the allowable temperature limit on the upper layer of Zirconia pebbles.
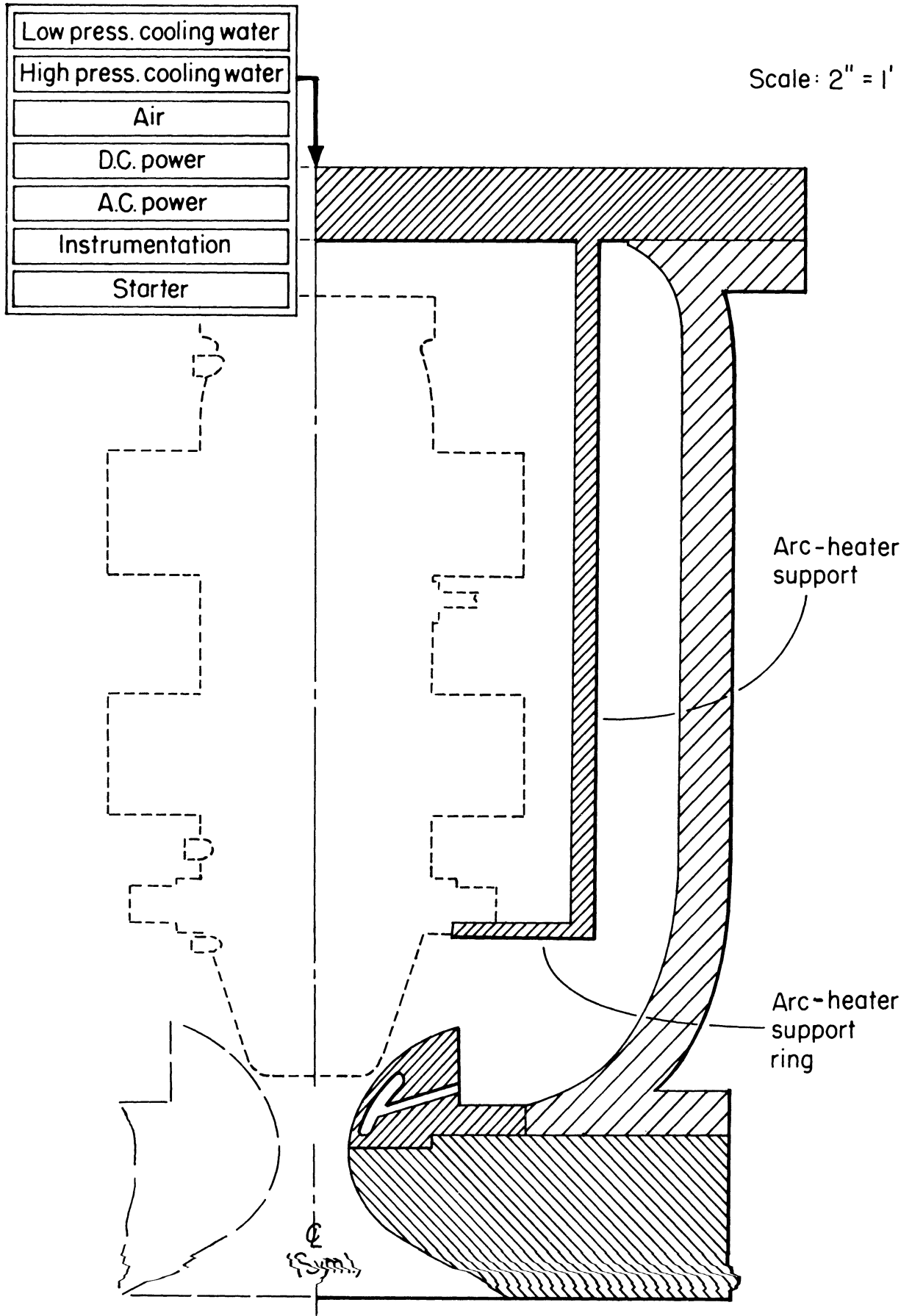
| Low press. cooling water |
| High press. cooling water |
| Air |
| D.C. power |
| A.C. power |
| Instrumentation |
| Starter |

Scale: 2" = 1'

Arc-heater
support

Arc-heater
support
ring

C (Sym.)

FIGURE 46.  ARC-HEATER SUPPORT.

134

# REFERENCES

1. Paschkis, V., and Persson, J., Industrial Electric Furnaces and Appliances, 2nd Ed, Interscience, New York, 1960.

2. Cobine, J. D., Gaseous Conductors, Dover, New York, 1958.

3. Phillips, R. L., "Fundamental Considerations in the Design of an AC Arc Heater," to be published as an ARL Tech. Doc. Rept.

4. Kaufmann, W., Ann. der Physik, Vierte Folge, Band 2, 1900.

5. Rother, H., Ann. der Physik, 6 Folge, Band 20, 1957.

6. Stine, H. A., Watson, V. R., NASA TN D-1331, 1962.

7. Morse and Feshbach, Methods of Theoretical Physics, Part I, McGraw Hill.

8. Chen, M. M., "Theory for a Fully-Developed, Laminar, Axial Positive Column," AVCO RAD Internal Memo 8-10-61; also Paper presented at Symposium for Engineering Aspects of Magnetohydrodynamics, Berkeley, Calif., April, 1963.

9. Resler, E. L., and Sears, W. R., J. Aeron. Sci., Vol. 25, April, 1958, p. 235.

10. Jakob, M., Heat Transfer, Vol. II, p. 112, Wiley, 1957.

11. Kivel, B., and Bailey, W., Research Report 21, December, 1957, AVCO-Everett Research Laboratories.

12. Nicholls, J. A., "Studies of AC Arc Heating Phenomena," Proposal submitted to Aerospace Research Labs, November, 1963.

13. Callaghan, E. E., and Maslen, S. H., NASA TN D-465, October, 1960.

# APPENDIX A

## MAGNETIC FIELD COIL COMPUTATIONS

### Resistance Calculation

For 1/4 in. O. D. x .030 in. wall copper tubing the copper cross-sectional area is:

$$\omega = .134 \text{ cm}^2$$

The resistivity of 85% IACS copper is

$$\rho = 2.03 \times 10^{-6} \text{ ohm-cm}$$

The resistance per foot is:

$$R = \rho/\omega = 4.62 \times 10^{-4} \text{ ohms/ft}$$

Since each pancake has 50 feet of tubing and there will be a total of 40 pancakes the total length of copper is 2000 feet. Then

$$R_{tot} = 4.62 \times 10^{-4} \times 2 \times 10^3 = .924 \text{ ohms}$$

### Heating Calculation

Consider two operating conditions; (1) the voltage drop across the coil is 250 volts and (2) the full open circuit voltage of the power supply is dropped across the coil, i. e., 500 volts. Then:

$$I_1 \cong 270 \text{ amps}$$

$$I_2 \cong 540 \text{ amps}$$

Now it can be shown for the coil in question that the temperature rise of the copper, $\Delta T$, at a given length, $\ell$, downstream of the cooling water insertion is

$$\Delta T = \frac{I^2 \rho}{\omega} \left[ \frac{1}{hp} + \frac{\ell}{\dot{w}} \right] \, {}^{\circ}F$$

where h is the heat transfer coefficient of the cooling water film, $\dot{w}$ is the weight flow of the coolant, and p is the wetted perimeter of the tubing cooling passage.

136

For the present case the second term in the brackets is much greater than the first and one has the usual expression

$$\Delta T \cong \frac{I^2 \rho \ell}{\omega \dot{w}} \; {}^{\circ}F$$

With the subscripts 1 and 2 denoting the two current levels given above one finds:

$$\Delta T_1 \cong 3.19 \times 10^{-2} \; (\ell/\dot{w})$$

$$\Delta T_2 \cong 12.76 \times 10^{-2} \; (\ell/\dot{w})$$

For a friction factor typical of smooth tubing and a pump pressure of 300 psi one finds

$$\dot{w} \ell^{1/2} = 1.89$$

Then for $\ell = 100$ feet

$$\Delta T_1 \cong 17^{\circ}F$$

$$\Delta T_2 \cong 68^{\circ}F$$

Furthermore $\dot{w} \cong 1.4$ gal/min per 100 feet so that the total pump output should be at least 28 gal/min at 300 psig.

# APPENDIX B
## CIRCUIT DESIGN CALCULATIONS

Subscripts:

$( \ )_p \sim$ primary air

$( \ )_s \sim$ secondary air

$( \ )_f \sim$ final conditions

$\dot{Q} \sim$ heat added to primary stream (BTU/sec)

$h \sim$ enthalpy (BTU/lb)

$\dot{w} \sim$ weight flow (lb/sec)

$P \sim$ arc power (kilowatts)

$\eta \sim$ overall efficiency

Now clearly:

$$\dot{w}_p h_p = \frac{56.88}{60} \eta P$$

and

$$h_f = \frac{\dot{w}_s h_s + \dot{w}_p h_p}{\dot{w}_s + \dot{w}_p} \quad .$$

It has been shown theoretically and verified experimentally that the arc power may be related to the external circuit parameters by

$$P = \frac{2}{\pi} \quad \frac{3}{2} \frac{V_\ell^2}{\omega L} \frac{e_a}{V_\ell} \left[ 1 - \frac{1}{3} \frac{2\pi^2}{9} \frac{e_a^2}{V_\ell} \right]^{\frac{1}{2}} \times 10^{-3}$$

where $V_\ell$ is the line voltage and $\omega L$ is the inductive reactance per phase in ohms. Now if one defines

$$\alpha \equiv \dot{w}_s / \dot{w}_p$$

138

the expression for the final enthalpy can be written

$$h_f = (h_p + \alpha h_s)/(1 + \alpha)$$

Since it will usually be true that

$$h_p >> \alpha h_s$$

one can write

$$h_f \cong h_p/(1 + \alpha)$$

Recalling the relation between arc power and primary air enthalpy one can easily obtain

$$(\omega L \times 10^3) = \frac{2}{\pi} \quad \frac{3}{2} \quad \frac{56.88}{60} \quad \frac{\eta V_\ell^2}{h_f (\dot{w}_s + \dot{w}_p)} \quad \frac{e_a}{V_\ell} \quad \left[ 1 - \frac{1}{3} \frac{2\pi^2}{9} \frac{e_a^2}{V_\ell^2} \right]^{\frac{1}{2}}$$

The following values have been specified:

$$V_\ell = 750 \text{ volts,} \qquad T_f = 3000^O R \text{ and } 6000^O R$$

at $\quad h_f = 815$ BTU/lb $(3000^O R)$, $\qquad .05 \leq (\dot{w}_s + \dot{w}_p) \leq .10$ lb/sec

at $\quad h_f = 2180$ BTU/lb $(6000^O R)$, $\qquad .10 \leq (\dot{w}_s + \dot{w}_p) \leq .15$ lb/sec

It is clear that one need only specify the final enthalpy, the total mass flow, and the arc voltage in order to find the proper line inductance to achieve those conditions. Notice the direct dependence upon the efficiency, $\eta$.

139